NOTE

Architectural morphogenesis of poplar grown in a shortened annual cycle system

Kei' ichi Baba[1]*, Yuko Kurita[2,3], Tetsuro Mimura[2]
[1]Research Institute for Sustainable Humanosphere, Kyoto University, Uji 611-0011, Japan.
*E-mail: kbaba@rish.kyoto-u.ac.jp
[2]Graduate School of Science, Kobe University, Kobe 657-8501, Japan
[3]Faculty of Agriculture, Ryukoku University, Otsu 520-2194, Japan

Abstract

Tree architecture is an important feature of plant environmental adaptation and affects many aspects of forestry, as well as both timber and orchard fruit production. However, studying tree architecture indoors in standard lab environments is challenging due to the large size and long growth cycles of trees. Here, we developed miniaturized poplar trees with branching architecture similar to field-grown trees by using a shortened annual cycle system. Control poplars grown under typical fixed conditions in a growth room had no branches and formed simple shapes consisting of a single stem and leaves. We observed simultaneous breaking of dormancy of several buds resulting in such architectural complexity. Our results suggest that apical dominance is lost in the shortened annual system as dormancy is broken. In contrast, apical dominance persisted in control trees grown under typical fixed conditions.

Introduction

Plant architecture depends on leaf phyllotaxy, branch angle, and branch frequency [1]. Tree architecture strongly affects light distributions in the canopy and carbon assimilation, and thus impacts wood production and quality in forestry and the timber-product industry [2, 3]. In addition, plant architecture is also an

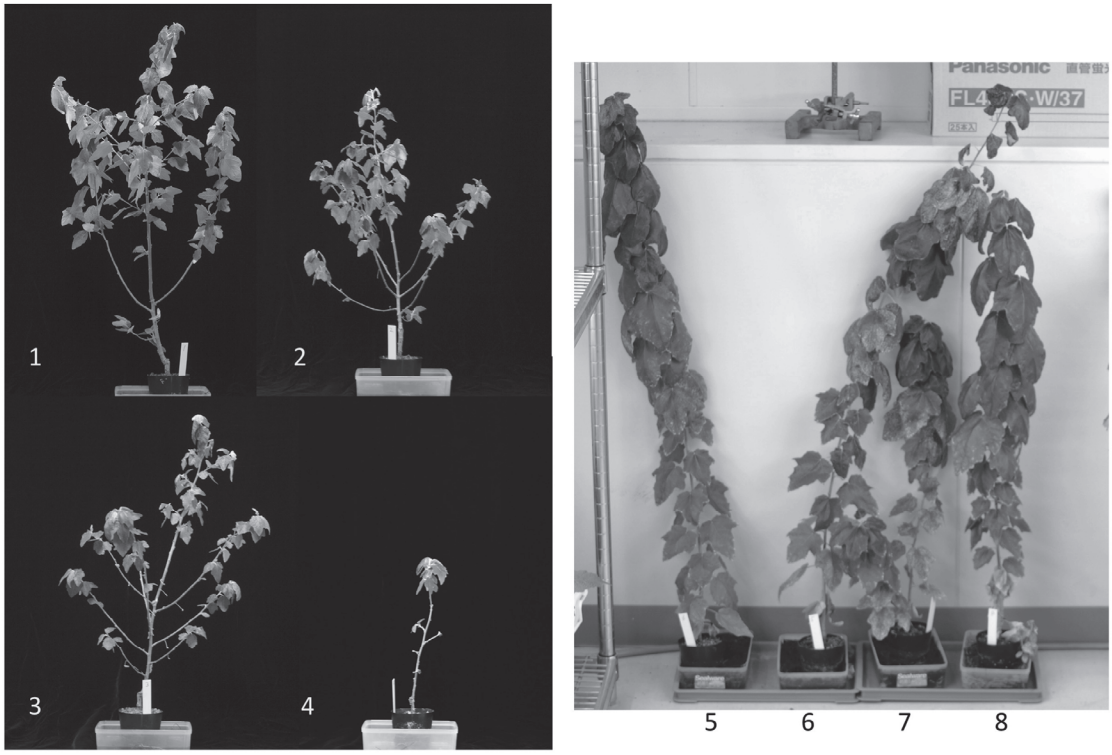

Fig. 1. Tree architecture after Stage 2 of the third cycle of the shortened annual cycle system (#1-4). Observations for the control trees (# 5-8, in Stage 1 only) were recorded at the same time.

NOTE

important horticultural trait that influences fruit yield and orchard quality [4, 5]. Despite its important economic implications, research on tree architecture is highly limited in typical indoor experimental environments given that tree morphogenesis spans many years and mature trees are typically too large and cumbersome to manage indoors. Because of these difficulties, computer modeling has been applied to predict the mature tree shape [2, 4] and some treatments or modifications in young plants have also been explored to achieve the desired architecture [3, 5]. In the present study, miniaturized poplar trees with branching patterns similar to that of field-grown trees were developed when grown under a shortened annual cycle system [6, 7]. This system reduces the annual cycle of poplar growth to a period of 4-5 months, and induces an architecture that differs greatly from control trees grown under typical fixed conditions in a growth room.

Materials and methods

Cuttings of 3-5 cm in length were obtained from poplar trees (*Populus alba* L.) grown in a growth room. The cuttings were potted (7.5 cm diameter, 6.5 cm depth) and cultured with 2000x diluted Hyponex fertilizer (N:P:K = 6:10:5, HYPONeX Japan, Osaka, Japan) applied at a depth of 0.5-2 cm. After confirmation of new shoot growth, poplars were cultured for three cycles of the shortened annual cycle system [6, 7], which mimicked periods of leaf color change, defoliation, dormancy, and breakage and growth all within a period of 4-5 months. This system consisted of three stages: Stage 1 with a long day at high temperature (14 h light, 24-28°C); Stage 2 with a short day at mid-temperature (8 h light, 15°C); Stage 3 with a short day and low temperature (8 h light, 5°C). Stages 2 and 3 were carried out in a plant growth chamber (LH-410PFD-SP, NK System, Osaka, Japan). Duration of Stages 1 and 2 was set at 1 month each, whereas the duration of Stage 3 was determined by leaf fall and ranged between 2-3 months. Control trees, prepared in a similar manner were subjected to Stage 1 only of the fixed condition. Tree height, defined as from the basal point of the bud to the apical tip, was measured at the end of each stage, and photos were taken of trees at the end of each stage, which were used to determine branch number.

Results and discussion

Four newly growing shoots from poplar cuttings were cultured for three rounds of the shortened annual cycle system. This system consisted of three conditions mimicking spring/summer (Stage 1), autumn (Stage 2), and winter (Stage 3). All of the new shoots underwent defoliation in Stage 3 and bud breaking at the beginning of Stage 1. In contrast, control shoots grown under fixed conditions (identical to Stage 1 conditions) displayed continuous growing of the first breaking shoot (or two for tree #7) which occurred at the beginning of the culturing of the cuttings. In the controls, no other buds broke and the leaves did not fall except for a small number at the lowest part of the stem. Figure 1 shows the tree architecture at the end of

Table 1. Branch number at the end of each stage.

culture condition	tree #	Cycle-Stage								
		1-1	1-2	1-3	2-1	2-2	2-3	3-1	3-2	3-3
Shortened annual cycle system	1	1	1	1	6	6	6	16	16	16
	2	1	1	1	8	8	8	22	22	22
	3	1	1	1	9	9	9	19	19	19
	4	1	1	1	3	3	3	3	3	3
control (Stage 1 only)	5	1	1	1	1	1	1	1	1	1
	6	1	1	1	1	1	1	1	1	1
	7	2	2	2	2	2	2	2	2	2
	8	1	1	1	1	1	1	1	1	1

Note: Single stem was shown as 1.

NOTE

Stage 2 in the third cycle (trees # 1-4), and control trees at the same time (trees # 5-8). Trees that were grown in the shortened annual cycle system developed multiple branches, whereas the control trees formed only a single stem, with the exception of tree # 7, which developed two stems in the basal region. Branch number increased every cycle for trees grown in the shortened annual cycle system (Table 1), whereas the number of branches did not increase for control trees. Branch number increased only in Stage 1 after dormancy (Stage 3), and not in Stages 2 or 3. Bud breaking occurred only at the beginning of Stage 1, at which time the branch number was determined. Each branch apex displayed apical dominance following initiation of growth.

Tree heights were recorded at the end of each stage in order to assess stem elongation (Fig. 2). The heights of three individual trees (# 1-3) increased at similar rates during each stage, exhibiting high and moderate increases in Stage 1 and Stage 2, respectively, but no change in height was observed in Stage 3, with the exception of the third cycle, in which (for unknown reasons) no growth was observed in Stage 2. Only tree # 4 failed to grow after the second cycle, despite it forming new leaves after each dormant phase (Stage 3). The control trees, grown under fixed conditions identical to those described for Stage 1, underwent exponential growth during the early period, after which the growth rate declined sharply and tree height became constant. Tree # 7 had two stems (Fig. 1) but only measurements of the longer stem are included in Fig. 2. This tree was also smaller than the other control trees, possibly due to nutrient sharing between the two stems. Trees # 1, 2, and 3 were shorter than 70 cm, whereas trees # 5, 6, and 8 were taller than 70 cm (Fig. 2). Variations in height were most likely due to differences in the numbers of stems and branches among these trees; trees # 1, 2, and 3 had many branches, whereas trees # 5, 6, and 8 had only one long stem. Total biomass was more or less the same between the trees grown in the shortened annual cycle and in the control systems (data not shown).

The architecture of the trees grown under the shortened annual system strongly resembled that of field-grown trees, albeit in miniature. This result suggests that our shortened annual cycle system more closely approximates natural conditions for poplar trees. Trees in the shortened annual cycle system produced three growth rings inside the stem [7], which accorded with the observed growth curves (Fig. 2). In contrast, the control trees had only a single ring despite having stem diameters comparable to those in the shortened annual cycle system.

Variations in shape from arbor to bush within woody species is thought to be associated with apical dominance, a classic explanation of which is that auxin from the apical bud directly suppresses the growth of the axillary bud. It has been known for decades that auxin flux in the shoot stem inhibits cytokinin synthesis at the node, which breaks axillary bud dormancy [8]. More recently, strigolactone, a root phytohormone, was also found to maintain axillary bud dormancy [9, 10]. Moreover, enhancement of the sugar supply might be necessary to break axillary bud dormancy [11]. Although details of the mechanisms underlying the poplar morphogenesis described in the present study remain unclear, simultaneous disruptions of the dormancy of several buds resulted in complex plant architecture, with many branches. The

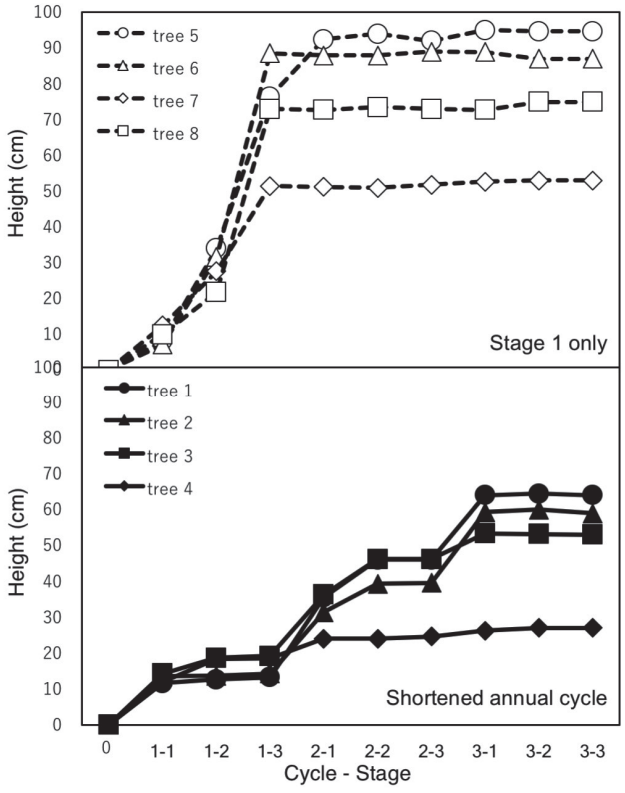

Fig. 2. Growth of trees under the shortened annual cycle system.

Tree height was measured at the end of each stage. Measurements of the control trees (in Stage 1 only) were recorded at the same time.

NOTE

dormant stage (Stage 3) of this shortened system could prevent apical dominance in the initial phase of the breaking of dormancy. In contrast, the control trees grown under fixed conditions (identical to Stage 1 conditions) experienced continued growth throughout apical dominance.

Acknowledgements

Financial support for this work was provided by the Research Institute for Sustainable Humanosphere, Kyoto University (Mission-1). We would like to thank Editage (www.editage.jp) for English language editing.

References

[1] Honda H, Hatta H, "Branching model consisting of two principles: Phyllotaxis and effect of gravity", *Forma*, 19, 198-196, 2004.

[2] Fernández M P, Norero A, Vera J R, Pérez E, "A functional–structural model for radiata pine (*Pinus radiata*) focusing on tree architecture and wood quality", *Ann Bot*, 108, 1155-1178, 2011.

[3] Spathelf P, "Reconstruction of crown length of Norway spruce (*Picea abies* (L.) Karst.) and Silver fir (*Abies alba* Mill.) – technique, establishment of sample methods and application in forest growth analysis", *Ann For Sci*, 60, 833-842, 2003.

[4] Migault V, Pallas B, Costes E, "Combining genome-wide information with a functional structural plant model to simulate 1-year-old apple tree architecture", *Front Plant Sci*, 7, 2065, 2017.

[5] İpek M, Arikan S, Pirlak L, Eşitken A E, "Effect of different treatments on branching of some apple trees in nursery", *Erwerbs-Obstbau,* 59, 119–122, 2017.

[6] Kurita Y, Baba K, Ohnishi M, Anegawa A, Shichijo C, Kosuge K, Fukaki H, Mimura T, "Establishment of a shortened annual cycle system; a tool for the analysis of annual re-translocation of phosphorus in the deciduous woody plant (*Populus alba* L.)", *J Plant Res*, 127, 545-551, 2014.

[7] Baba K, Kurita Y, Mimura T, "Wood structure of *Populus alba* L. formed in a shortened annual cycle system", *J Wood Sci*, Doi 10.1007/s10086-017-1664-x, 2017.

[8] Tanaka M, Takei K, Kojima M, Sakakibara H, Mori H, "Auxin controls local cytokinin biosynthesis in the nodal stem in apical dominance", *Plant J*, 45, 1028-1036, 2006.

[9] Gomez-Roldan V, Fermas S, Brewer P B, Puech-Page V, Dun E A, Pillot J, Letisse F, Matusova R, Danoun S, Portais J, Bouwmeester H, Beard G, Beveridge C A, Rameau C, Rochange S F, "Strigolactone inhibition of shoot branching", *Nature,* 455, 189-194, 2008.

[10] Umehara M, Hanada A, Yoshida S, Akiyama K, Arite T, Takeda-Kamiya N, Magome H, Kamiya Y, Shirasu K, Yoneyama K, Kyozuka J, Yamaguchi S, "Inhibition of shoot branching by new terpenoid plant hormones", *Nature*, 455, 195-200, 2008.

[11] Mason M G, Ross J J, Babst B A, Wienclaw B N, Beveridge, C A, "Sugar demand, not auxin, is the initial regulator of apical dominance", *PNAS*, 111, 6092-6097, 2014.

NOTE

Estimating net ecosystem production of tropical forest

(Laboratory of Radar Atmospheric Science, RISH, Kyoto University)

Tran Van Do

Abstract

In recent years, ecologists have focused on estimating Net Ecosystem Production (NEP) to understand the role of forest against increasing concentration of CO_2 in the atmosphere, a major concern in research and debates on global warming. This is due to the fact that NEP of a forest is the amount of carbon accumulated in a unit of area and time. In this study, NEP was estimated for tropical evergreen broadleaved forest in Northwestern Vietnam. The results indicated that one hectare of old-growth broadleaved forest can accumulate 2.59 Mg C ha^{-1} $year^{-1}$, which is higher than some other forests around the world.

Introduction

NEP is a fundamental property of ecosystems. It was originally defined as the difference between the amount of CO_2 fixed by photosynthesis in an ecosystem (gross primary production) and total ecosystem respiration (the sum of autotrophic and heterotrophic respiration). Based on this definition, NEP represents the organic carbon available for storage within the system or loss from it by export or non-biological oxidation. In other ways, NEP is usually described as the balance between Net Primary Production (NPP) and heterotrophic respiration in an ecosystem. Therefore, NEP is known as the rate of carbon accumulation in forest ecosystem. Estimating NEP is a gap in many forests. This study was conducted in Vietnam to understand capacity of tropical forests in sequestrating CO_2 against global warming and climate change.

Materials and methods

Study was conducted in a tropical evergreen broadleaved forests of Copia Natural Reserve, Northwest Vietnam at 21°23'N and 103°38'E. In the research area, mean annual rainfall was 1,277 mm, and mainly fell in the summer season between May and July. Mean monthly temperature ranged from 21 to 23°C in summer, and from 12 to 16°C in winter. The annual relative humidity is 80%.

On the site, a plot of 30 m × 30 m was established in old-growth forest for NEP estimation. The NEP or rate of carbon accumulation in a forest ecosystem is estimated as NEP = ΔM + ΔCr + Lf + Fp – Rs, where ΔM is aboveground biomass increment, ΔCr is coarse root increment, Lf is aboveground litterfall, Fp is fine root production, and Rs is heterotrophic respiration (soil respiration). ΔM was estimated basing on measuring diameter at breast height (*DBH*) of all living stems at time t_i and t_j ($t_j > t_i$), and applying allometry for AGB (aboveground biomass) in Eq. 1 [1];

$$\mathrm{AGB} = \rho \mathrm{E} \exp\left[\begin{matrix}-1.499 + 2.148\, ln(DBH) + \\ 0.207(ln(DBH))^2 - 0.0281(ln(DBH))^3\end{matrix}\right] \qquad (\mathbf{1})$$

with ρ is wood specific gravity.

ΔCr was estimated basing on alloemtry between CRB (coarse root biomass; root with φ > 2 mm) and AGB as $CRB = 0.489 \cdot AGB^{0.890}$ [2]. Lf was estimated basing on litter trap technique, which was set up systematically under forest canopy. Fp was estimated basing on continuous inflow method using sequence soil core sampling and litter bag technique [3]. Rs was estimated basing on a closed chamber method (CC-method) using an infra-red gas analyzer – IRGA [4].

Results and discussion

Decomposition of dead fine roots was 0.03 g m^{-2} d^{-1}, mortality was 0.07 g m^{-2} d^{-1}, and fine root production was 1.00 g m^{-2} d^{-1} in old-growth forest (Figure 1). Very small amount of fine roots died, indicating

NOTE

longevity of fine roots in the study site is long. Meanwhile, half of dead fine roots was decomposed to release CO_2 to the atmosphere. It may indicate that after two years all dead fine roots will be decomposed completely. Therefore, soil nutrient in tropical old-growth forest Vietnam is high.

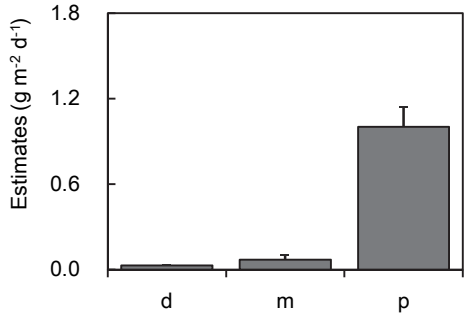

Figure 1. Fine root production (p), mortality (m), and decomposition (d), bars indicated ±SE (Standard error).

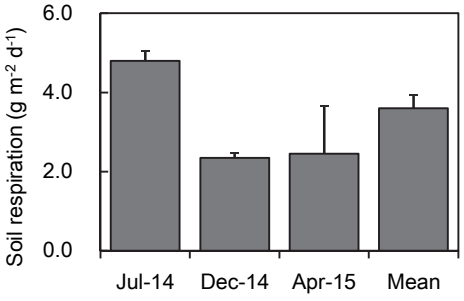

Figure 2. Soil respiration in different seasons, bars indicated ±SE (Standard error).

Total NPP in the present study area was 8.61 g m^{-2} d^{-1} (Table 1). In which, aboveground litterfall contributed 46.7%, reduced to AGB increment (37.1%), to fine root production (11.6%), and to coarse root increment (4.6%). Belowground NPP accounted for 16.2%, which was much lower than that of aboveground NPP (83.8%)

Table 1. Contribution of each compartment to total NPP

	Belowground NPP		Aboveground NPP		Total
	ΔCr	Fp	Lf	ΔM	
g biomass m^{-2} d^{-1}	0.40 ± 0.10	1.0 ± 0.14	4.02 ±0.45	3.19 ± 0.24	8.61
g C m^{-2} d^{-1}	0.2	0.5	2.01	1.595	4.31
Ratio (%)	4.6	11.6	46.7	37.1	

Soil respiration was seasonal dependent, which was higher in summer and lower in winter. In summer, soil respiration was nearly 5 g m^{-2} d^{-1}, while in winter was 2.2 g m^{-2} d^{-1} with annual mean of 3.6 g m^{-2} d^{-1} (Figure 2). In the summer, there are higher temperature and humidity leading to higher activities of soil microorganisms, which decompose organic matter to release CO_2. Meanwhile, in winter temperature may drop to 7^{o}C and it is very dry. Therefore, activities of soil microorganisms reduce. There was high variation of soil respiration in April, which is known as season transition between winter and summer. In this time, daily fluctuation of temperature between day and night is high, leading to much higher soil respiration in day time compared to that of night time.

Total NEP in evergreen broadleaved old-growth forest in Northwestern Vietnam was 0.71 g C m^{-2} d^{-1}, equaling to 2.59 Mg C ha^{-1} $year^{-1}$.

References

[1] Chave J, Andalo C, Brown S, Cairns M A, et al. (2005) Tree allometry and improved estimation of carbon stocks and balance in tropical forests. Oecologia 145:87-99.
[2] Mokany K, Raison RJ, Prokushkin A S (2006) Critical analysis of root: shoot ratios in terrestrial biomes. Global Change Biology 12:84-96.
[3] Tran VD, Akira O, Tamotsu S (2016) Estimation of fine-root production using rates of diameter-dependent root mortality, decomposition and thickening in forests. Tree Physiology 36:513-523.
[4] Bekku Y, Koizumi H, Nakadai T, Iwaki H (1995) Measurement of soil respiration using closed chamber method: An IRGA technique. Ecological Research 10:369-373.

RECENT RESEARCH ACTIVITIES

Wood selection in Japanese traditional tea ceremony room

(Laboratory of Biomass Morphogenesis and Information, RISH, Kyoto University)

Suyako Tazuru-Mizuno and Junji Sugiyama

Identification of wood heritages has provided beneficial information on the origin, historical background, wood selection and also new perspectives. In specific, historical cultural exchanges would be one of the possible factors that influence the wood selection in Japan. Recently, microscopic wood identifications were performed on the decorative and structural elements of several Japanese traditional tea ceremony rooms "Chashitsu" in Kyoto, Japan [1]. Although Japanese tea ceremony rooms are well-known as representative expression of "Wabi-Sabi" the Japanese senses of beauty, scientific wood identification has not seen as important in the past.

For wood identification, minimum amount of samples that are necessary for making preparation were collected carefully from deteriorated parts or cracks so as not to alter the appearance and strength. Hand-sectioned samples were observed under an optical microscope and the samples were identified on the basis of microscopic anatomical features. However, in many cases, it is not easy to collect enough size of samples from old valuable wooden artifacts. In many cases, only one tiny sample can be provided. In order to preserve such a precious tiny sample, synchrotron X-ray microtomography (SRX-ray μCT) that is non-destructive and non-invasive method has been widely applied. Our investigation recently revealed this method is effective for identification and observing anatomical structure [2] [3]. From Japanese traditional tea ceremony room, it was difficult to get enough size of samples; SRX-ray μCT was also applied to identify the wood species.

As a result, the unique wood usage peculiar to tea ceremony rooms was revealed. For instance, combination usage of *Pinus densiflora* and Zoboku (wood with bark) or *Cryptomeria japonica* and Zoboku for Tokonoma was confirmed. Furthermore, some results concerning about the wood selection envisaged a very unique cultural interaction between the architectural styles of Korean peninsulas and Japan. Now, other investigation of tea ceremony rooms in regard to wood species has been started in Kansai area. In order to deeper the "Wabi-Sabi concept" in wood selection and reveal the linkage among Asian counties, wood identification would be more and more important.

Acknowledgements

The synchrotron radiation experiments were performed at the BL20XU in SPring-8 (Japan) with the approval of the Japan Synchrotron Radiation Research Institute (JASRI. Project Nos. 2009B1093, 2009B1981, 2010A1932, 2011B1239 and 2016B1743). Part of this study was supported by the Database for the Humanosphere (Xylarium) of RISH, Kyoto University, as a collaborative program. This work was supported by Cultural Properties Division (Kyoto Prefectural Board of Education), Nobotokean tea room and Konchi-in Temple.

References

[1] Mizuno (Tazuru) S, Sugiyama J, "Wood identification of Building Components of the Tea Room Hasso-seki of Konchi-In Temple Designated as an Important Cultural Property", *Mokuzai Gakkaishi*, 57, 1, 14-19, 2011.

[2] Tazuru S, "A Scientific Identification of the Species of Trees Used for Tea-ceremony Rooms: The newest Method". *The Journal of Chanoyu*, 27, 59-66, 2017. (in Japanese)

[3] Hairi C, Nugroho W, Tazuru S, Sugiyama J, "Identification of wooden keris sheath using synchrotron X-ray microtomography", 67th Annual Meeting of Japan Wood Research Society, 2017.

RECENT RESEARCH ACTIVITIES

Extracellular glycolipids and glucans secreted by a selective lignin-degrading fungus, *Ceriporiopsis subvermispora*

(Laboratory of Biomass Conversion, RISH, Kyoto University)

Hiroshi Nishimura and Takashi Watanabe

A white-rot fungus, *Ceriporiopsis subvermispora*, known to be a selective lignin-degrading fungus, decomposes lignin and hemicelluloses in wood prior to the decomposition of cellulose. Because of its potential applicability and usefulness of selective lignin degradation in the industry, understanding the mechanism of selective ligninolysis has been studied. However, fundamental knowledge, especially the role of secondary metabolites and extracellular glucans in wood decay, is still insufficient to unveil this unique wood degradation mechanism. Secondary metabolites secreted by wood rot fungi play varied roles such as transport of wood biomass components, redox reactions of metal ions for wood degradation, and defense and symbiotic signals in the microbial community. In particular, the roles of extracellular secondary metabolites in selective white-rot fungus are key for selective ligninolsis at a site far from the hyphae and extracellular enzymes. Extracellular glucans, mucilaginous surroundings of hypha called "sheath", are produced by wood-rot fungi and play multiple roles in the lignolysis. Here, we focus on extracellular glycolipids and glucans and report secretion and chemical structure of them (Figure 1).

Cerebrosides are a kind of sphingolipids and composed of hexose and a ceramide (*N*-acylsphingosine) moiety. These compounds are known as strong amphipathic substances and potential signal molecules in the microbial community. First, we isolated cerebroside from *C. subvermispora*. *C. subvermispora* was incubated for 2-4 weeks in three different types of culture media: wood, basal liquid, and stable-isotope labeled with ^{13}C- and ^{15}N- medium. Next, we determined the chemical structure of cerebrosides. The structure was analyzed by LC-ESI-MS, GC-EI-MS, and NMR experiments in combination with stable-isotope labeled information. As results, we report three glucocerebrosides, isolated from a white-rot fungus, *Ceriporiopsis subvermispora*. The structural differences originate from the sphingoid moiety having (8*E*)- or (8*Z*)-double bonds and methyl branches at the olefinic C-9 carbon atom. We found an accumulation of cerebrosides in the sheath and a different expressed pattern of cerebroside in a wood-degrading medium and a liquid medium.[1]

We analyzed the structure of the sheath of *C. subvermispora* by transmission electron microscope, NMR followed by stable-isotope labeling and methylation analysis. We conclude that the sheath polysaccharide is composed of comb-like β-1,3 glucan branching glucopyranosyl residues at *O*-6 positions.[2] Further studies are needed to understand biological activities and the metabolism of cerebrosides and the sheath.

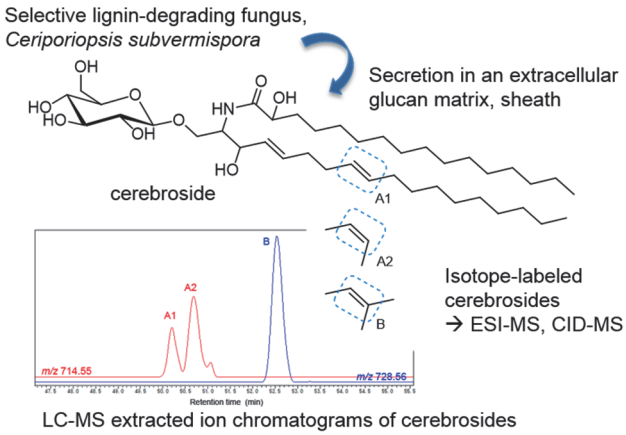

Figure 1. Extracellular metabolites, cerebrosides secrete in the sheath of *C. subvermispora.* (Outline)

Acknowledgements

We acknowledge collaborative programs, DASH/FBAS and ADAM, of Research Institute for Sustainable Humanosphere (RISH), Kyoto University and Zero-Emission Energy (ZE) research program, of Institute of Advanced Energy (IAE), Kyoto University.

References

[1] Nishimura, H., D. Yamaguchi, and T. Watanabe, "Cerebrosides, extracellular glycolipids secreted by the selective lignin-degrading fungus *Ceriporiopsis subvermispora*", *Chem. Phys. Lipids*, 203, 1-11, 2017.

[2] Suzuki, D., H. Nishimura, K. Yoshioka, R. Kaida, T. Hayashi, K. Takabe, and T. Watanabe, "Structural characterization of highly branched glucan sheath from *Ceriporiopsis subvermispora*", *Int. J Biol. Macromol.* 95, 1210-1215, 2017.

RECENT RESEARCH ACTIVITIES

Structure, Biosynthesis, and Bioengineering of Lignocellulose and Phenylpropanoid Metabolites for Future Biorefinery

(Laboratory of Metabolic Science of Forest Plants and Microorganisms, RISH, Kyoto University)

Toshiaki Umezawa, Yuki Tobimatsu, Shiro Suzuki, Masaomi Yamamura, Takuji Miyamoto, and Rie Takada

It is becoming increasingly important to establish a sustainable society by reducing our heavy reliance on fossil resources. As lignocellulosic biomass represents the most abundant renewable and carbon-neutral resources on earth, technologies to improve their utilizations are key for realizing the goal. In this context, we investigate structure, biosynthesis and bioengineering of lignocellulosic biomass using various model plants and biomass crops. In addition, we are interested in understanding biosynthesis of plant-derived phenylpropanoid metabolites displaying various useful biological activities. Our program typically integrates research ideas and approaches based on chemistry, biochemistry, and molecular biology.

Among a wide variety of biomass feedstocks, large-sized grass species, such as *Erianthus*, *Sorghum*, sugarcane, and bamboo, have attracted particular attention especially due to their high biomass productivity and superior environmental adaptability. To explore new breeding strategies to improve the production of fuels and materials from grass biomass, we seek to develop transgenic rice plants that produce biomass with improved utilization properties. Our research particularly focuses on manipulating lignin, a phenylpropanoid polymer accounting for 15-30 wt% of lignocellulosic biomass.

We have developed various rice transgenic lines in which specific genes encoding enzymes and transcription factors functioning in lignin biosynthetic pathway are down- and/or up-regulated. Some of our developed transgenic lines appeared to display notably enhanced biomass properties that can be exploited for productions of bioenergy and biomaterials [1-3]. In parallel, we are working on selective breeding of grass crop varieties, such as *Erianthus* spp. and *Sorghum* spp., with superior lignins suited for bioenergy and biomaterial productions [4]. In addition, we also work on development of new analytical methods using various chemical methods, NMR spectroscopy, and fluorescence imaging techniques, to scrutinize elusive details of architecture and development of lignocellulosic biomass [5].

In another front, aiming at biological production of useful phytochemicals, we have been characterizing plant and microbial enzymes involved in formations of bioactive phenylpropanoids such as lignans and norlignans. Our recent projects include elucidation of the biosynthesis of antitumor podophyllotoxin in *Anthriscus sylvestris* [6], unravelling crystal structures of hinokiresinol synthases, unique enzymes responsible for the enantioselective formation of bioactive norlignans [7], and identification of new enzymes/genes involved in the formation of estrogenic mammalian lignans (enterolignans) via human intestinal bacteria [8].

Selected Publications and Presentations (FY2016)

[1] Koshiba T, Yamamoto N, Tobimatsu Y, Yamamura M, Suzuki S, Hattori T, Mukai M, Noda S, Shibata D, Sakamoto M, Umezawa T. (2017) *Plant Biotechnol.* **34**:7-15.

[2] Lam PY, Tobimatsu Y, Takeda Y, Suzuki S, Yamamura M, Umezawa T, Lo C. (2017) *Plant Physiol.*, **174**:972-985.

[3] Takeda Y, Koshiba T, Tobimatsu Y, Suzuki S, Murakami S, Yamamura M, Rahman M, Takano T, Hattori T, Sakamoto M, Umezawa. (2017) *Planta*, **246**:337-349.

[4] Miyamoto T, Mihashi, A, Yamamura M, Tobimatsu Y, Suzuki S, Takada R, Kobayashi Y, Umezawa T. (2017) Abstracts of the 2017 annual meeting of the Japan Society for Bioscience, Biotechnology and Agrochemistry.

[5] Tobimatsu Y. (2017) A ‘‘Double Click’’ for illuminating plant cell walls. *Cell Chem. Biol.* **24**:246-247.

[6] Kumatani M, Yamamura M, Ono E, Shiraishi S, Umezawa T (2017) Abstracts of the 67th Annual meeting of the Japan Wood Research Society.

[7] Azuma A, Saka N, Suzuki S, Yamamura M, Mikami B, Umezawa T (2017) Abstracts of the 67th Annual meeting of the Japan Wood Research Society.

[8] Hisadome N, Suzuki S, Utsumi R, Umezawa T. (2017) Abstracts of the 2017 annual meeting of the Japan Society for Bioscience, Biotechnology and Agrochemistry.

RECENT RESEARCH ACTIVITIES

Shikonin is a new model for accumulation studies of lipophilic substances in plants

(Laboratory of Plant Gene Expression, RISH, Kyoto University)

Akifumi Sugiyama and Kazufumi Yazaki

Bioactive substances often have hydrophobic properties. It makes actually sense as those substances should penetrate across the plasma membrane to exhibit their activities inside the cells, where hydrophobicity is beneficial in terms of the membrane permeability. In plants, lipophilic secondary metabolites are often secreted out of the cells and accumulated in apoplastic space, e.g. furanocoumarins are accumulated in oil gland after excretion form the epithelial cells, and monoerpenes are often accumulated in subcuticular cavities after biosynthesis in secretary cells in many plant species. However, the secretion mechanisms of those lipophilic metabolites are largely unknown.

Shikonin derivatives are medicinal compounds found only in a limited number of boraginaceaeous medicinal plants. *Lithospermum erythrorhizon* (purple gromwell) is a representative, which has been used as a medicinal plant over a thousand years for burns, wounds, frostbite, inflammation, and hemorrhoids as external use, and for internal use it is effective for leukemia and tumors. As these naphthoquinone compounds have bright red color, it has been used as a natural dye to stain cloths, especially silk, to obtain beautiful purple color, which was a representative color of highest public servant in Nara Era. These characteristics nicely fit to the purpose of Mission 5 “Quality of the Future Humanosphere”, especially Submission 5-1 “Harmonization of human health and the environment”. The wild plants are, however, facing to extinction, because the useful part is the roots and therefore harvest of *L. erythrorhizon* directly reflects the reduction of individual number. Also epidemic of plant viruses is another cause of the endangerment. To keep the sustainable supply of this plant, more fundamental studies are necessary.

Hairy roots are valuable materials for fundamental studies of root function. From *L. erythrorhizon*, we formerly showed that a virulent *Agrobacterium rhizogenes* strain ATCC15834 can be used to establish fast growing hairy roots of this plant [1]. We have been using this hairy root system to study biosynthetic regulation and secretion mechanism of shikonin derivatives, as it can be kept aseptically and stably subcultured, and also maintain the same metabolic function as the intact roots. Cultured hairy roots of *L. erythrorhizon* are capable of producing shikonin derivatives in the dark, while it is strongly inhibited by light irradiation and the shikonin production is also susceptible to ammonium ion as well. These characteristics are almost identical as dedifferentiated cultured cells of this plant. Moreover, the shikonin accumulation occurs only in the epidermal cells in hairy roots, which is the same as in the intact root. Using cultured hairy roots as a model of secretion system of lipophilic metabolites, we have been studying the secretion mechanism of lipids from plant cells [2]. Details are described by our PhD student, K. Tatsumi, in this issue.

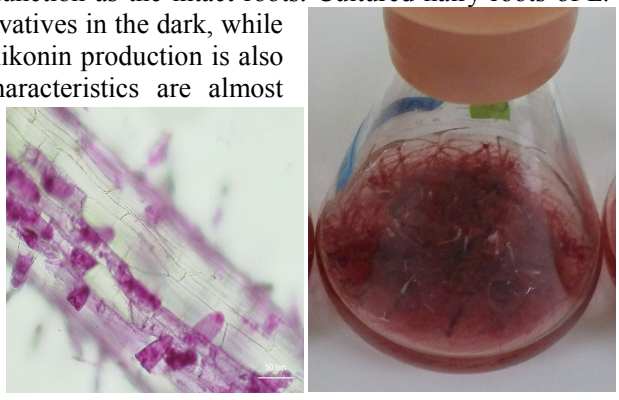

Hairy roots of *L. erythrorhizon* producing shikonin

References

[1] Yazaki, K., Tanaka, S., Matsuoka, H., and Sato, F. (1998). Stable transformation of *Lithospermum erythrorhizon* with *Agrobacterium rhizogenes* and shikonin production of the transformants. Plant Cell Rep., 18, 214-219.

[2] Tatsumi, K., Yano, M., Sugiyama, A., Sato, M., Toyooka, K., Aoyama, T., Sato, F., Yazaki, K. (2016) Characterization of shikonin derivative secretion in *Lithospermum erythrorhizon* hairy roots as a model of lipid-soluble metabolite secretion from plants, Frontiers Plant Sci. 7, 1066.

RECENT RESEARCH ACTIVITIES

Forecast of Localized Heavy Rain by Combining Coherent Doppler LIDAR and Numerical Model

(Laboratory of Atmospheric Sensing and Diagnosis, RISH, Kyoto University)

Jun-ichi Furumoto

Recent study, the impact of coherent Doppler LIDAR (CDL) radial velocity on the forecast of localized heavy rain was examined. For simulating localized heavy rain case, which occurred in Tokyo on 24 Jul. 2015, I used the four-dimensional vibrational data assimilation (4D-VAR) and three-dimensional vibrational (3D-VAR) system for use with a high-resolution numeral model, Weather Research and Forecasting Model - Advanced Research (WRF-ARW).

This is because clouds which occurs rain are generated by updraft with convective instability, and the exact location of convection initiation is essentially determined by the location of updrafts. So, I observed wind condition in detail at boundary layer by using CDL, and get convergence. Assimilating the wind velocity of the boundary layer to WRF helps to improve precision of localized heavy rain forecasts. I had observed the radial wind velocity of the boundary layer at Nihombashi, Tokyo from May 2015 to May 2016 by using CDL whose observation range was from 100m to 4km and resolution was 100m. First, I examined the impact of 3D-VAR, and had an impact on lower wind condition near the place of CDL. However, WRF-ARW was not able to strengthen convergence. 3D-VAR examination realized the shortage of observation range.

Second, I examined the impact of 4D-VAR by which 5 data of radial wind velocity every 6 minutes assimilated to WRF-ARW, and strengthened a convergence line, approximately 30km long, on the boundary layer around the spot of CDL. However, the convection was not able to rain on the WRF-ARW because of observation range. In the sensitivity experiment to assimilate artificial wind, precipitation was calculated when assimilating strong lower wind convergence. Therefore, to predict localized heavy rain in advance, it is one of the effective way to assimilate the observation data of lower wind.

In the future, we complete our developing coherent Doppler Lidar and will examine the impact of assimilating observational data of multiple CDLs with expanded observation range into WRF-ARW and further discuss the assimilation method by 4D-VAR to LES (Large Eddy Simulation).

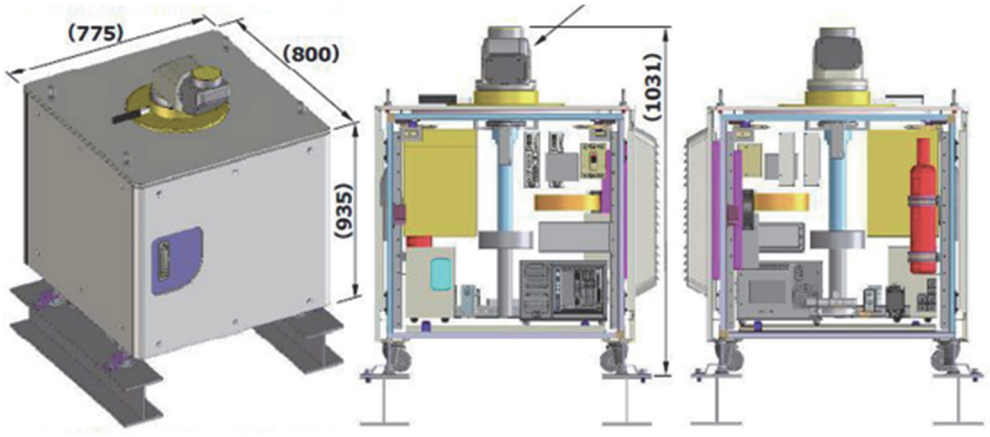

Fig. 1. Coherent Doppler Lidar under development in our laboratory

RECENT RESEARCH ACTIVITIES

Is there a stratospheric pacemaker controlling the daily cycle of tropical rainfall?

(Laboratory of Atmospheric Environmental Information Analysis, RISH, Kyoto University)

Takatoshi Sakazaki

No matter where you live, rain seems to fall more often at certain times of day, whether it is seen in the daily afternoon rainstorm or a typical overnight shower. Indeed, statistically, long-term average rainfall tends to cluster at certain times of the 24-hour cycle, but that time frame varies depending on location. Notably, rainfall in the tropics exhibits a large, 12 h Sun-synchronous variation with coherent phase around the globe. A long-standing, but unproved, hypothesis for this phenomenon is excitation by the prominent 12 h atmospheric tide, which itself is significantly forced remotely by solar heating of the stratospheric ozone layer.

We investigated the relative roles of large-scale tidal forcing and more local effects in accounting for the 12 h variation of tropical rainfall. A model of the atmosphere run with the daily cycle of solar heating artificially suppressed below the stratosphere still simulated a strong coherent 12 h rainfall variation (~50% of control run). This finding demonstrates that stratospherically forced atmospheric tide propagates downward to the troposphere and contributes to the organization of large-scale convection.

As an example, Figure 1 shows the daily cycle of rainfall over the Maritime Continent (Indonesia and its surrounding oceans). Observed rainfall (blue curve) shows two peaks, separated by roughly 12 hours, indicating of a 12 h variation. Modeling results with and without the daily cycle solar heating of ozone layer (red and black curves, respectively) show that the double peak of rainfall is accounted for only if the 12-hour atmospheric tidal wave, which is largely excited by the ozone heating, is included.

We found that a daily disturbance from the upper atmosphere leaves its footprints on tropical rainfall. The present results could also lead to the understanding of the excitation of tropical atmospheric waves by moist convection, to the evaluation of climate models, and to the understanding of the recently discovered lunar tidal rainfall cycle. [1]

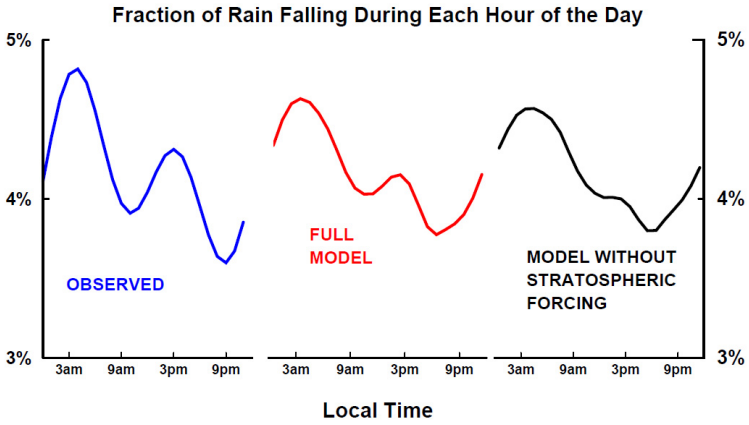

Figure 1. Fraction of the total rainfall, as a function of time of day, for a region including much of Indonesia and its surrounding oceans. Observations show strong peaks at early morning and mid-afternoon. Our modeling captures the observed modulation, only when upper atmospheric forcing that excites atmospheric tidal wave is included.

Acknowledgments

I thank the co-authors of this project, Keven Hamilton, Chunxi Zhang, and Yuqing Wang for their contributions. Figure 1 was produced with helps of K. Hamilton. I am supported by the Japan Society for Promotion of Science, Overseas Research Fellow.

Reference

[1] Sakazaki T., K. Hamilton, C. Zhang, and Y. Wang, “Is there a stratospheric pacemaker controlling the daily cycle of tropical rainfall?”, *Geophysical Research Letters*, 44, 1998-2006, doi:10.1002/2017GL072549, 2017.

RECENT RESEARCH ACTIVITIES

Three-dimensional tomography of the ionosphere over Japan based on GPS-TEC observations

(Laboratory of Radar Atmospheric Science, RISH, Kyoto University)

Mamoru Yamamoto and Hiroyuki Hashiguchi

Real-time information of the ionospheric electron distribution is important for the correction of the measurement errors in satellite navigation. We developed three-dimensional ionosphere tomographic analysis system under collaboration with Dr. Susumu Saito at Electronic Navigation Research Institute, Dr. C.-H. Chen at National Cheng Kung University (Taiwan), and Dr. Akinori Saito at Graduate School of Science, Kyoto University. The tomography is based on the GPS-TEC data from selected 200 stations of GOENET, and the analysis technique reported by Gopi et al. [1]. The developed system consists of four parallel processes; parallel decoding of BINEX binary data, estimation of instrument bias, two-dimensional fluctuated and absolute TEC distribution analyses and the three-dimensional tomographic analysis. The real-time tomography started in April 2016. The 3D ionospheric plasma distribution is obtained at every 15 minutes with about 6 minutes latency, and the results are open to public from http://www.enri.go.jp/cnspub/tomo3/ [2]. An example results on June 27, 2016 is shown in Figure 1.

We now try to improve this real-time system. The first point is to analyze past data. We keep the same way as to the real-time analysis. As the real-time system use 200 selected stations, we selected the same number of stations on January 1st of each year. Also, in order to improve computation speed of this analysis, we ported our analysis system to the super computer system A (Camphor 2) of Kyoto University. This super computer consists of 1800 nodes, and each node comprises 68 cores and 112GB of memory. We assigned 10-day data analysis to each node, and used 37 nodes to analysis one-year data. This whole one-year analysis takes about 10 hours, which corresponds to about 230 times improvement of the computation time. Also, in the future, we will enhance our analysis area by including data from Korea and/or Taiwan.

References

[1] Seemala, G. K., Yamamoto, M., Saito, A. and Chen, C.-H.: Three-dimensional GPS ionospheric tomography over Japan using constrained least squares, *J. Geophys. Res. Space Phys.*, **119**, 3044-3052, 2014.

[2] Saito, S., S. Suzuki, M. Yamamoto, C.-H. Chen, and A. Saito, Real-time ionosphere monitoring by three-dimensional tomography over Japan, *J. Inst. Navig.*, in press, 2017.

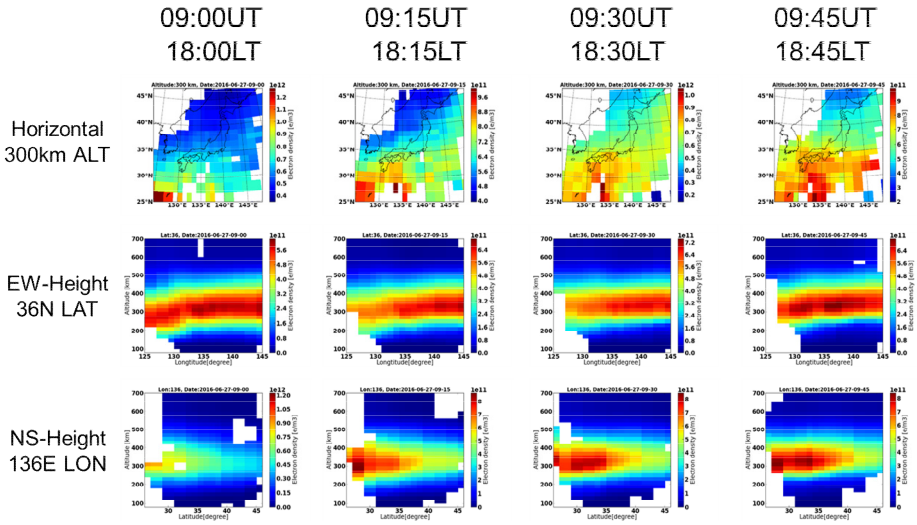

Figure 1: Example of real-time 3D tomography of the ionospheric plasma density over Japan. The real-time analyses are conducted at every 15 minutes with about 6 minutes latency [2].

RECENT RESEARCH ACTIVITIES

Diversity in reproductive strategies is likely linked to invasion success of ants

(Laboratory of Ecosystem Management and Conservation Ecology, RISH, Kyoto University)

Chin-Cheng (Scotty) Yang

A number of mechanisms/traits have been proposed to explain successful invasion of ants, reproductive strategy, however, receives relatively less attention simply because most of studies have focused on supercolony, unicoloniality and competitive superiority as underling mechanisms. To strengthen our understanding, my laboratory has been devoting research efforts on characterizing the association of diversity of reproduction modes and success of invasive ants in recent years. Here I would like to briefly summarize recent findings from our laboratory regarding this particular topic.

Worker reproduction in yellow crazy ant

We reported recently that workers of invasive yellow crazy ants (*Anoplolepis gracilipes*) are capable of reproducing regardless queen presence or not [1]. Observation indicated that a very high proportion of worker-produced eggs serve as a main food source for certain groups of colony members, especially for larvae of early instar whose diet relies exclusively on the worker-producing eggs (Fig. 1). These findings suggest that worker reproduction may have played a role in provisioning vital protein nutrition in the colony. Data are being collected to empirically demonstrate how invasion of *A. gracilipes* is facilitated by the worker reproduction.

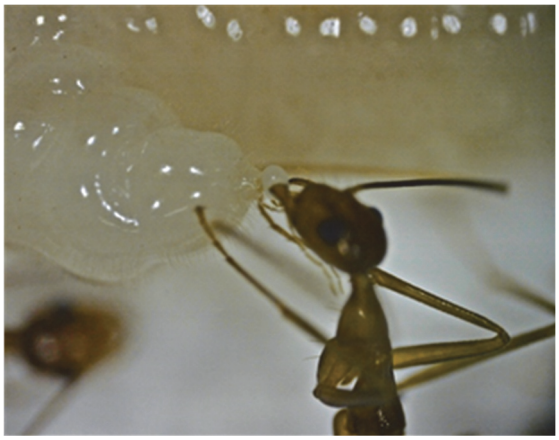

Figure 1. A worker of yellow crazy ant is feeding an egg to a queen-destined larva. Note this egg is infertile and is predominately produced by an ant worker. As such type of eggs generally serves as food for colony members, it is also termed ‘‘trophic egg’’.

Parthenogenesis of exotic *Strumigenys* ants

Strumigenys rogeri Emery1890, originating from Africa, has been considered as a widespread tramp species as this ant is found distributed in numerous non-native ranges including Taiwan. We found that queens of this ant species reproduce asexually throughout where they were collected in Taiwan [2]. Furthermore, unmated queens are able to produce both workers and young queens (asexually) under laboratory conditions in as short as 39 days. These findings suggest that asexual reproduction may have helped this tramp ant overcome some invasion barriers that otherwise may prevent their establishment and subsequent dispersal in Taiwan and elsewhere.

Acknowledgements

I would like to express the sincerest gratitude to the Future Development Funding Program, Kyoto University Research Coordination Alliance (KURCA) for its financial support.

References

[1] Lee CC, Nakao H, Tseng SP, Hsu HW, Lin GL, Tay JW, Billen J, Ito F, Lee CY, Lin CC, Yang CC. Worker reproduction of the invasive yellow crazy ant *Anoplolepis gracilipes*, *Frontier in Zoology*, 14, 24, 2017a. (doi: 10.1186/s12983-017-0210-4)

[2] Lee CC, Hsu SF, Yang CC, Lin CC. Thelytokous parthenogenesis in invasive dacetine ant *Strumigenys rogeri* (Hymenoptera: Formicidae) in Taiwan. *Entomological Science*, 2017b. (in press)

RECENT RESEARCH ACTIVITIES

Novel process for fabricating high-modulus cellulose-based products

(Laboratory of Active Bio-based Materials, RISH, Kyoto University)

Kentaro Abe and Hiroyuki Yano

Cellulose is the most abundant natural polymer on earth. It is insoluble in water because of its inter- and intra-molecular hydrogen bonds and it occurs in plant cell walls in the form of crystalline nanofibers, the so-called cellulose microfibrils. Since this stable structure prevents it from dissolving even in common organic solvents, the fabrication of cellulose-based films and textiles often requires the use of special solvents. For example, toxic carbon disulfide has been used to prepare regenerated cellulose films, also known as Cellophane. However, the dissolution and regeneration processes deteriorate the Young's modulus of cellulosic products because of crystal conversion from Cellulose I to Cellulose II.

This study proposes a novel process for fabricating high-modulus films based on cellulose nanofibers. Instead of dissolution process, dried pulps were mechanically disintegrated into nanofibers in NaOH solutions. NaOH treatments loosened the hydrogen bonding between cellulose microfibrils in dried pulps. Furthermore, the preparation of a highly concentrated suspension (8%) of cellulose nanofibers using a ball-mill was attempted. In our previous study, a suspension containing a maximum of only 2% cellulose nanofibers was achieved by bead-milling because of high viscosity restrictions [1]. Therefore, in this study, a planetary ball-mill was used, which is a more powerful and effective piece of equipment for high viscous suspensions.

After ball-milling for 90 min a highly concentrated suspension (8%) of cellulose nanofibers with a uniform diameter of approximately 20–50 nm was prepared. The nanofiber suspensions prepared in the NaOH solution had both the crystal forms of Cellulose I and Cellulose II although Cellulose II gradually increased with increasing milling time. The suspensions were formed into hydrogels after neutralization and the formation of hydrogels is effective for the fabrication of cellulose nanofiber-based films. The hydrogel sheets were hot-pressed into thin films at 120 °C (Fig. 1). Young's modulus of the films was significantly higher compared to that of typical regenerated cellulose films due to some remaining Cellulose I (Table 1). Changes in the milling conditions and the apparatus used for nano-fibrillation need to be further optimized in order to maintain more cellulose I in the nanofibers leading to higher-modulus products. We believe that our method will facilitate the mass production of cellulose nanofibers as it also facilitates subsequent drying of hydrogels to fabricate films.

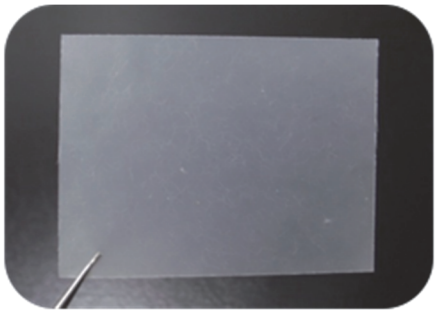

Figure 1. High-strength film based on cellulose nanofibers prepared by a ball-milling for 90 min in 8% NaOH solution.

Table 1. Average tensile property of cellulose nanofiber film prepared by a ball milling for 90 min in 8 % NaOH solution.

	Density (g/cm^3)	MOE (GPa)	MOR (MPa)	Break at strain (%)
8 %NaOH 90 min	1.46	9.3 (0.4)	100.2 (3.6)	2.4 (0.2)

Note: standard deviations are given in parentheses.

Reference

[1] Abe K, *Cellulose*, **23**, 1257-1261, 2016.

RECENT RESEARCH ACTIVITIES

Recent studies on production of sustainable materials by using natural resources

(Laboratory of Sustainable Materials, RISH, Kyoto University)

Soichi Tanaka, Kenji Umemura, and Kozo Kanayama

One of the main theme in our laboratory is the substitution of the fossil resource-based materials by the natural resource-based ones. In this article, the recent studies on the theme were introduced from the viewpoint of the promotion of usage of the fiber material derived from plant, and of the development of the adhesives (or the binder) derived from natural resources.

Promotion of usage of fiber material derived from plant

Though wood is the representative plant-derived material, its usage has been insufficient in terms of the reduction of fossil resource-consumption. It is required for the wider usage of wood to enhance the performance and reliability of wood and wood-based materials. Chemical treatment, or introduction of chemicals into wood, is one of the major methods for the enhancement. In the conventional treatment, however, distribution of chemicals in wood was irregular, leading to the inadequate performance and reliability. This irregularity can be categorized to macroscopic irregularity, indicating that the chemically treated wood includes the untreated cells in its structure; and microscopic irregularity, indicating that each cell includes the untreated regions in its amorphous structure. The macroscopic irregularity is mainly caused by the aspirated pits that disturb the flow of chemical solution in tracheid for coniferous wood. Then, we assumed that the water hammer phenomenon can be applied to reduce the macroscopic irregularity by penetrating the pits, which is now under examination. Meanwhile, for reducing the microscopic irregularity, focus was placed on the diffusion of chemicals into cell walls during conditioning, or process of evaporating solvent from wood impregnated with chemical solution. The microscopic irregularity was clarified to be controlled by the relative humidity and temperature during the conditioning [1].

Bast fiber of kozo (*Broussonetia kazinoki* × *B. papyrifera*) has been used as a raw material for Japanese paper, called washi. The supplement of the fiber, however, has been decreasing with the decrease in the production of washi. To increase the fiber supplement, focus was placed on the development of a new bast fiber-based material that can be used in huge industries (e.g. automotive industry). It was required for such a material to have high rigidity and strength. In our study, the process of producing the fiber board was applied to produce the fiber material derived from kozo-bast fiber. It was indicated that the long fiber unique to kozo made it difficult to control the strength and Young's modulus, which may be related to the difficulty in controlling the arrangement of the long fiber in the materials.

Development of adhesives derived from natural resources

In our previous research, the feasibility of applying natural raw materials to the adhesive for wood-based materials has been studied. The mixture of sucrose and some other natural materials (citric acid, ammonium dihydrogen phosphate (ADP), or wattle tannin) was confirmed to act as the adhesive, in which the attribution of the caramelization of sucrose was indicated. In our recent study, to improve the low pH and mechanical properties of the particle board bonded with sucrose-ADP mixture, the calcium carbonate was added to the mixture. The feasibility of using the mixture of sucrose and ammonium nitrate (AN) as a new natural adhesive was also investigated. Bagasse of sweet sorghum (*Sorghum bicolor* L. Monech), known as an agricultural waste, has been also regarded as a fiber materials, and thus the utilization of the bagasse and citric acid for manufacturing of particleboard was also studied in recent years [2].

References

[1] Tanaka, S., M. Seki, T. Miki, K. Umemura, and K. Kanayama, "Solute diffusion into cell walls in solution-impregnated wood under conditioning process IV: effect of temperature on solute diffusivity," *Journal of Wood Science*, DOI 10.1007/s10086-017-1658-8.

[2] Kusumah, S. S., K. Umemura, K. Yoshioka, H. Miyafuji, and K. Kanayama, "Utilization of Sweet Sorghum Bagasse and Citric Acid for manufacturing of particleboard I: Effects of pre-drying treatment and citric acid content on the board properties," *Industrial Crops and Products*, vol. 84, pp. 34-42, 2016.

RECENT RESEARCH ACTIVITIES

Structural Investigation for Development of CLT Construction Method

(Laboratory of Structural Function, RISH, Kyoto University)

Akihisa Kitamori and Hiroshi Isoda

1. Introduction

Toward establishment of sustainable society, the higher engineered technique for wooden buildings of low environmental impact has been attracted attention such as Cross-laminated timber (CLT), which can effectively utilize low-quality wood materials and enables to compose a reasonable wall structure. Due to progress of research on materials and construction methods, it has become possible to design those CLT buildings by general methods in recent years.

Figure 1. Two types of CLT construction methods.

Two types of structure systems have been developed for CLT building; its wall structure is composed by assembling of narrow size panels (Figure1, left) or by large size panels with openings (Figure1, right). The former enables to acquire a high ductility due to metal connectors, while the latter generally has high strength performance and easy construction characteristics.

2. Research Subjects

We have focused on the research of CLT building in terms of following subjects for example.

1) **Estimation of in-plane bending strength of CLT member** is trying to develop a simulation model for determining the allowable strength. The influence of defects such as knot and finger joint distributed on each layer and also the lamination effect which is a reinforcement due to cross laminate layer are taken into consideration in the model. This research aims to provide the proper estimation for the in-plane mechanical property of CLT which is important when used as vertical structural element such as shear wall.

2) **Clarifying the load carrying mechanism of shear wall CLT panel** conducts an analytical approach of FEM by focusing on the crash behavior at the bottom of the CLT wall panel due to stress concentration around the connector hole. The influence of vertical load which becomes significant when in the mid-rise building subjected to seismic load is the major point of interest. The digital image correlation method is also employed in order to obtain the stress distribution.

3) **Evaluation of in-plane shear property of CLT wall panel with opening** is studying the influences of stress concentration at the in-corner of opening. L and T shaped specimens with various size configurations were employed for the static tests, and the bending stress distribution of non-linear shape along the cross section was observed. Then the reduction factor of shear strength was calculated in combination with the effect of rolling shear property obtained by the test.

3. Future Plan

CLT construction system is progressing. Different type of metal connectors have been developed and need to be evaluated. Long-term phenomena or durability of CLT construction is also important subject of research. Besides, combination use of CLT with steel or reinforced concrete structure as composite structure system is also highly expected. Taking above into consideration, we are conducting research aimed at further expanding utilization of CLT.

Figure 2. Experiment examples by research subjects (1)-(3)

RECENT RESEARCH ACTIVITIES

Microstructural analysis of carbon composite from phenolic resin and cellulose nanofiber

(Laboratory of Innovative Humano-Habitability, RISH, Kyoto University[1], Lignyte Co., Ltd.[2], Research Center for Biomaterials, LIPI[3])

Yoshikazu Onishi[1, 2], Toshimitsu Hata[2], Isamu Ide[2], Subyakto[3], and Yusup Amin[3]

Carbon materials with high specific surface area have been used in various fields such as CO_2 gas adsorbent, and electrodes for electric double layer capacitors. The micropores and mesopores of the carbon have great influence on the property of the materials. Micropores less than 2 nm are suitable for CO_2 adsorbent. On the other hand, micropores contribute to the improvement of capacitance, and mesopores contribute to rapid charge / discharge performance in EDLC. Controlling microstructure of carbon material is important because of the dependence of pore size distribution on the required property.

We have conducted microstructural analysis on carbon materials from thermosetting phenol resin. We have prepared carbon composites of phenol resin and cellulose nanofiber (CNF), which is one of the wood components in order to develop porous carbon materials from phenol resin. CNF is renewable resource and porous structure is uniformly formed. In this study, carbonization and activation treatment were carried out by adding potassium hydroxide to composite of phenolic resin and CNF at the same time. The microstructure of obtained carbon composite from phenolic resin and CNF was observed with transmission electron microscopy (TEM).

Phenol, CNF, formaldehyde, and hexamethylene-tetramine were mixed in a reaction vessel. The temperature was kept at 85°C during stirring for 1 hour. Potassium hydroxide, KOH aqueous solution with 50 % was added to the sample and stirred for 30 minutes, and then moisture was removed in a vacuum condition. The obtained residue was dried at 120°C for 24 hours to obtain carbon precursor of phenolic resin and CNF composite containing KOH. The obtained carbon precursor was heat-treated at 800°C for 1 hour. The microstructure of carbon composite of phenolic resin and CNF was observed with TEM.

TEM image of carbon composite of phenolic resin and CNF is shown in Fig. 1. Fig. 1(a) shows the region of the carbonized phenolic resin and Fig. 1(b) shows that of carbonized CNF. Carbonized phenolic resin seems to have relatively large pores compared to those observed for carbonized CNF, in which fibrous texture was observed with oriented state. Smaller pores compared to those of phenol resin were observed. From this result, it is confirmed that the pore diameter developed in the carbon composite differ between the region of phenolic resin and CNF even if the same activator was used.

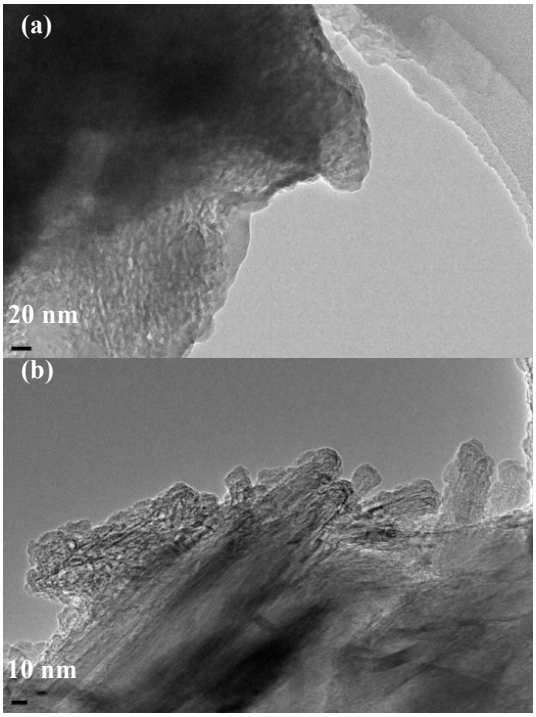

Figure 1. TEM image of carbon composite of phenolic resin and CNF. A: region of carbonized phenolic resin, B: region of carbonized CNF.

From the TEM observation, however, drastic change is necessary on pore structure corresponding to micropores and mesopores in order to get carbon composite of phenolic resin and CNF with high specific surface area.

RECENT RESEARCH ACTIVITIES

Simulations and Modeling of Geospace Environment

(Laboratory of Computer Space Science, RISH, Kyoto University)

Yoshiharu Omura, Yusuke Ebihara, and Satoko Nakamura

We have conducted a series of test particle simulations of obliquely propagating whistler mode wave-particle interaction [1], showing that the perpendicular wave electric field can play a significant role in trapping and accelerating relativistic electrons through Landau resonance. A further theoretical and numerical investigation verifies that there occurs nonlinear wave trapping of relativistic electrons by the nonlinear Lorentz force of the perpendicular wave magnetic field. We have performed a subpacket analysis of chorus waveforms observed by the Van Allen Probes [2], and calculated the energy gain by the cyclotron acceleration through Landau resonance. We compare the efficiencies of accelerations by cyclotron and Landau resonances in typical events of rapid electron acceleration observed by the Van Allen Probes. By performing test particle simulations of relativistic electrons scattered by electromagnetic ion cyclotron (EMIC) rising tone emissions, we find a nonlinear scattering process named SLPA (Scattering at Low Pitch Angle) totally different from the nonlinear wave trapping. The nonlinear wave trapping, occurring for high pitch angles away from the loss cone, scatters some of resonant electrons to lower pitch angles, and a fraction of the electrons is further transported into the loss cone by SLPA after being released from the wave trapping [3].

Geomagnetically induced currents (GIC) is known to be hazardous to the power grid system. When great magnetic storms occur, the magnitude of GICs increases in particular at high latitudes where auroral electojet flows in the ionosphere. Previously, the power grid system in Japan is regarded to be safe to the GICs because Japan is situated at geomagnetically low latitude. In order to assess whether the power grid system in Japan is definitely safe for extreme geomagnetic storms, we have conducted numerical simulations. First, we modeled propagation of the electomagnetic fields transmitted from the ionosphere to the ground by the Finite-difference time-domain (FDTD) method. A global relief model provided by NOAA and a global map of sediment Thickness provided by Gabi Laske and Guy Masters were incorporated to derive a three-dimensional electrical conductivity that is required to calculate the geomagnetically induced electric field (GIC). Secondly, we modeled the 500 kV power grid system consisting of >100 substations and power lines. From the requirement of continuity of the electric current, we calculated the GIC flowing in the power grid system in Japan for given GIE and the power grid model. Figure 1 shows an example of the simulation result. The distribution of GIC appears to be complex because of non-uniform ground conductivity, and uneven distribution of the power grid system.

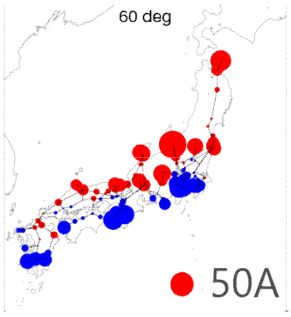

Figure 1. Example of simulated GIC in the power grid system in Japan. The radius of the circle represents the magnitude of GIC.

References

[1] Hsieh, Y.-K, and Y. Omura, Nonlinear dynamics of electrons interacting with oblique whistler-mode chorus in the magnetosphere, *J. Geophys. Res. Space Physics*, *122*, 675-694, 2017.

[2] Foster, J. C., P. J. Erickson, Y. Omura, D. N. Baker, C. A. Kletzing, S. G. Claudepierre, Van Allen Probes Observations of Prompt MeV Radiation Belt Electron Acceleration in Non-Linear Interactions with VLF Chorus, *J. Geophy. Res. Space Physics*, *122*, 324-339, 2017.

[3] Kubota, Y., and Y. Omura, Rapid precipitation of radiation belt electrons induced by EMIC rising tone emissions localized in longitude inside and outside the plasmapause, *J. Geophys. Res. Space Physics, 122*, 293-309, 2017.

RECENT RESEARCH ACTIVITIES

Human Safety on Electromagnetic Fields

(Laboratory of Applied Radio Engineering for Humanosphere, RISH, Kyoto University)

Junji Miyakoshi, Shin Koyama, Naoki Shinohara, Tomohiko Mitani, and Yohei Ishikawa,

We increasingly live in a roiling environment of electromagnetic fields (EMF). The main origins of this increase are the fast-rising use of cell phones and wireless local area networks together with the proliferation of cell phone base stations and other related facilities throughout the world. In the near future, they will likely be joined by a rapid proliferation of wireless power supplies. Accordingly, unease has grown among many people concerning the potential effects of these fields on health, the assessment of the EMF effect has therefore become a major social demand.

Research at this laboratory has focused on quantitative analysis of a clear response to EMF exposure at the cellular and genetic levels. The results of the assessments have been presented in regard to the occurrences and the mechanisms of EMF genotoxicity (e.g., chromosomal aberration, micronucleus formation and DNA damage), and the responses to EMF in gene expression and in signal transduction mechanisms [1]-[3]. As shown in Figure 1, for research performed to assess the biological effects of EMF, we construct an exposure system in a cell-culture incubator with wireless energy transmission by resonance power transmission, and then assess the cytogenetic toxicity involved in carcinogenicity and other effects of EMF. For assessment of EMF effects on immune function, a field of research recommended by the World Health Organization (WHO), we analyze cytokine secretion, phagocytosis, and other related activities. The results have become essential materials for discussions on EMF biological effects. Through our membership in WHO, the International Agency for Research on Cancer, and the International Commission on Non-Ionizing Radiation Protection, we have participated in and contributed to international conferences on EMF assessment.

The rapid increase in use of EMF will continue in the coming years with widespread utilization of noncontact energy transmission technology, including wireless power supply systems for stationary and moving electric vehicles. Given this trajectory, it is essential to determine the safety levels and elucidate the effects and mechanisms of EMF based on scientific data. This requires the advancement of related research and effective utilization of leading-edge life science technology.

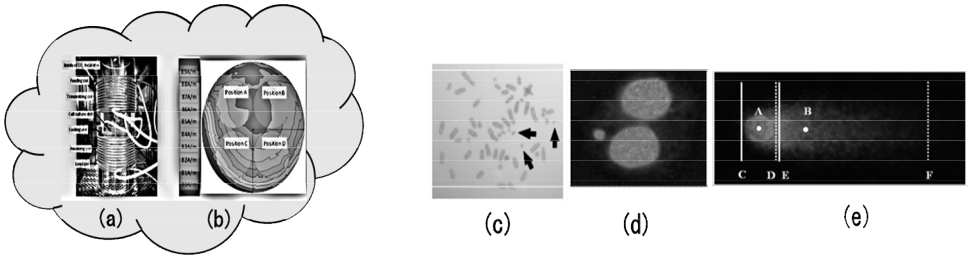

Fig. 1. Left:(a) Exposure system and (b) the distribution of electromagnetic fields; Right: Samples of genotoxicities, (c) chromosome aberration, (d) micronucleus, and (e) comet assay.

References

[1] K. Mizuno, N. Shinohara, J. Miyakoshi. Expression of heat shock proteins in human fibroblast cells under magnetic resonant coupling wireless power transfer. Energies 8, 12020-12028. (2015)

[2] K. Mizuno, N. Shinohara, J. Miyakoshi. In vitro evaluation of genotoxic effects under magnetic resonant coupling wireless power transfer. Int. J. Environ. Res. Public Health. 7;12(4):3853-63. (2015)

[3] S. Koyama, E. Narita, N. Shinohara, J. Miyakoshi. Effect of an intermediate-frequency magnetic field of 23 kHz at 2 mT on chemotaxis and phagocytosis in neutrophil-like differentiated human HL-60 cells. Int. J. Environ. Res. Public Health. 17;11(9):9649-59. (2014)

RECENT RESEARCH ACTIVITIES

Novel Space Environment Monitor, Instrument, and Space Mission Concepts

(Laboratory of Space Systems and Astronautics, RISH, Kyoto University)

Hiroshi Yamakawa, Hirotsugu Kojima, and Yoshikatsu Ueda

Space Debris Observation, Modelling, and Mitigation

The space debris problem is tackled from observation (space situational awareness), trajectory evolution, and mitigation points of view. 1) A method to identify the size, shape, and rotation, and to determine the trajectory of known space debris using range Doppler data of MU (Middle and Upper) Radar, RISH, Kyoto Universiry, is investigated with some successful observation results. 2) A study to investigate space debris trajectory evolution focusing on objects smaller than 1 cm has been started to shed light on geomagnetic field effects. 3) Space debris mitigation (orbit control) using Lorentz force by positive charging effect is studied. Lorenz force is based on the interaction between an electro-statically charged debris and the Earth's plasma environment. The orbit control method to decrease the altitude using Lorentz force is studied focusing on decreasing semi-major axis, enlarging eccentricity, and lowering perigee distance. 4) An on-orbit space debris observing system is studied assuming an optical sensor onboard a satellite. The required specifications of optical sensors and ranges of observable space debris are investigated for application to removal sequence.

Electromagnetic Space Propulsion Systems

Recently, new propulsion systems that utilize electromagnetic forces acting on a charged spacecraft were proposed. The Lorentz force that acts when a charged object goes across the Earth's magnetic field and the Coulomb force that acts on among the charged objects can be employed to control the orbit of charged spacecraft or space debris by controlling the electrostatic potential of the object with charged particle emitters. One of our studies is to evaluate feasibility and performance of such "electromagnetic orbital control" regarding both orbital dynamics and plasma physics by using numerical simulation on the super computer system of Kyoto University. We 1) proposed a new charging model that enables to compute the surface potential fast and precisely by considering a velocity distribution of emitted particles, 2) proposed a new secondary electron emission model for particle simulations that can simulate much like the actual physics than conventional methods, and 3) revealed the thrust performance of an electric solar wind sail, a novel propulsion system which obtains its thrust by deflecting the ions in solar wind with numerous positively charged tethers.

Miniaturization of plasma wave receiver system

Plasma wave receiver is one of the essential instruments for space environment exploration; however, conventional receiver has a problem in its large weight and size. In order to overcome this problem, we have been miniaturized plasma wave receiver by developing Application-Specific Integrated Circuits (ASIC) for plasma wave receivers. We succeeded in developing miniaturized plasma wave receiver by realizing analog circuit, which is especially large part of the receiver, using ASIC. This miniaturized receiver will be onboard the SS-520-3 sounding rocket, which will launch in the December of this year to resolve the cause of ion outflow phenomena at the cusp region. In addition, we aim to develop a mixed-signal ASIC chip for one-chip plasma wave receiver. The mixed-signal ASIC chip includes all analog and digital circuits for plasma wave receiver. One-chip plasma wave receiver allows to reduce weight and size of the instruments drastically, and it will contribute for increasing opportunities of plasma wave observation.

Quantitative evaluation of basic properties of nano bubbles in water

The electric and electrochemical performance of nano bubble (NB) in pure water, is reported herein. Recently, NB has found applications in various fields, However, the detailed mechanism underlying the performance of NB is not known, although the relevance of ions (proton and hydroxide ion) in solution has been discussed. Therefore, we investigated NB through electric and electrochemical measurements. First, we conducted a preliminary experiment in an nano bubble generator and a measuring device for the concentration of nano-particles. We also measured the electrical conductivity and found that the amount of flowing gas and the gas species did not influence the NB concentration.

ABSTRACTS (PH D THESIS)

Study of bacterial cellulose synthase by recombinant protein

**(Graduate School of Agriculture,
Laboratory of Biomass Morphogenesis and Information, RISH, Kyoto University)**

Shi-jing Sun

Functional analysis of cellulose synthase was conducted with recombinant protein. Given its easiness, bacterial cellulose synthase is used in this study. First of all, cellulose-synthesizing activity was successfully reconstituted in living cell of *Escherichia coli* by expressing the minimal required subunits CesA and CesB of *Gluconacetobacter*. Then this system, named as "CESEC (cellulose-synthesizing *E. coli*)" was used for checking enzymatic activity of point-mutants, for which site-directed mutagenesis was designed based on the structural model of bacterial cellulose synthase published in 2013 [1]. The obtained data were consistent with this model and previous data, and furthermore spotlighted the pivotal role of sulfur–arene interaction by cysteine in FFCGS motif and surrounding aromatic residues. However, the product of CESEC was a non-native structure of cellulose II, indicating that the reconstituted activity was incomplete or partially denatured. It is then absolutely required to find missing factor(s) for the native cellulose synthase activity. CESEC will be one of the tools useful for identifying such factors by reconstitution approach in following researches.

Introduction

In general, recombinant protein allows variable experiments to be conducted like site-directed mutagenesis and large scale production of protein. It is therefore a useful tool to analyze protein. Cellulose synthase is enzyme of hetero-subunit complex in cell membrane. Given high difficulty to handle membrane proteins with complex associated however, fewer studies have been conducted for cellulose synthase with recombinant protein, and then our understanding of cellulose biosynthesis is limited yet. In this thesis, recombinant cellulose synthase was intensively used for exploring its enzymatic mechanism.

Bacterial model was selected in this thesis given its convenience to use. First, cellulose-synthesizing activity was successfully reconstituted in living cell of *Escherichia coli* by conventional method of heterologous expression of protein. This system, which we named as "CESEC (cellulose-synthesizing *E. coli*), was then demonstrated to be useful tool for the study of cellulose synthase: effect of point-mutation to the activity was surveyed in order to explore catalytic reaction at the level of amino acid residue.

Reconstitution of cellulose-synthesizing activity in *E. coli* [2]

Expression vector of bacterial cellulose synthase was constructed by cloning *cesA* and *cesB* genes of *Gluconacetobacter xylinus* JCM9730, which are the minimally required subunits of bacterial cellulose synthase. These two genes are in a same gene cluster, and then introduced into the vector as it is, together with the upstream sequence of *cesA* gene (Shine-Dalgarno sequence or ribosomal binding site). In addition, c-di-GMP, a small cyclic nucleotide, is another essential factor for cellulose synthesis in bacteria. For producing c-di-GMP in the cell, expression vector of DGC (diguanylate cyclase or c-di-GMP synthase) was constructed by inserting the gene into pBAD33 vector, which can be maintained together with pQE. These two plasmid DNA were then introduced into an *E .coli* strain XL1-Blue (Figure 1) and then transformant by carrying both plasmids were selected by antibiotics.

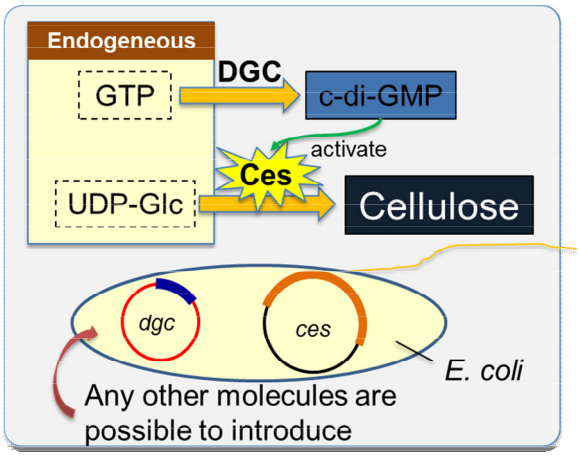

Figure 1. A schematic diagram of CESEC, cellulose-synthesizing E. coli

ABSTRACTS (PH D THESIS)

It was shown by western blotting that this *E. coli* transformant expresses CesA and CesB proteins in cell membrane correctly. As well, by LC/MS analysis, production of c-di-GMP in the cell was confirmed specifically when DGC was expressed. Finally it was shown that cellulose is produced by this *E. coli* transformant only when CesA, CesB and DGC protein was expressed, reconfirming that two proteins of CesA/ CesB and a nucleotide c-di-GMP are the required factors for cellulose biosynthesis in bacteria.

Analysis of the product in dried state demonstrated that synthesized cellulose was not in the native structure of cellulose I, but crystallized into cellulose II. However GPC analysis showed that weight-averaged molecular weight of the produced cellulose is as high as 700. These indicate that the reconstituted cellulose synthase still keeps the polymerizing activity but lacks crystallization (microfibril formation) mechanism. The reason for this partial denaturation has to be clarified for understanding the machinery to synthesize cellulose as microfibril with crystallographic polymorph I.

Functional analysis of CesA protein with site-directed mutagenesis [3]

The *E. coli* transformant established above uses conventional plasmid DNA for expressing cellulose synthase protein. It is accordingly easy to introduce any mutations to cellulose synthase for testing its effect to enzymatic activity. Then, several point mutants of CesA was prepared by site-directed mutagenesis for counting their cellulose-synthesizing activity to explore roles of amino acid residues in catalysis.

Mutation was designed on sequence similarity and structural model that was reported in 2013 [1]. A significant reduction of activity by mutation was observed when mutation matters (like s mutation of catalytic residue Asp333 to Asn), while an unexpected reduction of activity was found for a mild mutation of cysteine in FFCGS motif, which is well conserved in bacterial type CesA protein. Structural model in 2013 [1] spotlighted the “main chain” carbonyl of this cysteine as one of the keys to locate the molecular end of growing cellulose, which is the acceptor of glucosyltransfer reaction. Given this hypothesis, one can suppose that “side chain” of this cysteine could be replaced by other side chain unless the mutation is deteriorative. However, in addition to deteriorative mutations like valine or phenylalanine, mild mutation to alanine or even serine abolished cellulose-synthesizing activity. This indicates side chain thiol has an active role in catalysis. Probably sulfur–arene interaction between the side chain thiol and surrounding aromatic residues (Phe291, Tyr292, and Phe306) plays a role for cellulose-polymerizing reaction.

Concluding remarks

Cellulose synthesis is not only a chemical reaction to elongate glucan chain by successive transferring reaction, but also a physical reaction to assemble polymer chains into a supemolecular structure – cellulose microfibril. Cellulose-synthesizing activity reconstituted into *E. coli* in this study, CESEC, is a useful tool for studying biochemistry and biophysics of cellulose synthase to understand the mechanism of cellulose biosynthesis in molecular and supermolecular level.

Acknowledgements

LC/MS analysis was done with DASH system (CER and RISH, Kyoto University). Electron microscopic observation was done with ADAM system (RISH, Kyoto University).

References

[1] Morgan, J. L. W., Strumillo, J., Zimmer, J. 2013. Crystallographic snapshot of cellulose synthesis and membrane translocation, *Nature,* **493:** 181-186.

[2] Imai, T., Sun, S.-j., Horikawa, Y., Wada, M., Sugiyama, J. 2014. Functional reconstitution of cellulose synthase in *Escherichia coli*, *Biomacromolecules,* **15:** 4206-4213.

[3] Sun, S.-j., Horikawa, Y., Wada, M., Sugiyama, J., Imai, T. 2016. Site-directed mutagenesis of bacterial cellulose synthase highlights sulfur–arene interaction as key to catalysis, *Carbohydr.Res.,* **434:** 99-106.

ABSTRACTS (PH D THESIS)

Thermal Stabilization of Nanocellulose by Chemical Modification

(Graduate School of Agriculture, Laboratory of Active Bio-based Materials, RISH, Kyoto University)

Melissa Agustin

The utilization of cellulose has recently expanded into applications that take advantage of its deconstructed fibers, a material known as nanocellulose. Among the various applications of nanocellulose, its use as a reinforcing filler has drawn tremendous interest among researchers. The inherent excellent mechanical properties of crystalline nanocellulose, which was reported to be as strong as Kevlar, make it a good candidate as reinforcing filler in polymer composite preparation. The poor thermal stability of nanocellulose, however, limits its potential to reinforce polymer matrices with high melting points such as polyamide or polycarbonate. In order to expand the application of nanocellulose to reinforce polymer matrices with high melting points (>220oC), this study was conducted to improve the thermal stability of nanocellulose by chemical modification.

In Chapter 2, acetylation, which is the simplest and most commonly used chemical modification technique for cellulose, was carried out on bacterial cellulose (BC), which was chosen to eliminate the effect of hemicellulose. The effect of degree of polymerization (DP) on the thermal stability of BC before and after acetylation was studied systematically. BC with varying viscosity-average degree of polymerization (DPv, 1100, 500 and 300) were prepared by acid hydrolysis and were acetylated to a degree of substitution (DS) of about 0.4. Based on the results of thermogravimetric analysis (TGA), thermal stability decreased with decreasing DPv, which was attributed to the increase in the number of reducing ends (REs) as DPv decreased. Acetylation improved the thermal stability of BC and the degree of improvement increased with decreasing DP. Furthermore, it was found out that possible protection of reducing ends by acetyl group contribute to the high degree of improvement in thermal stability in BC with low DP.

The effect of the structure of the esters on thermal stability of nanocellulose was evaluated and the results were presented in Chapter 3. BC nanofibers (DPv of 1100) and nanocrystals (DPv of 300) were esterified to a DS of about 0.40 with various types of esters: short and long straight-chain; cyclic (adamantoyl, ADM); aromatic (benzoyl, BNZ); and branched (pivaloyl, PIV). TGA results showed that the temperature at maximum weight loss rate (Tmax) increased after esterification but the structure of the ester groups showed no varying effect on Tmax. Esters with straight aliphatic chain showed lower 5% weight loss temperature (WLT) than those of the bulky esters of ADM, BNZ, and PIV. Pyrolysis-gas chromatography-mass spectrometry analysis revealed that deprotection or the removal of the ester groups was found to be the main event occurring at the initial stage of thermal degradation of nanocellulose esters. From the structure and types of pyrolysis products, it was found that straight-chain esters deprotect by condensation reaction which was proposed to be driven by the presence of alpha hydrogens. Bulky esters of ADM, BNZ, and PIV which do not possess alpha hydrogens deprotect by direct ester bond cleavage. Deprotection by direct ester bond cleavage was found to require higher temperature than deprotection by condensation reaction, thus resulting to higher 5% WLT of ADM, BNZ, and PIV esters than those with straight chain esters.

The thermal stability of nanocellulose esters was further evaluated in Chapter 4 by investigating their resistance against thermally-induced depolymerization and discoloration. Films of BC esters with and without α-hydrogens were heated isothermally at various temperatures for 1h in nitrogen or in air. The changes in molecular weight distribution of the residual cellulose were evaluated by gel permeation chromatography. Results showed that esterification alters the rate of thermally-induced depolymerization of

nanocellulose. BNZ and PIV esters without α-hydrogens showed higher resistance against thermally-induced depolymerization than acetyl and myristoyl esters with alpha hydrogens, in nitrogen and in air. The resistance of BNZ and PIV esters against depolymerization was also complemented by its resistance against thermal discoloration. The delay of depolymerization translates to the inhibition of the formation of REs which can be active sites for thermal discoloration.

In Chapter 5, the effect of esterification on wood-based cellulosic pulps and nanofibers (WCNF) were investigated to understand the effect of hemicellulose on thermal stability. The degree of improvement in thermal stability of wood-based pulps is a function of DS. Esterification to a DS of 0.3 yielded esters with lower thermal stability than those esterified to a DS of 0.6, which must have completely esterified the hemicellulose. Similar to BC, BNZ and PIV esters of pulps also showed higher weight-loss resistance than those with straight-chain esters. Because of the higher reaction rate of benzoylation over pivaloylation, benzoylation was chosen to modify WCNF. Benzoylated WCNF showed higher resistance against thermal weight-loss and thermally-induced depolymerization and discoloration than the untreated WCNF.

Finally, in Chapter 6, the overall findings of the study were summarized. The thermal stability of nanocellulose can be improved by esterification with ADM, BNZ, and PIV; which do not possess alpha hydrogens. Despite the presence of amorphous hemicellulose, the thermal stability of benzoylated wood-based cellulosic pulps can be comparable to that of benzoylated BC nanofibers. On the other hand, the thermal stability of benzoylated WCNF was only comparable to that of the BC nanocrystals with a DPv of 300. Even though a high degree of improvement in thermal stability of low-DP nanocelluloses (BC nanocrystals and WCNF) can be achieved after esterification, the esterified low-DP nanocelluloses cannot surpass the thermal stability of esterified high-DP nanocelluloses. It is therefore recommended to optimize the preparation of nanocellulose, in a way that will minimize depolymerization, so that subsequent chemical modification will be more effective.

ABSTRACTS (PH D THESIS)

Nesting Biology of the Drywood Termite, *Incisitermes minor* (Hagen)

**(Graduate School of Agriculture
Laboratory of Innovative and Humano-habitability, RISH, Kyoto University)**

S. Khoirul Himmi

The invasive drywood termite, *Incisitermes minor* (Hagen) (Isoptera: Kalotermitidae) is considered to be the most destructive drywood termite in the western United States (USA). The colonies live entirely within a single piece of wood. Because of this hidden ecology, *I. minor* can be easily transported around the world within an infested piece of wood as a result of human activities. Originally from the southwestern USA and northern Mexico, infestations of this invasive species have been reported in Canada, China, and Hawaii, and more than half of the prefectures in Japan. The cryptic lifestyle of drywood termites makes it difficult to study their foraging behavior and to detect infestations in wood. In recent years, X-ray Computed Tomography (CT) has been developed as a reliable indirect method to analyze termite nests without damaging.

The present study aims to elaborate the nesting biology of *I. minor*, focusing on the observation of initial nest-founding in natural environment and X-ray computed tomographic (CT) analysis of the nest-gallery systems of *I. minor*.

Evaluation of initial nest-founding by *I. minor* reproductives

The evaluation of initial nest-founding of *I. minor* reproductives following the nuptial flight was conducted on six commercial timber species. The timbers included three Japanese timbers, hinoki (*Chamaecyparis obtusa* Endl.), karamatsu (*Larix leptolepis* Gord.), and sugi (*Cryptomeria japonica* D. Don), and three USA timbers, Douglas-fir (*Pseudotsuga menziessi* Mirbel), western red cedar (*Thuja plicata* Donn ex D. Don) and spruce (*Picea sitchensis* Bong. Carriere). The infested timbers were recorded in detail by identifying position of excavated holes on timbers (sapwood, heartwood, and border line of sapwood and heartwood), and the location of excavated holes on timber set-up (closed gap (CG) area, open gap (OG) area, cross-sectional surface (CS) area, bottom surface (BS) area, and upper surface (US) area of the timbers).

The results suggested that *I. minor* reproductives showed timber preferences in establishing the royal chamber to initiate the colony. The order of preferred timber species was as follows: hinoki, spruce, western red cedar, sugi, Douglas-fir, karamatsu. The current results showed nesting preferences among these six commercial timbers corresponded to previous report on feeding preferences. The reproductives of *I. minor* expressed nest-site selectivity on a preferred part of the timbers, i.e, on the springwood part of the annual growth rings on the sapwood part of the timbers. The reproductives of *I. minor* also showed selectivity in determining their nest-site location in response to the timber arrangement, namely by preferring the CG area. The results corresponded to previous reports which suggested that *I. minor* royal pairs like wood cracks, crevices or holes as sites at which to excavate the first royal chamber.

X-ray CT analysis of the nest-gallery systems of *I. minor*

We conducted CT scan to capture the structure of initial chambers excavated by *I. minor* as part of nest-founding activities and foraging; to observe first year development of the chambers; to monitor colonization process of foraging groups of *I. minor* in extending the nest-gallery to previously unoccupied timber; and to visualize how drywood termites establish and maintain their nest-gallery systems in response to the internal structure of fibers, growth rings and other anatomical properties of timbers. The selected timbers were imaged using an X-ray CT apparatus (Y.CT Modular320 FPD, YXLON International GmbH, Germany) maintained at Kyushu National Museum. The X-ray data obtained during the scanning process will be stored in files containing two-dimensional (2D) image stacks (*.raw image file), with each file representing a single 2D image-slice of the timbers. The 2D CT image stacks for each timber will be rendered into 3D images (each 2D image slice was 0.3 mm in thickness) by using volume graphics

software (VGStudio MAX 2.1, Volume Graphics GmbH, Germany).

The structure of initial chamber excavated by the royal pair of *I. minor* resembled European pear-shape and cashewnut-shape, in response toward timber anatomical properties. Those chambers were established in the springwood of the sapwood, and were carefully excavated beneath the surface to follow the direction of annual growth rings, and avoided the summerwood. *In situ* observation of the first year development of initial chambers suggested that royal pairs of *I. minor* can start breeding new colony members in the first six months, and by the end of the first year, an incipient colony can have 0 – 5 new members. The development of royal chambers in the first year showed a preference for the springwood part of the particular growth rings where the entrance holes were excavated.

We also evaluated the structure of initial chamber which was established by group of foragers, mediated by the foraging activities of individuals that attacked adjacent surface of a new timber. The result indicated that drywood termite has greater foraging flexibility in response of environmental conditions. In extending the nest-gallery, *I. minor* also expressed selectivity in foraging by selecting favorable excavation areas, and showed adaptability with respect to the timber environment. In the absence of primary reproductives, the colony showed dynamic change in its caste composition through the emergence of replacement reproductives. The results also suggested that replacement reproductives can emerge from the pseudergate stage. However, the sexes of the replacement reproductives, the time interval before they emerge and the suitable conditions required to facilitate the emergence of replacement reproductives are not yet fully understood.

During colonization and foraging within wood, the internal structures of fibers and growth rings and other anatomical properties influenced the way drywood termites established their nest-gallery. The nest-gallery excavations demonstrated continual adaptation by foragers to anatomical constraints in selecting favorable areas of less dense wood fiber inside the timbers. The colony also exhibited defense mechanisms with which to protect the colony, such as by sealing a tunnel leading to the outer environment using cement pellets. The sticky hydrated pellets were observed in the chambers inside the nest-gallery, even in the first six months of new nest establishment.

ABSTRACTS (PH D THESIS)

Evaluation of the Nutritional Requirement and Wood Decay Properties of a Termite Mushroom, *Termitomyces eurrhizus*

**(Graduate School of Agriculture,
Laboratory of Innovative Humano-habitability, RISH, Kyoto University)**

Kazuko Ono

The *Termitomyces eurrhizus* mushroom has high potential market value. The fungi in this genus are called "termite mushrooms", and have a symbiotic relationship with Mactotermitinae termites. Since to date, most researchers have been focused on this symbiotic relationship, the biological and physiological properties of the fungi themselves are less understood. The purpose of this study was to evaluate the possibility of artificial cultivation of *T. eurrhizus* by examining the nutritional characteristics of the fungus.

Fig. 1. The fruit bodies of *T. eurrhizus* from the comb in the termite nest

Screening of strains and media of *T. eurrhizus* collected in Japan

Strains of *T. eurrhizus* collected in Okinawa Prefecture were screened for the following experiments. Four strains were selected from 27 strains. Strain T3, collected from Okinawa Main Island, had low media specificity and grew tractably. Strain T11 from Ishigaki Island was easy to handle, with a medium growth rate on any media. Strain T25, collected from Iriomote Island, had low media specificity and grew fast, while T26 from Iriomote Island grew very fast on any media.

Effects of carbohydrate substrates on vegetative mycelial growth of *T. eurrhizus*

Effects of carbohydrate substrates on the mycelial growth of *T. eurrhizus* were surveyed using 4 strains. Thirteen carbohydrates were tested in this experiment, and all the 4 strains showed the most rapid growth on the fructose- and maltose-containing media. In addition, all the 4 strains grew positively on mannose-, sucrose- and trehalose-containing media. *T. eurrhizus* might utilize starch and cellulose similarly, and demonstrated a poor ability to catabolize lactose.

Wood decaying properties of *T. eurrhizus*

The decay properties of *T. eurrhizus* were examined. Three softwood species, akamatsu (*Pinus densiflora)*, sugi (*Cryptomeria japonica)* and hinoki (*Chamaecyparis obtuse)*, and two hardwood species, buna (*Fagus crenata)* and konara (*Quercus miyagii)*, were used as wood specimens. Scanning Electron Microscope (SEM) observations suggested that *T. eurrhizus* could only attack the surfaces of small wood samples (1.0 (R) × 1.0 (T) × 0.5 (L) cm). There was no significant difference in mass-loss rate between heartwood and sapwood specimens exposed to *T. eurrhizus* for 12 weeks. Moreover, the mass loss rates of

ABSTRACTS (PH D THESIS)

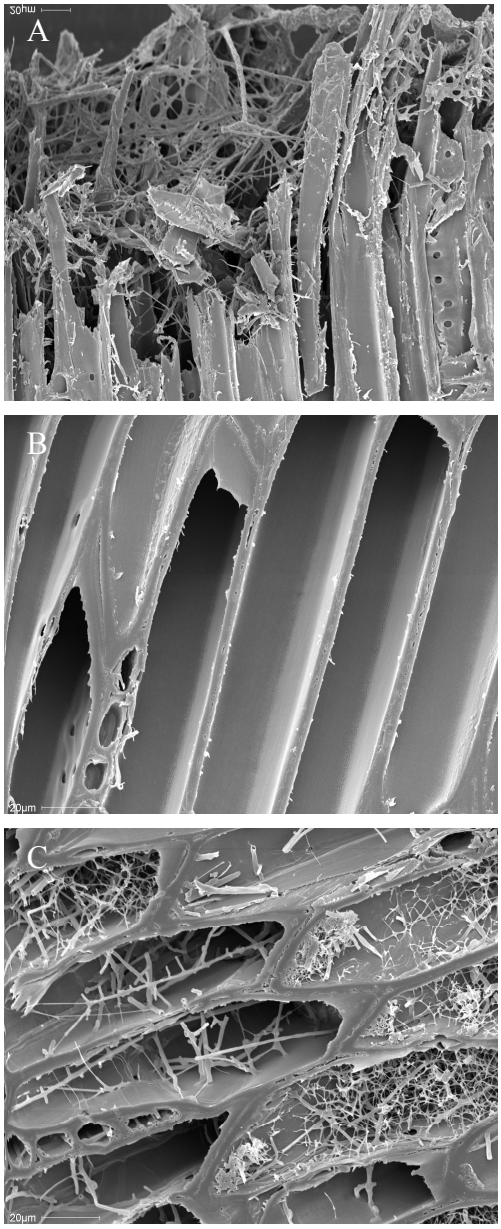

Fig. 2. SEM images of decayed wood samples of sapwood of sugi (*Cryptomeria japonica)*
A: The surface of sample decayed by *T. eurrhizus*
B: Core sample decayed by *T. eurrhizus*
C: Core sample decayed by *Trametes versicolor*

softwood specimens were generally higher than those of hardwood specimens. Chemical analyses of decayed wood specimens suggested that *T. eurrhizus* does not have high lignin-degradation ability, even though it has been categorized as a white-rot fungus.

Decay properties of *T. eurrhizus* on moso bamboo (*Phyllostachys edulis*)

Decay property of the fungus against moso bamboo, *Phyllostachys edulis*, was investigated. *T. eurrhizus* preferentially catabolized free sugars in the bamboo. The bamboo showed a high concentration of starch (approx. 1%), which the fungus found difficult to utilize.

Laccase activity in *T. eurrhizus*

The existence of laccase, one of lignin decomposing enzymes, was detected using Bavendamm test. This is a simple detection method of phenol-oxidase activities. *Termitomyces eurrhizus* strains did not show positive results except for one strain. The results suggested that *T. eurrhizus* has laccase but its activity is very weak.

From the results of these experiments, the use of fine wood chips or sawdust is strongly recommended as a media matrix for the artificial cultivation of *T. eurrhizus*. Wood species with lower lignin content are more favorable. Fagaseae trees such as Japanese beech (*Fagus crenata*), which are preferentially used for the media matrix of mushroom production in Japan, would not be suitable for *T. eurrhizus*. On the other hand, sugi (*Cryptomeria japonica*) and moso bamboo (*Phyllostachys edulis*), which are the most easily obtained forest resources in Japan, have been suggested as possibilities for use as a media matrix for *T. eurrhizus*.

ABSTRACTS (PH D THESIS)

A study of foraging behavior and physiological adaptation of western drywood termite: a framework for development of novel bandage system

**(Graduate School of Agriculture,
Laboratory of Innovative Humano-habitability, RISH, Kyoto University)**

Choi BaekYong

The western drywood termite, *Incisitermes minor* (Hagen), is one of invaded insect species, and was firstly reported in Japan in 1976. Since that date, 24 out of 47 prefecture have been infested by *I. minor*.

With current pest management industry standard for detection/inspection (visual searching) and remedial treatment (wood injection), it is hard to prevent drywood termite infestations for some reason including; 1) the lack of knowledge of foraging behavior and biological adaptations of drywood termites that involve survival in environmental stresses and 2) the high proportion of remedial intervention which only intends to kill drywood termites present at the time of application, whereas no preventive treatment which intends to stop or prevent reinfestation. Consequently, the drywood termite management should understand the foraging behavior and biological adaptations of drywood termites to provide a framework for improving efforts at detection and control when treatment is necessary

Quantitative observation of the foraging tunnels in Sitka spruce ad Japanese cypress caused by the drywood termite *I. minor* by 2D and 3D X-ray computer tomography (CT)

The cryptic lifestyle of drywood termites makes it difficult to study their foraging behaviour and to detect infestations in hidden regions. As CT scanning results show, the development of tunneling is affected by the physical constraints of knows with their high density, high extractive, and lignin contents. Based on these factors, foragers caused distinguished tunneling patterns based on the physical properties of wood during gallery construction. The Foragers primarily excavate along the earlywood in radial direction towards the outer surface of the wood to establish the primary and satellite chambers, followed by mainly superficial longitudinal expansion with occasional lateral deviations. These unique foraging patterns aid the development and optimization of the application of new remedial treatment using solid carbon dioxide as a chilling agent.

The role of physiological elements on cold tolerance of *I. minor*

Unlike endothermic animals, termites regulate the body temperature by the temperature of the environment evolving a diversity of competitive biological adaptation to ensure the survival under non-optimal temperature. This present section investigated on the correlation between genetic advance physiological elements and cold tolerance of three most widely distributed pest species in Japan: *Reticulitermes speratus* (Kolbe), *Coptotermes formosanus* Shiraki, and *I. minor*. First, to estimated and compared the SCP and the LLT of tested termite species using an ultra cooling freezer. Second, to measure the biological variations in an individual group of termite species to compared and identified correlation between the natural cryoprotectants and cold tolerance of three structural pests in Japan.

Table 1. Mean wet and dry mass, water relations, CP, and total lipid composition (mean ± SE) of three termite species

Elements	*I. minor*	*C. formosanus*	*R. speratus*
Wet body mass (mg)	9.96 ± 0.17^{a}	3.07 ± 0.02^{b}	2.08 ± 0.03^{c}
Dry body mass (mg)	2.78 ± 0.04^{a}	0.64 ± 0.01^{b}	0.41 ± 0.01^{c}
TBW content (%)*	72.0 ± 0.6^{c}	78.6 ± 0.5^{b}	80.1 ± 0.3^{a}
Low RH − CP** ($\mu gH_2O\ cm^{-2}\ h^{-1}\ mmHg^{-1}$)	(M) 2.11 ± 0.04^{b} (H) 3.36 ± 0.09^{b}	(M) 28.67 ± 0.67^{a} (H) 42.13 ± 0.86^{a}	(M) 31.26 ± 0.67^{a} (H) 42.04 ± 0.90^{a}
Body lipid (% of dry weight)	28.45 ± 0.53^{a}	17.32 ± 0.42^{c}	19.93 ± 0.49^{b}
Cuticular lipid (% of dry weight)	17.97 ± 0.41^{a}	9.10 ± 0.21^{b}	7.28 ± 0.25^{b}
Trehalose (% of dry weight)	0.28 ± 0.03^{c}	1.35 ± 0.3^{a}	1.04 ± 0.15^{b}
SCP (°C)	-12.6 ± 0.3^{a}	-9.3 ± 0.2^{b}	-5.7 ± 0.2^{c}
Heat of crystallisation (°C)	$\leq 0.8^{a}$	$\leq 0.3^{b}$	$\leq 0.2^{b}$
Heat of crystallisation (Sec.)	77 ± 4^{a}	30 ± 3^{b}	23 ± 2^{c}
LLT_{50}(°C)	-14.0 ± 0.2^{a}	-10.2 ± 0.2^{b}	-6.3 ± 0.1^{c}
LLT_{95}(°C)	-22.1 ± 0.2^{a}	-12.6 ± 0.1^{b}	-9.8 ± 0.2^{c}

Mean in the same column followed by different letters are significantly different ($P < 0.05$, ANCOVA, Tukey's HSD)
*wet weight **cuticular permeability
(M) denotes surface area estimation using Meeh's formula, (H) denotes surface area estimation using Haagsma's formula

Unlike subterranean termites, western drywood termites cannot retreat from unfavourable conditions when it is necessary to escape. It is therefore not unreasonable to assume that the desiccation and cold

hardiness tolerance of *I. minor* could be higher than subterranean termite species. Of the low temperature stresses that *I. minor* can overcome by a genetic advance in physiological elements such as water relation and cuticular structure. The SCP varied between -10.5 and -14.5°C while LLT ranged from -13.9 and -14.8 °C for LLT_{50} and below -22.0°C for LLT_{95}. Cold tolerance may influence by some physiological elements including low body water content and harder cuticle structure. As known termite cryoprotectant, trehalose, there was no clear indication that it function as a natural cryoprotectant in *I. minor*. Low concentration of trehalose may affect by their heritage physiological ecology.

Investigation of thermal conductive properties of structural timbers at low temperature region using solid carbon dioxide as a chilling agent

Knowledge of the thermal conductive properties of wood at low temperatures aids the development and optimization of the application of a lethal cold temperature treatment for drywood termites. This section explains the relationship between the thermal conductive properties of wood at low temperatures and important factors, the microstructural and anisotropy of wood.

The results indicate that the thermal conductive properties of wood at low temperatures are mainly affected by the composition and morphological properties of wood (i.e., density/ratio of earlywood and latewood, a proportion of heartwood and sapwood, pattern of growth ring). In particular, thermal conductive properties are mainly dependent on the pattern of the growth ring itself at low temperatures.

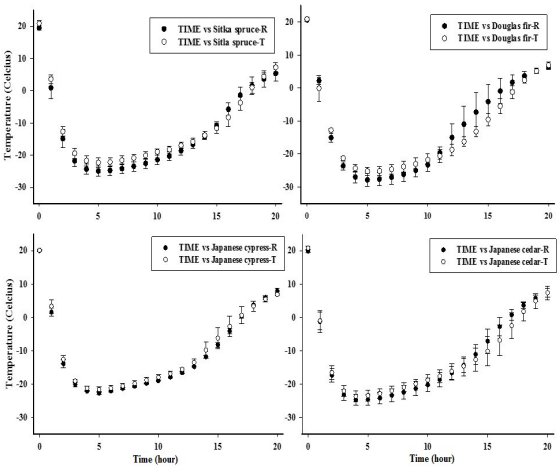

Figure 1. Comparison of the thermal conductive properties values obtained in both tangential and radial direction using solid carbon dioxide slabs

Novel application of a two-in-one bandage system for improving remedial and preventive treatment of drywood termite control

This section has presented a two-in-one bandage system, which combines of two or more treatment approaches with different mechanisms can cooperatively prohibit drywood termite eradication and prevent re-infestation. microstructural and anisotropy of wood using solid carbon dioxide as a chilling agent.

The effectiveness of the remedial treatment in a two-in-one bandage system was highly influenced by the microstructure of the wood and the dosage of the chilling agent. However, using polyurethane bandage system requires a much less chilling agent (1,200g CO_2 snow) to generate the core temperature of timber achieved a lower than required critical thermal minimum (CT_{min}) of drywood termite in the first 3 h in the much larger volume of structural timber (0.0115 m^{-3} of softwood). It explains the importance of designing and material selection for the insulation system to maximize the heat transfer properties of solid carbon dioxide. Regards the insecticidal activity evaluations, the difference in the mortality data indicates that there was a significant interaction between the dosage and the exposure time. With continuous exposure at the lowest concentration, worker health did not suffer significantly due to a delayed avoidance response of the termites. Meanwhile, with continuous exposure at higher concentrations, termites were overwhelmed by the excessive amounts of imidacloprid, which required more resources and time to cope with the stress, enhancing the recognition of advanced symptoms.

Although this study shows promise for improved methods of control and prevention for drywood termites, there is potentially adjusting this new control technique/device to meet the needs of the pest management industry. Area of potential future works is to develop the supercritical mixture of the chilling agent and insecticide. Using the supercritical CO_2 mixture, it would reduce the application time and cost for the pest management industry. In the current design, the increase the property of insulation of two-in-one bandage system by the implement of other insulative materials

ABSTRACTS (PH D THESIS)

Simulation Study on Enhancements of Energetic Heavy Ions in the Magnetosphere

(Graduate School of Engineering, Laboratory of Computer Space Science, RISH, Kyoto University)

Yohei Nakayama

Introduction

One of the dynamic phenomena emerging in the geospace is the substorm. During the substorm, reconfiguration of the magnetic field takes place in the magnetosphere and the energetic charged particles are enhanced. In particular, singly charged oxygen (O^+) ion is known as the most responsible ion species for the substorm. Many observations show that energetic O^+ ions (tens of keV) rapidly increase in the inner magnetosphere and contribute significantly to the ring current during substorms. In spite of many studies, the energization process of the O^+ ion in the inner magnetosphere is still a controversial issue. In the present study, we perform test particle simulations in a global MHD electromagnetic fields [1]. Using the test particle simulation result, we reproduce spatiotemporal variations of distribution function and flux of O^+ ion after the substorm-time acceleration based on the Liouville theorem [2]. Through the numerical studies, the global trajectories and accelerations of O^+ ions from their source regions and their contributions to the energetic O^+ ions in the inner magnetosphere are examined.

Oxygen Injection in the Plasmasheet during the Substorm

We focus on an acceleration of O^+ ion around the nightside magnetic reconnection region, which can be thought as the most dynamic region during the substorm. Mechanisms of the enhancement of the dawn to dusk electric field and of subsequent accelerations of O^+ ions due to the intensive electric field are investigated in detail. In the inner magnetosphere, our simulation reproduces a realistic flux enhancement with the O^+ ion such as the dispersion-less structure, the dispersed structure and the nose structure which are often observed by in-situ observations as shown in Fig. 1. In addition to the dispersion structures, our simulation shows that another type of structure named void structure in the inner magnetosphere (Fig. 2). The structure is observed by the Van Allen Probes HOPE instruments. We reveal that the generation mechanisms of the void structure consist of the formation of the strong equatorward flow in the low pressure region and tailward flow in the high pressure region and the intense non-adiabatic acceleration of O^+ ions.

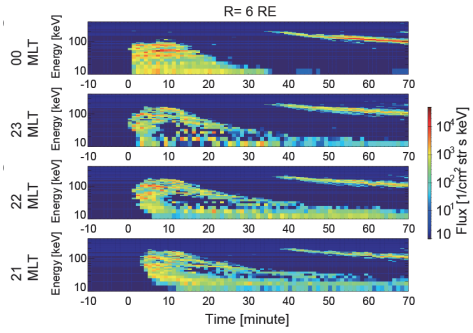

Fig. 1. Energy versus time spectrograms of the differential flux of the O+ ions at fixed positions

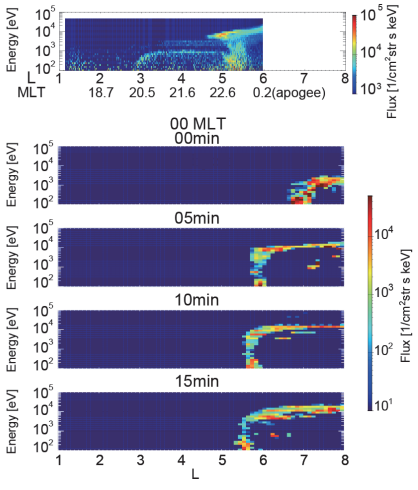

Fig. 2. Observation and Energy-L spectrograms of the simulated O^+ ions at 00 MLT in the equatorial plane.

Substorm-time O^+ outflow from the ionosphere

We also examine variations of O^+ outflow during the substorm and their impacts on the enhancement of energetic O^+ in the inner magnetosphere. We reveal that, during the substorm growth phase, O^+ ions at tens of eV are extracted from the dayside polar region due to the region 1, resulting in the enhancement of the warm O^+ ions (hundreds of eV) in the lobe (Fig. 3). This process works as a "pre-conditioning" of the O^+

ion. After the substorm onset, the enhanced warm O^+ ions are non-adiabatically accelerated to tens of keV and injected to the inner magnetosphere. A combination of the pre-conditioning and the non-adiabatic acceleration of the O^+ establishes a realistic O^+ ring current. At the same time, the initial brightening occurs in the midnight aurora region, then up to a few keV O^+ ions are extracted and directly supplied to the inner magnetosphere, developing a fraction of the O^+ ring current (Fig. 4).

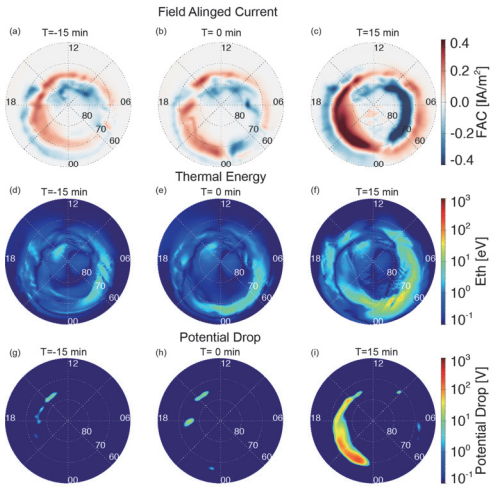

Fig. 3. MHD conditions and auroral outflow parameters at 1000 km altitude.

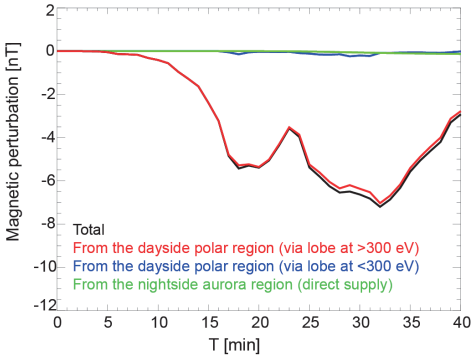

Fig. 4. Magnetic perturbation on the ground due to the several groups of O^+ ion.

Conclusion

This thesis addresses important issues and contributes to understand the big picture of the O^+ ion energization during substorms. Global paths of O^+ ions from the ionosphere to the inner magnetosphere have been tracked, and the realistic spatiotemporal flux has been reproduced by the large-scale computer simulations. During the growth phase of the substorm, the large scale region 1 FAC results in the extraction of warm O^+ ions from the dayside polar region. The O^+ ions transported to the lobe region with the adiabatic heating due to the convection electric field. The warm (hundreds of eV) O^+ ions are directed to the acceleration region in near-earth plasma sheet via the lobe region which is work as the "preconditioning". After the onset substorm expansion phase, the rich and warm O^+ ions are rapidly (within minutes) energized up to tens of keV under the effect of the large dawn-to-dusk electric field. This acceleration that occurs in the non-adiabatic manner, leading to the formation of the void structure in energy-L spectrograms. This is consistent with in-situ observations. The energetic O^+ ions via lobe significantly contribute to the O^+ ring current build up. At the same time, the auroral acceleration process thermalizes the ionospheric O^+ ions to hundreds of eV. Consequently, they are supplied to the inner magnetosphere and contributes to a fraction of the O^+ ring current. From the results, we have concluded that a combination between the pre-conditioning of the warm O^+ ion (hundreds of eV) in the lobe due to the enhancement of the midday part of the region 1 FAC and the non-adiabatic acceleration in the near-earth plasmasheet is the dominant energization process for the ring current O^+ ion during the substorm.

Acknowledgements

Computation in the present study was performed with the KDK system of Research Institute for Sustainable Humanosphere (RISH) at Kyoto University as a collaborative research project. This study was supported by KAKENHI, Grant-in-Aid for Scientific Research (B) 15H03732.

References

[1] Ebihara, Y., M. Yamada, S. Watanabe, and M. Ejiri (2006), Fate of outflowing suprathermal oxygen ions that originate in the polar ionosphere, J. Geophys. Res., 111, A04219, doi:10.1029/2005JA011403.

[2] Tanaka, T., A. Nakamizo, A. Yoshikawa, S Fujita, H. Shinagawa, H. Shimizu, T. Kikuchi, and K. K. Hashimoto (2010), Substorm convection and current system deduced from the global simulation, J. Geophys. Res. 115, A05220, doi:10.1029/JA014676.

ABSTRACTS (PH D THESIS)

Advanced Beam Forming by Synthesizing Spherical Waves For Progressive Microwave Power Transmission

(Graduate School of Engineering, Laboratory of Applied Radio Engineering for Humanosphere, RISH, Kyoto University)

Takayuki Matsumuro

Development of various beam electromagnetic field by synthesizing spherical waves is established to deepen microwave power transmission technology. For the realization of space-based solar power system with large-scale microwave power transmission, early social implementation of terrestrial systems with a short distance and continuous development in the market are important. Progressive microwave power transmission technology for suppressing the interference with other wireless systems and the effect for the human body is required especially for the terrestrial systems. To deal with the problem, we investigate the ideal electromagnetic fields designed by the set of spherical waves, which are basis functions of Maxwell's equation. Two tasks for the further technological progress are focused in this study: miniaturization of the receiving antenna for the ubiquitous power source, and minimization of energy leakage for beam-type microwave power transmission.

An operation principle of a high-directivity radiation phenomenon from the point source is clarified. It is well known the radiation from multipoles at the origin, which can be considered as the limit of small antennas, is the spherical wave. The high-directivity radiation phenomenon can be obtained by involving spherical waves of the different order. We derive the directivity of the synthesized spherical wave from the uncertainty relation of angular momentum and angle. It is also shown that the intrinsic wave source is assumed to exist on the surface of the cutoff region by the estimation of the effective aperture of the synthesized spherical wave (Fig.1). Moreover, we discover that multipoles can be replaced by a spherical dielectric resonator with finite size. By using a dielectric resonator that is smaller than the cutoff region, it is possible to realize a compact radiation system with the larger effective aperture than the physical cross-section. A design method for degenerating all spherical wave modes of the spherical dielectric resonator with a multilayered structure is developed (Fig.2). Degeneration of TE11-mode and TM11-mode is enabled by the spherical dielectric resonator structure with a center conductor. Degeneration of TE-mode and TM-mode of higher order is enabled by the spherical dielectric resonator structure with anisotropic permittivity. We also develop an evaluation method and equipment for spherical symmetry of the dielectric constant of a fabricated spherical dielectric resonator. The multilayered spherical dielectric resonator gives a basic structure of the compact receiving antenna for the ubiquitous power source.

An effective design method of low-leakage microwave beam by synthesizing spherical wave is developed. Beam electromagnetic field is optimized to the minimum leakage for the input of the array antenna element. The beam electromagnetic field is obtained by combining outgoing and incoming spherical waves with the same amplitude. It is shown that a strict Gaussian beam without paraxial approximation is synthesized by spherical waves when side lobes of the beam are minimized. The design formula of the optimum beam waist radius according to the transmission distance is also derived. The effective range where the edge level can estimate the leakage power of the system is investigated by the simulation. Moreover, we propose a single-frequency retrodirective system using a beam pilot signal with the low-leakage beam design. The multipath propagation caused by the ground or the sea surface of the terrestrial microwave power transmission can be eliminated by using the beam pilot signal. It is shown that the retrodirective system operates stably even when the atmospheric refractive index has a spatial distribution. We also develop a dual-mode dielectric resonator antenna element ideally with infinitesimal dipole characteristics. The dual-mode dielectric resonator antenna is proposed as a common array antenna element for the beam pilot signal and microwave power. This involves a cross-shaped hemispherical dielectric resonator structure, and an isolation level exceeding 60 dB has been experimentally measured between the orthogonal ports of the fabricated antenna. The single-frequency retrodirective system improves the reliability of the terrestrial microwave power transmission.

The comprehensive studies from the clarification of the principle for the compact antenna to the proposal of the terrestrial microwave power transmission system are pursued. This research is hoped to contribute to

ABSTRACTS (PH D THESIS)

the early social implementation of progressive microwave power transmission and the realization of the space-based solar power station.

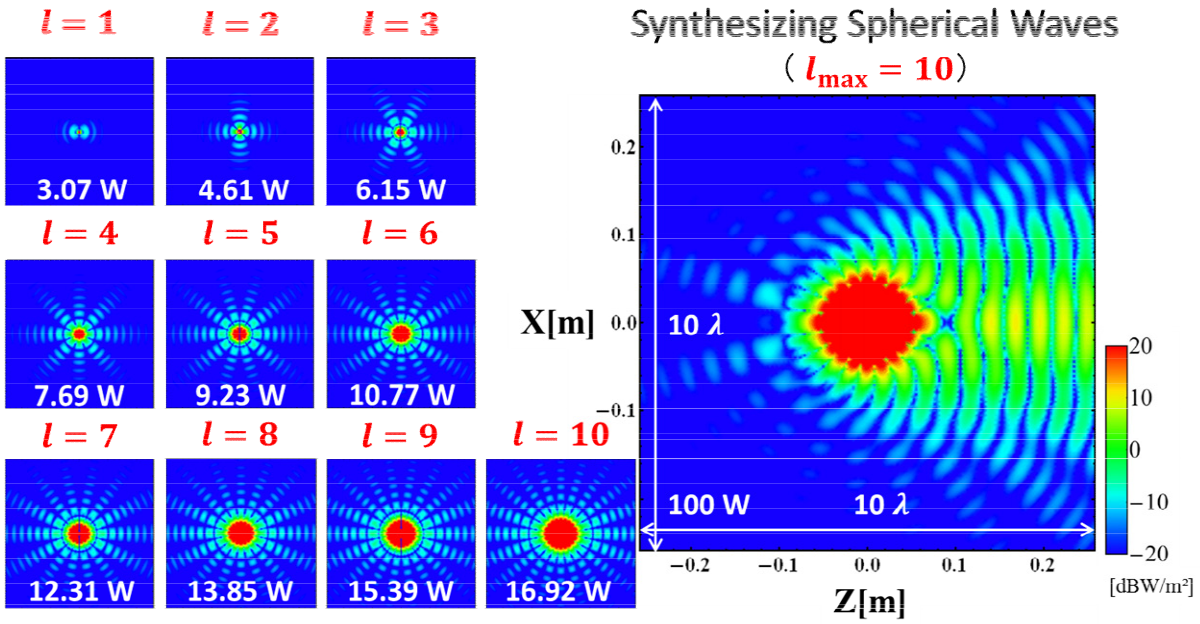

Fig.1. Electromagnetic Field by Synthesizing Spherical Waves

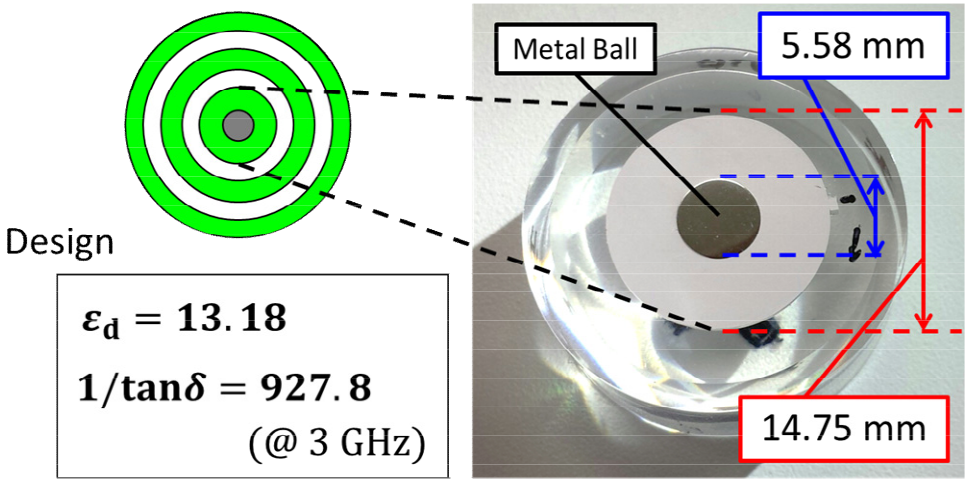

Fig.2. Developed Di-electric Resonator Antenna

ABSTRACTS (PH D THESIS)

On Asteroid Deflection Techniques Exploiting Space Plasma Environment

**(Graduate School of Engineering,
Laboratory of Space Systems and Astronautics, RISH, Kyoto University)**

Kohei Yamaguchi

Introduction

The collision of the asteroid with the Earth is one of the devastating disaster which has been studied by many astronomers and researchers. In this thesis, two techniques to deflect an asteroid with unacceptable Earth colliding risk away from the original course are proposed and studied. Compared with the method proposed before, the effectiveness of the methods has been extended by exploiting the space plasma environment. The first method is the kinetic impactor (KI) which sends a spacecraft to impact against the target asteroid for deflection. To increase the impact velocity, the electric solar wind sail (E-sail), which generates the thrust acceleration force with the interaction between the charged conducting tethers and the solar wind plasma stream, is assumed as the propulsion system. Second method is the Coulomb force attractor, which tows the asteroid by using the electrostatic attraction between the asteroid and the spacecraft both of which are artificially charged.

Electric solar wind sail kinetic impactor

The E-sail [1] is the next-generation space propulsion system. The E-sail based spacecraft has many long thin conducting tethers which are connected to electron guns mounted on the spacecraft main body (see also a conceptual sketch shown in Fig. 1). The tethers are charged up through the loss of electrons caused by the electron gun and interact with the natural solar wind plasma stream. Since the E-sail enables a spacecraft to generate the thrust force without consuming any reaction mass, it can be attractive to increase the impact high velocity required by KI technique.

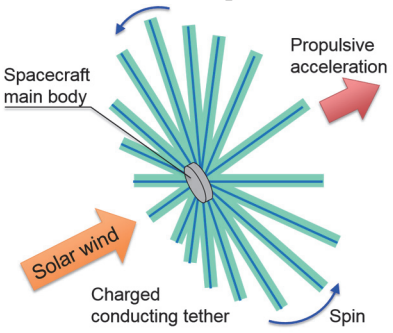

Figure 1. A conceptual sketch of the E-sail based spacecraft.

The advanced solar wind force model is proposed considering the configuration of the E-sail base spacecraft. The direction and the magnitude of the solar wind thrust force of the E-sail is expressed as a function of the attitude of the E-sail. To reduce the energy required to change the direction of the thrust force by changing the attitude of the E-sail, a new orbital maneuvering technique not changing the attitude of the spacecraft actively but changing the voltage of the conducting tethers is also proposed and investigated. The usage of the maneuvering technique has been proven by analytical and numerical approach.

Finally, numerical simulations of the E-sail KI are performed for the scenario created from fictional Earth impactors. The mass of the asteroids is assumed to be 1.0×10^{9} kg and the mass of the projectile mounted on the E-sail is assumed to be 1,000 kg. The trajectory of the E-sail to impact to the asteroid is solved in an optimal frame work. The results show that the E-sail KI achieves deflection distances larger than the Earth radius for Apollo asteroids which has a semi-major axis larger than 1 au. Figure 2 is an example of the optimized trajectory of the E-sail. Results for the Aten asteroid which has the semi-major axis smaller than 1 au, on the other hand, the deflection distance achieved by the E-sail KI is smaller than the Earth radius. To investigate the characteristics of the E-sail KI, trajectory optimization for the solar sail which produces the thrust force by reflecting the Sun light with a large thin mirror is also performed. Since the solar radiation pressure force is proportional to the inverse of the square solar distance of the spacecraft, the thrust

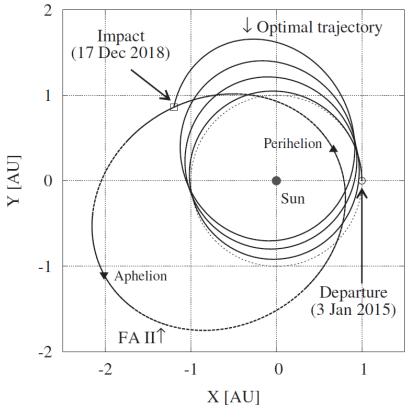

Figure 2. An example of the optimal trajectory for E-sail.

ABSTRACTS (PH D THESIS)

acceleration magnitude of the solar sail rapidly increased when the spacecraft spirals inward to impact against Aten asteroid. On the other hand, the thrust force of the E-sail varies as the inverse of the solar distance and thus the E-sail experiences a small reduction on thrust when the spacecraft spirals outward to impact against Apollo asteroid. These results show that the E-sail KI is more effective to deflect Apollo asteroids.

Coulomb force attractor

The gravitational tractor [2] which tows the asteroid by using the gravitational attraction between a target asteroid and a massive spacecraft has been proposed and studied. The Coulomb force attractor extends the towing force by an electrostatic attraction between the asteroid and the spacecraft. Both the spacecraft and the asteroid are artificially charged and the electrostatic force is introduced.

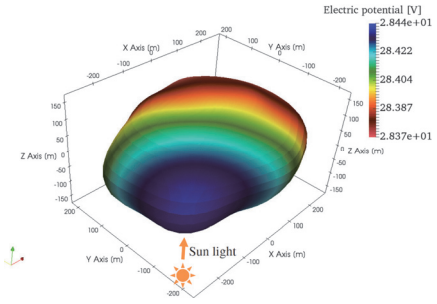

Figure 3. Natural charging analysis for a conductive asteroid.

The Coulomb force attractor cannot be used without charging the asteroid artificially. To study the charging mechanisms of a conductive asteroid, three-dimensional asteroid charging model is developed based on the finite element method. The voltage of the asteroid is formulated based on the three dimensional mesh to model the realistic shape of the asteroid. Current flows which are caused by the space plasma surrounding the target asteroid are modeled as the equivalent current sources. They are, currents caused by the primary electrons and protons, the secondary electron current caused by the incidence of the primary particles, photoelectron currents caused by the Sun illumination. To solve this non-linear problem, a numerical solver has also been developed. Our tool successfully works to solve the natural charging phenomenon of a conductive asteroid as shown in Fig. 3. The results for artificial charging cases show that the asteroids composed with conductive material can be charged artificially.

The dynamics of the charged spacecraft in the vicinity of the charged asteroid is also formulated. The equations of motion are formulated for the rotating reference frame fixed in the initial heliocentric motion of the centroid of the asteroid. By numerically integrating these equations, it is demonstrated that the electrostatic attraction is effective to extend the change in the position and velocity of the asteroid. The achievable deflection distances between the asteroid and the Earth at the predicted Earth impact date are also calculated for fictional Earth impactor to investigate the effectiveness of the Coulomb force attractor. An 8.73×10^7 kg of asteroid artificially charged -20 kV is assumed to be a target. The spacecraft is charged up to 20 kV and the mass is assumed to be 500 kg. The eccentricity of this asteroid is assumed to be about 0.2. Such small asteroid is difficult to be deflected by using the gravitational attraction. In addition, achievable deflection distance is not so affected by the change in time to start towing. The result shown in Fig.4 tells that the Coulomb force attractor can extend the deflection distance of the asteroid with a small mass and small eccentricity efficiently.

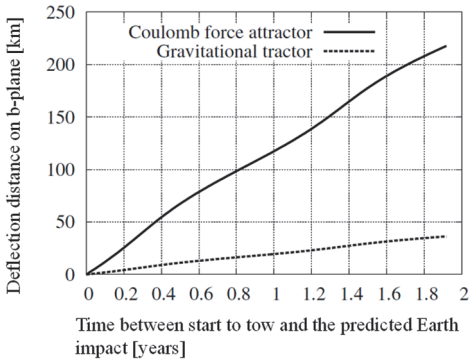

Figure 4. Comparison of the achievable deflection distances by two methods.

Acknowledgements

This work was supported by a JSPS KAKENHI grant 15J08268. Computation time was provided by the SuperComputer System, Institute for Chemical Research, Kyoto University.

References

[1] Janhunen, P., "Electric Sail for Spacecraft Propulsion," *Journal of Propulsion and Power*, vol. 20, pp. 763-764, 2004.

[2] Lu, T. E. and Love, G. S., "Gravitational Tractor for Towing Asteroids," *Nature*, vol. 438, pp. 177-178, 2005.

ABSTRACTS (MASTER THESIS)

Stable-isotope labeling and analysis of extracellular metabolites, ceriporic acids, produced by *Ceriporiopsis subvermispora*

(Graduate School of Agriculture, Laboratory of Biomass Conversion, RISH, Kyoto University)

Takaaki Kono

Wood-rotting fungi are the only organisms that can decompose wood because the lignin in wood cell walls is hard to degrade. Biodegradation of lignin is an essential role and characteristic feature of wood-rotting fungi in the ecosystem. Lignin degradation by fungi is explained as mostly to the fungal enzymatic activity of ligninolytic enzymes. However, not only ligninolytic enzymes but also metabolites secreted by fungi have known to important in the lignin degradation system.[1,2] Here, we have focused on a wood-rotting fungus, *Ceriporiopsis subvermispora*, which has the ability to decompose lignin in preference to cellulose. Thus, the fungus, *C. subvermispora*, recognized as a selective lignin-degrading fungus. Previous studies reveal that the importance of secondary metabolites of *C. subvermispora*. [1,2]

Stable-isotope (non-radioactive) labeling has been used to study metabolites of *C. subvermispora* and has been determined the structure and diversity of them.[2] High-resolution mass spectrometry enables the establishment of incorporation of heavy atoms from precursor substrates into different metabolic products. Here, we try to understand metabolic dynamics of extracellular metabolites, ceriporic acids, by stable-isotope labeling experiments. We analyzed intra- and extracellular metabolites and observed several metabolites that can separate as isotopically labeled compounds based on the mass difference.

Acknowledgements

Collaborative programs, Development and Assessment of Sustainable Humano-sphere/Forest Biomass Analytical System (DASH/FBAS), and Analysis and Development System for Advanced Materials (ADAM), of Research Institute for Sustainable Humanosphere (RISH), Kyoto University are acknowledged.

References

[1] Nishimura, H., Sasaki, M., Seike, H., Nakamura, M., Watanabe, T., “Alkadienyl and alkenyl itaconic acids (ceriporic acids G and H) from the selective white-rot fungus *Ceriporiopsis subvermispora*: a new class of metabolites initiating ligninolytic lipid peroxidation”, *Org. Biomol. Chem.* 10, 6432-6342, 2012.

[2] Nishimura, H., Murayama, K., Watanabe, T., Honda, Y., Watanabe, T., “Diverse rare lipid-related metabolites including ω-7 and ω-9 alkenylitaconic acids (ceriporic acids) secreted by a selective white rot fungus, *Ceriporiopsis subvermispora*”, *Chem. Phys. Lipids*, 165, 97-104, 2012.

ABSTRACTS (MASTER THESIS)

A new *O*-methyltransferase gene involved in antitumor lignan biosynthesis in *Anthriscus sylvestris*

(Graduate School of Agriculture, Laboratory of Metabolic Science of Forest Plants and Microorganisms, RISH, Kyoto University)

Masato Kumatani

Lignans are phenylpropanoid dimers that are linked at C-8 position of their propyl side chains [1] and isolated from stem, heartwood, leaf, root, flower and fruit of a wide variety of plants [2]. Some lignans are known for having various physiological activities including antitumor, antiviral and antioxidative. Especially, podophyllotoxin is known as an antitumor lignan and used as a precursor for the chemical synthesis of the anticancer drugs etoposide, teniposide and etopophos [3]. However, the availability of this lignan is limited because of overharvesting podophyllotoxin-forming plants. Hence, stable and large scale production of podophyllotoxin has been paid attention [3].

Biosynthetic pathways of antitumor lignans have been studied using several plants, and some pathways were proposed. In a biosynthetic pathway of *A. sylvestris*, Sakakibara et al. proposed the pathway from matairesinol to yatein based on feeding experiment using stable isotope-labeled precursors [4]. Recently, cDNA encoding thujapilcatin *O*-methyltransferase (TJOMT), which catalyzes a conversion from thujaplicatin to 5-*O*-methylthujaplicatin, was identified from *A. sylvestris* [5]. But, the 5-*O*-methylthujaplicatin *O*-methyltransferase (5MTJOMT), catalyzes a conversion from 5-*O*-methythujaplicatin to 4,5-*O*,*O*-dimethylthujaplicatin, has not been identified. A set of genes involved in the podophyllotoxin biosynthetic pathway was not completely isolated in any plants including *A. sylvestris*. Isolation of all genes enables biological productivity of podophyllotoxin in future.

In this study, based on a correlation analysis between patterns of 5MTJOMT activity and of gene expression among different organs of *A. sylvestris*, several putative OMT sequences which had more than 0.2 correlation coefficient were selected as 5MTJOMT candidate genes. Then, recombinant proteins were prepared from each gene, and checked whether the recombinant protein had any activity with potential substrate. A lysate of the recombinant protein having OMT activity for 5-*O*-methylthujaplicatin was purified by affinity chromatography and desalted by gel filtration chromatography, and kinetic analysis for 5-*O*-methylthujaplicatin was conducted.

Eight genes were selected as 5MTJOMT candidate genes by correlation analysis. Among 5MTJOMT candidate genes, AsOMT95 having a moderate correlation coefficient (R = 0.43) showed OMT activity for 5-*O*-methylthujaplicatin and 4-demethylyatein. In addition, the catalytic efficiency (k_{cat}/K_m) of AsOMT95 for 5-*O*-methylthujaplicatin and 4-demethylyatein was 1.78 and 4.07 min^{-1} μM^{-1}, respectively. In *A. sylvestris*, 4-demethylyatein has not been detected and lignan biosynthetic pathway via 5-*O*-methylthujaplicatin was proposed based on feeding experiments. Therefore, it was suggested that *AsOMT95* is a gene involved in methylation of 5-*O*-methylthujaplicatin, i.e., *As5MTJOMT*.

References

[1] R.D Haworth (1942) The chemistry of the lignan group of natural products. *Journal of the Chemical Society*, 448-456.
[2] W.D. Macrae and G.H.N Towers (1983) Biological activity of lignans. *Phytochemistry* **23**, 1207-1220.
[3] S. Farkya, V.S. Bisaria and A.K. Srivastava (2004) Biotechnological aspects of the production of the anticancer drug podophyllotoxin. *Applied Microbiology and Biotechnology*, **65**, 504-519.
[4] N. Sakakibara, S. Suzuki, T. Umezawa and M. Shimada (2003) Biosynthesis of yatein in *Anthriscus sylvestris*. *Organic & Biomolecular Chemistry* **1**, 2474-2485.
[5] S.K. Ragamustari, T. Nakatsubo, T. Hattori, E. Ono, Y. Kitamura, S. Suzuki, M. Yamamura1 and T. Umezawa (2013) A novel *O*-methyltransferase involved in the first methylation step of yatein biosynthesis from matairesinol in *Anthriscus sylvestris*. *Plant Biotechnology* **30**, 375-384.

ABSTRACTS (MASTER THESIS)

Generation and characterization of rice *CAD2 CAldOMT1* double mutants with altered lignin content and structure

(Graduate School of Agriculture, Laboratory of Metabolic Science of Forest Plants and Microorganisms, RISH, Kyoto University)

Naoyuki Matsumoto

Lignin, an abundant aromatic polymer derived from oxidative couplings of monolignols and related phenylpropanoids, is one of the major components of lignocellulosic biomass. Bioengineering of lignin has long been a major research focus, especially because lignin negatively impacts numerous biomass utilization processes such as chemical pulping and bioethanol production. More recently, engineering lignin to facilitate its conversion into value-added aromatic commodities has also received considerable attention. In this context, our laboratory has been studying lignin engineering using rice, a grass model plant, to explore molecular breeding approaches for improving the properties of grass biomass.

Recent studies in our laboratory have demonstrated that regulations of rice lignin biosynthetic genes encoding cinnamyl alcohol dehydrogenase (CAD) and 5-hydroxyconiferaldehyde *O*-methyltransferase (CAldOMT) differently impact structures and properties of rice lignocellulose. Downregulation of *OsCAD2*, one of the major rice CAD genes, leads to unusual incorporation of *p*-hydroxycinnamaldehydes into lignin polymers along with a slight reduction in lignin content [1]. On the other hand, downregulation of *OsCAldOMT1*, a major rice *CAldOMT*, resulted in altered lignins largely depleted in syringyl and tricin units [2,3]. Both *OsCAD2*- and *OsCAldOMT1*-deficient rice displayed significantly increased biomass saccharification efficiency compared to wild-type rice [1,2]. Interestingly, however, they show distinctively different time-dependent saccharification profiles, suggesting that differences in lignin content/structure of the two lignin-modified rice differently affect the properties of lignocellulose. In this study, to further investigate the relationship between altered lignin content/structure and lignocellulose properties of *OsCAD2*- and *OsCAldOMT1*-deficient rice, new double-knockout mutants for *OsCAD2* and *OsCAldOMT1* (*cad2 caldomt1*) were generated, and their modified lignocellulose structure as well as enzymatic saccharification efficiency were assessed comparatively with the previously developed rice transgenics in which either of *OsCAD2* or *OsCAldOMT1* alone is downregulated.

Anticipated *cad2 caldomt1* double knockout mutants were successfully generated via targeted mutagenesis in *OsCAD2* single knockout background [1] using CRISPR/Cas9 expression vector designed to target *OsCAldOMT1*. Genotyping for selected T_0 lines suggested that they have bi-allelic mutations that should lead loss of *OsCAldOMT1* function. Chemical and NMR analyses on cell walls isolated from *cad2 caldomt1* clearly demonstrated that they produce altered lignins affected by loss-of-functions of both *OsCAD2* and *OsCAldOMT1*. Our preliminary saccharification experiments suggested that *cad2 caldomt1* T_0 lines also displayed synergistic increase in saccharification efficiency via loss-of-functions of both *OsCAD2* and *OsCAldOMT1*, although a deeper investigation should be conducted with T_1/T_2 progeny lines. Overall, we contemplate that further analysis of the developed rice transgenic lines would provide new insights into molecular breeding approaches to improve grass biomass for future biorefinery.

References

[1] Koshiba, T., Murakami, S., Hattori, T., Mukai, M., Takahashi, A., Miyao, A., Hirochika, H., Suzuki, S., Sakamoto, M., and Umezawa, T. "*CAD2* deficiency causes both *brown midrib* and *gold hull and internode* phenotypes in *Oryza sativa* L. cv. Nipponbare", *Plant Biotechnol.* 30, 365-373, 2013.

[2] Koshiba, T., Hirose, N., Mukai, M., Yamamura, M., Hattori, T., Suzuki, S., Sakamoto, M., and Umezawa, T. "Characterization of 5-Hydroxyconiferaldehyde *O*-Methyltransferase in *Oryza sativa*", *Plant Biotechnol.* 30, 157-167, 2013.

[3] Matsumoto, N., Lam, P.Y., Takeda, Y., Suzuki, S., Lan, W., Yamamura, M., Sakamoto, S., Lo, C., Ralph, J., Tobimatsu, Y., Umezawa, T. "Delineating lignin biosynthetic pathway in monocots: a rice *O*-methyltransferase involved in the formation of syringyl and tricin lignin components in rice cell walls", *Proceedings of Lignobiotech IV Symposium,* O19, 2016.

ABSTRACTS (MASTER THESIS)

Metabolic engineering for isoprene production in algae

**(Graduate School of Agriculture,
Laboratory of Plant Gene Expression, RISH, Kyoto University)**

Takuya Asano

Isoprene is a volatile C5 hydrocarbon, 2-methyl-1,3-butadiene, which is used for the production of synthetic rubber and adhesives in a large amount [1]. The overall consumption over the world is ca. 1 million tons, while the source of isoprene is currently almost completely dependent on petrochemicals, for instance the isolation from C5 cracking fraction [2]. Because of the latent risk of resource depletion and also for lowering environmental load, isoprene production by living organisms have been attempted in recent years [3,4].

In nature, many microorganisms and plant species are known to emit isoprene to atmosphere. In particular, isoprene represents ca. 50% of plant-derived volatile organic compounds (PVOC) emitted to the air, which is calculated to be ca. 50 Tg carbon per year on the earth [5]. In order to establish the isoprene production by metabolic engineering, isoprene synthase gene was searched in plant species that are known as isoprene emitter plants. The first isoprene synthase gene was identified in poplar in 2001, and in Kyoto University another isoprene synthase gene PaIspS was isolated from *Populus alba* in 2005 [7].

We first tried to produce isoprene in transgenic plants, and used Arabidopsis as a model. However, the production level was too low, and more importantly the recovery of isoprene from the leaves seems to be practically unfiesible. From these experiences we are trying to express *PaIspS* in a couple of microorganisms. The results are now summarized as a publication.

Acknowledgements

This study was conducted as collaboration with Dr. Kentaro Ifuku, Dr. Hideya Fukuzawa, and Dr. Masataka Kajikawa of Graduate School of Biostudies of Kyoto University, and Dr. Tomonori Okumura of Research Institute of Environment, Agriculture and Fisheries, Osaka Prefecture. This study was supported in part by a grant of Mission 5-2 of RISH, Kyoto University.

References

[1] Bentley, F.K., Zurbriggen, A., Melis, A., 2014. Heterologous expression of the mevalonic acid pathway in cyanobacteria enhances endogenous carbon partitioning to isoprene. Mol. Plant, 7, 71-86.

[2] Weissermel, K., Arpe, H.J.,1992. Industrial Organic Chemistry. JohnWiley&Sons, NewYork..

[3] Whited, G.M., Feher, F.J., Benko, D.A., Cervin, M.A., Chotani, G.K., McAuliffe, J.C., La Duca, R.J., Ben-Shoshan, E.A., Sanford, K.J., 2010. Development of a gas-phase bioprocess for isoprene-monomer production using metabolic pathway engineering. Ind.Biotechnol. 6, 152-163.

[4] Ye, L., Lv, X., Yu, H. (2016) Engineering microbes for isoprene production. Metab. Eng. 38, 125-135.

[5] Sharkey, T.D., Yeh, S., Wiberley, A.E., Falbel, T.G., Gong, D., Fernandez, D.E., 2005. Evolution of the isoprene biosynthetic pathway in kudzu. Plant Physiol. 137, 700-712.

[6] Miller, B., Oschinski, C., Zimmer, W., 2001. First isolation of an isoprene synthase gene from poplar and successful expression of the gene in *Escherichia coli*. Planta 213,483-487.

[7] Sasaki, K., Ohara, K., Yazaki, K., 2005. Gene expression and characterization of isoprene synthase from *Populus alba*. FEBSLett. 579, 2514-2518.

ABSTRACTS (MASTER THESIS)

Discovery of prenyltransferase gene specific for phenylpropanoids

**(Graduate School of Agriculture,
Laboratory of Plant Gene Expression, RISH, Kyoto University)**

Tomoya Takemura

Preny is a collective name of isoprenoid residues, which are often attached to aromatic compounds, either directly to the aromatic ring by *C*-*C* bound or via *O*- or *N*-atoms on the ring systems [1]. The most simple and abundant prenyl residue is dimethylallyl that is composed of 5 carbon atoms, and as minority geranyl- (C10) and farnesyl- (C15) residues occur in nature [2]. Prenylated compounds are frequently reported as biological active compounds isolated from various medicinal plants. The activities are fairly divergent according to their chemical structures, such as, anti-bacterial, anti-tumor, anti-HIV activities as well as estrogenic activity and anti-tyrosinase effect [3-6].

Prenyltransferase for aromatic substrate is the responsible enzyme for the biosynthesis of prenylated aromatic compounds. Thus far, many prenyltransferases are identified for flavonoids, phloroglucinols, coumarins, but that specific for simple phenylpropanoids (C6-C3) have not been identified. In this study, we made attempts to discover the first prenyltransferase gene for phenylpropanoids. The most well-known prenylated phenylpropanoid is artepillin C, which is diprenylated 4-coumaric acid. A representative plant that contains artepillin C in a high amount is *Baccharis dracunculifolia* (Asteraceae) originated in Brazil, which is an important ingredient of Brazilian propolis. Adding to this plant, some other plant species in Asteraceae contain this prenylated phenylpropanoid, while the content is generally low.

By use of large scale EST information of several medicinal plants collected by Kazusa DNA Reseaerch Institute, we could narrow down a candidate plant, from which a candidate gene coding for prenyltransferase was found. We are currently summarizing these results for publication.

Acknowledgements

This study was supported by Dr. Hideyuki Suzuki of Kazusa DNA Research Institute; Dr. Hikaru Seki of Graduate School of Engineering, Osaka University; Dr. T. Yamaura of Nippon Shinyaku Co.; and LC-IT-TOF/MS privided by DASH/FBAS of RISH, Kyoto University.

References

[1] Yazaki, K., Sasaki, K., Tsurumaru, Y., Prenylation of aromatic compounds, a key diversification of plant secondary metabolites. Phytochemistry, 70 (15-16), 1739-1745 (2009).

[2] Botta, B., Vitali, A., Menendez, P., Misiti, D., Delle, M.G., 2005. Prenylated flavonoids: Pharmacology and biotechnology. Curr. Med. Chem. 12, 713-739.

[3] Appendino, G., Gibbons, S., Giana, A., Pagani, A., Grassi, G., Stavri, M., Smith, E., Rahman, M., 2008. Antibacterial cannabinoids from *Cannabis sativa*: A structure-activity study. J. Nat. Prod. 71, 1427-1430.

[4] Kapche, G.D.W.F., Fozing, C.D., Donfack, J.H., Fotso, G.W., Amadou, D., Tchana, A. N., Bezabih, M., Moundipa, P.F., Ngadjui, B.T., Abegaz, B.M., 2009. Prenylated arylbenzofuran derivatives from *Morus mesozygia* with antioxidant activity. Phytochemistry 70, 216-221.

[5] Kim, S.J., Son, K.H., Chang, H.W., Kang, S.S., Kim, H.P., 2003. Tyrosinase inhibitory prenylated flavonoids from *Sophora flavescens*. Biol. Pharm. Bull. 26, 1348-1350.

[6] Lee, J., Oh, W.K., Ahn, J.S., Kim, Y.H., Mbafor, J.T., Wandji, J., Fomum, Z. T., 2009. Prenylisoflavonoids from *Erythrina senegalensis* as novel HIV-1 protease inhibitors. Planta Medica 75, 268-270.

ABSTRACTS (MASTER THESIS)

Analysis of lipid transport machinery using *Lithospermum erythrorhizon*

**(Graduate School of Agriculture,
Laboratory of Plant Gene Expression, RISH, Kyoto University)**

Kanade Tatsumi

Higher plants produce a variety of lipophilic compounds. Representatives are cutin and wax that are primary metabolites, whereas there are a number of hydrophobic secondary metabolites, for example monoterpenes and furanocoumarins as well as several alkaloids. Many of these compounds are secreted out from particular cells at specialized tissues like glandular trichomes, oil glands, and also from epidermal cells [1] [2]. To date, however, secretory processes of lipophilic secondary metabolites from plant cells are largely unknown especially at the molecular level [3].

An herbal medicinal plant *Lithospermum erythrorhizon* Sieb. et Zucc. produces shikonin derivatives, red naphthoquinone pigments in the root bark. These pigments are highly lipophilic, and almost exclusively secreted out of the cells. This study aims to elucidate the secretion mechanisms of lipophilic metabolites using shikonin as a model due to several reasons, i.e. high productivity, visibility as a red pigment, and clear reversible regulation of its production by light and medium compositions [4].

By use of inhibitors of vesicle transport, cytochalasin D, an inhibitor of actin filament polymerization and Brefeldin A, an inhibitor of the adenosine diphosphate (ADP)-ribosylation factor/guanine nucleotide exchange factor (ARF/GEF) protein system, we find that these inhibitors strongly inhibit shikonin secretion without suppressing its biosynthetic activity. These data suggest that secretion of shikonin derivatives into the apoplast utilizes, at least partly, the pathways common to the ARF/GEF system and actin filament polymerization [5].

From our current data, we estimate that shikonin derivatives are dissolved in common lipids. In order to identify the lipids co-localized with shikonin, we have analyzed lipid extracts from cultured cells using LC-TOF-MS. We expect to summarize these results as a publication in near future.

Acknowledgements

We thank Dr. Yozo Okazaki and Dr. Kazuki Saito (RIKEN CSRS) for LC-TOF-MS of lipid analysis, Dr. Mayuko Sato and Dr. Kiminori Toyooka (RIKEN CSRS) for electron microscopy, and Dr. Takashi Aoyama (ICR, Kyoto University) for conforcal microscopy. This study was supported by a grant of mission 5-1 of RISH, Kyoto University.

References

[1]Lange, B. M., and Croteau,R. “Genetic engineering of essentiall oil production in mint” *Curr. Opin, Plant Biol*., 2; 139-144. (1999).
[2]Voo S S, Grimes H D, Lange B M. “Assessing the biosynthetic capabilities of secretory glands in citrus peel” Plant Physiol., 159, 81-94. (2012).
[3] Tabata M, Mizukami H, Hiraoka N, Konoshima M. “Pigment formation callus cultures of *Lithospermum erythrohizon*” *Phytochemistry* 13, 927-932. (1974).
[4] Widhalm, J. R., Jaini, R., Morgan, J. A., and Dudareva, N. “Rethinking how volatiles are released from plant cells” *Trends Plant Sci.*, 20, 545-550. (2015).
[5] Tatsumi K, Yano M, Kaminade K, Sugiyama A, Sato M, Toyooka K, Aoyama T, Sato F, Yazaki K. “Characterization of Shikonin derivative secretion in *Lithospermum erythrorhizon* hairy roots as a model of lipid-soluble metabolite secretion from plants”. *Front Plant Sci.* 7,1066. (2016).

ABSTRACTS (MASTER THESIS)

A study on real-time spatio-temporal variations of precipitable water vapor with a dense GNSS receiver network

**(Graduate School of Informatics,
Laboratory of Atmospheric Sensing and Diagnosis, RISH, Kyoto University)**

Naoki Ito

We have employed the GNSS meteorology method to measure the PWV (Precipitable Water Vapor), which is the integrated amount of water vapor along the zenith angle. We will try to establish the real-time prediction technique of the local torrential rain, utilizing the time and spatial variations of PWV within a small range in advance to the rainfall. We deployed the hyper-dense GNSS receiver networks around Uji and Shigarki with inter-station distances of few kilometers. We observed the PWV fluctuations occurred within a small horizontal scale, then we studied a relation between the PWV increase and rainfalls.

With the Uji network, we analyzed the PWV variations on September 3, 2012, when a localized heavy rain was observed. The averaged PWV for stations increased before a meteorological radar detected the rain clouds. The spatial distribution of PWV between the GPS stations increased to about 5 mm. The Shigaraki network is installed in hilly forests, so we need to compensate the effect of the difference due to elevation difference (Figure 1). We estimated the averaged PWV from July to September in 2016 to define the bias at each station. After removing this bias from the measured PWV, the spatial variation of PWV between the stations was suppressed by about 73 %.

For a real-time estimating of PWV, we need to know the accurate satellite orbit and clock information on real-time, which are corrected by referring to GEONET. Difference of PWV between the real-time analysis and the post processing with the final orbit was 0.82 mm in standard deviation. The usage of inexpensive single-frequency (SF) receivers would be beneficial for economic reasons. We implemented software to correct the effect of ionosphere delays on SF observations (the SEID model). By applying SEID for SF PWV retrieval, the error of PWV compared to the double-frequency (DF) solution was about 1.34 mm in standard deviation.

.

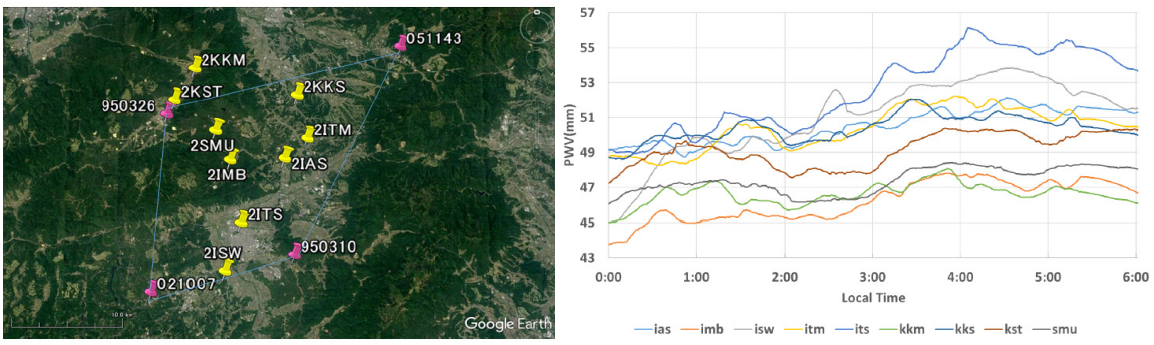

Figure 1. (left) The dense network of GNSS receivers installed near Shigaraki MU observatory in Shiga, Japan. (right) Temporal variations of the precipitable water vapor (PWV) observed from the Shigaraki dense GNSS receiver network.

ABSTRACTS (MASTER THESIS)

Observation of Temperature Profiles in Equatorial Region with EAR-RASS

**(Graduate School of Informatics,
Laboratory of Atmospheric Sensing and Diagnosis, RISH, Kyoto University)**

Hiraku Tabata

This study aims to continuously measure temperature profiles in the tropical troposphere (up to about 15-17 km) with high accuracy and high time-resolution by adopting Radio Acoustic Sounding System (RASS) (Figure 1) to the Equatorial Atmosphere Radar (EAR) at Kototabang, west Sumatra, Indonesia (Fukao et al, 2003). We arranged high-power speaker boxes and constructed a sound transmitting system in the EAR.

Because propagation of sound waves in the atmosphere is largely affected by the background winds, we employed a 3D ray-tracing of acoustic waves in order to predict the shape of acoustic wave fronts (Figure 2). Then, we selected appropriate antenna beam directions of EAR that satisfy the Bragg condition, i.e., the wave number vectors for radar waves and the target acoustic waves must be parallel.

As a result, we observed temperature profiles from 2 km to 5-12 km continuously with the time and height resolutions of about 3 minutes and 150 m, respectively. Several temperature profiles were obtained up to about the tropopause at 16 km, although observation period was short. RMS of difference of temperature in the upper troposphere between EAR-RASS and radiosondes was about 0.3 K. We also showed the effect of sound source power and frequency of sound signal on RASS observation quantitatively. We examined two methods of temperature correction by wind velocity.

EAR-RASS results are useful for the studies of peculiar atmospheric phenomena in the equatorial regions, such as the intense cloud convection, structure of the boundary layer, atmospheric waves, and so on.

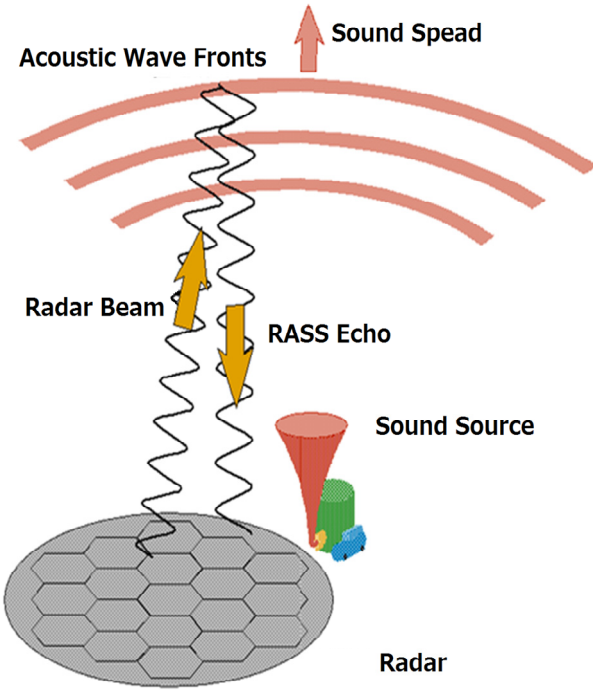

Figure 1. Radio Acoustic Sounding System (RASS).

Reference

[1] S. Fukao, H. Hashiguchi, M. Yamamoto, T. Tsuda, T. Nakamura, M.K. Yamamoto, T. Sato, M. Hagio, and Y. Yabugaki, Equatorial Atmosphere Radar (EAR): System description and first results, *Radio Science*, 38 (3), doi:10.1029/2002RS002767, 2003.

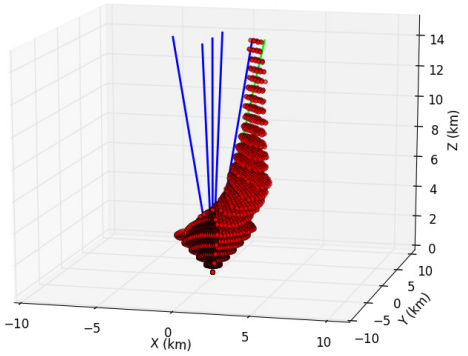

Figure 2. 3D plot of ray-tracing.

ABSTRACTS (MASTER THESIS)

Development of reception system for estimating ionospheric total electrons content from new beacon satellites

**(Graduate School of Informatics,
Laboratory of Radar Atmospheric Science, RISH, Kyoto University)**

Keiichi Iwata

Accurate measurement of the ionosphere helps to improve stability of satellite operations. Also it is useful to monitor the environment. For example, ground fluctuations by the earthquake fluctuates the total electron content (TEC) of the ionosphere. Radio-wave ray paths from the beacon satellite vary by the TEC. Because the effect is different at different frequencies, TEC can be estimated by analyzing the phase difference between signals at two different frequencies. Now 150MHz and 400MHz signals are used. However, beacon satellites are old, so only 3 satellites can now be used. There are plans for new beacon satellites. In this research, we developed a receiving system corresponding to the new beacon satellites.

The new type satellites are planned to be launched in September 2018; TBEx and COSMIC-2. Because transmitters on these satellites send signals at 150/400/965/1067 MHz. It is the necessary to correspond with higher and more frequencies than the current system. The current system has a stable operation record over a long term. We tried to develop the new receiver by using multiple SDR devices. So that we use then SDR boards to receive three frequencies.

In selecting a SDR, we examined the characteristics of SDRs and the beacon satellite transmitter. In addition, analysis frequency of system software also improves, we increased the speed. We developed prototype of the new receiver, and compared it with the current GRBR system as shown in Figure 1. This comparison experiment was successful, and we got similar results from both receivers. We also found that slight deviation of observation start timing of SDR does not have a big influence. However, we found that the data-loss is a severe problem. To avoid this problem, we needed to lower the spec by reducing data acquisition rate.

We were successfully developed the new digital receiver for the satellite-ground beacon experiment. However, there are three future tasks; further test of signals with frequencies other than 150MHz and 400 MHz, analysis method improvement that enables any frequency combination, and more stability with keeping higher data rates.

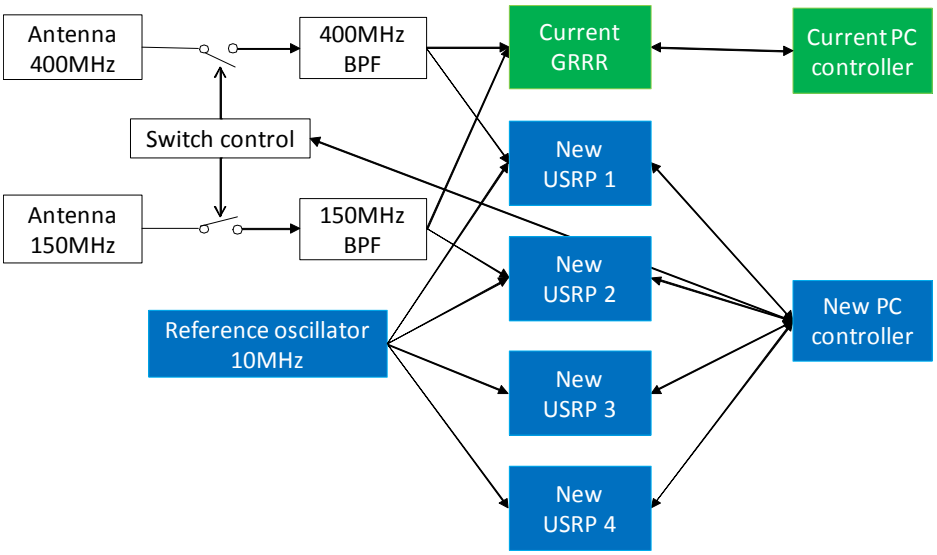

Figure 1. Block diagram for the comparison experiment between new and current beacon receivers.

ABSTRACTS (MASTER THESIS)

Study on atmospheric structure based on simultaneous observations with UAV and the MU Radar

**(Graduate School of Informatics,
Laboratory of Radar Atmospheric Science, RISH, Kyoto University)**

Takashi Mori

Over the past few years, an Unmanned Aerial Vehicle (UAV) has increasingly attracted attention as a new instrument for atmospheric measurements. Radiosonde balloons, which have been often used for atmospheric observations in the troposphere and lower stratosphere, move due to background winds and cannot measure at an aimed place. Therefore, autonomous UAV is being developed and operated to overcome this problem.

Observation field campaigns called the Shigaraki UAV-Radar Experiment (ShUREX) were carried out in 2015 and 2016, in which the UAVs developed by the University of Colorado were flown near and over the MU radar to simultaneously observe the atmospheric column over the radar [1, 2].

This thesis presents considerations of atmospheric structure by using observation data obtained during the ShUREX campaign for mainly two subjects.

As subject 1, simulations for large temperature variations measured by the UAV flying horizontally in strong echo layer were performed. The temperature variation over 20 minutes could be reproduced supposing the vertical profile of temperature and the vertical wind estimated from displacement of the echo layer. As a result, the large difference in temperature was caused by air parcel with adiabatic temperature change entering the oscillating inversion layer due to vertical wind.

As subject 2, comparisons between vertical profiles of squared refractive index gradient estimated from the observation data with UAV and the MU radar were performed. In the stratified layers, the profiles estimated from UAV and the MU radar agreed well except in some regions, which was caused by small inversion layers. On the other hand, the profile estimated from the MU radar was overall larger than that estimated from UAV in turbulent layers, which was probably caused by not distinguishing backscatter models. It was confirmed that other factors except for refractive index gradient contributed to the radar echo power when turbulent scatter is expected.

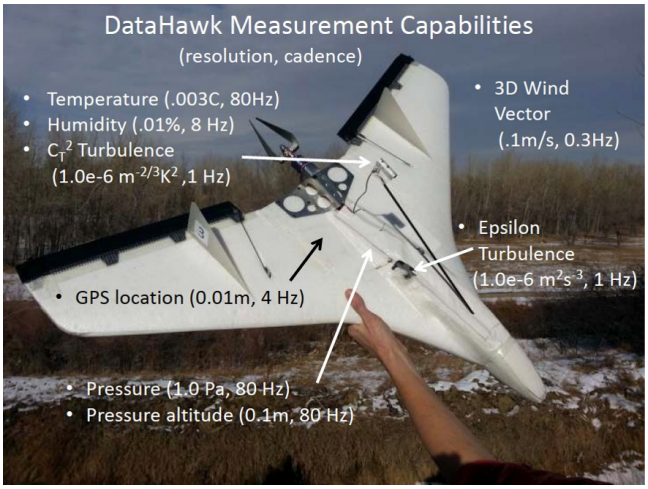

Figure 1. The University of Colorado DataHawk UAV [1].

References

[1] Lawrence, D. A. and Balsley, B. B., High-resolution atmospheric sensing of multiple atmospheric variables using the DataHawk small airborne measurement system, *Journal of Atmospheric and Oceanic Technology*, 30 (10), 2352-2366, 2013.

[2] Lakshmi Kantha, Dale Lawrence, Hubert Luce, Hiroyuki Hashiguchi, Toshitaka Tsuda, Richard Wilson, Tyler Mixa, and Masanori Yabuki, Shigaraki UAV-Radar Experiment (ShUREX2015): An Overview with Preliminary Results, *Progress in Earth and Planetary Science*, doi:10.1186/s40645-017-0133-x, 2017.

ABSTRACTS (MASTER THESIS)

Optically transparent materials from cellulose nanofiber (CNF)-stabilized resin-in-water Pickering emulsion

(Graduate School of Agriculture, Laboratory of Active Bio-based Materials, RISH, Kyoto University)

Subir Kumar Biswas

Introduction

CNF-reinforced optically transparent composites of high-performance have been developed a decade ago.[1] The composites were fabricated by impregnating acrylic resin monomer into the CNF-sheet. The CNF-sheet is very stiff due to the hydrogen (H) bonding among the nanofibers and hence, its resin impregnated composite is difficult to mold into a three-dimensionally (3D) curved material. To accomplish 3D-molding with optical transparency, CNF-suspension could be mixed with liquid resin, however, hydrophilic CNF-suspension and hydrophobic acrylic resin are typically immiscible. These drawbacks virtually hinder the fabrication of CNF-reinforced high-performance transparent materials that could be used in many exciting applications, such as contact lenses, substrate for curved displays, microlens arrays and so on.

Experimental

To overcome above two limitations, a Pickering emulsification process is developed. First, CNF-suspension was mixed with acrylic resin monomer (ABPE-10) at a concentration of 10% CNFs to the resin followed by vigorous agitation in a high-speed blender (37,000 rpm). The obtained emulsion was vacuum-filtered to get a CNFs/resin mat. The mat was then hot-pressed by placing between respective substrates to fabricate planar, 3D-molded, or micro-patterned composites (Fig. 1). The thermal, mechanical and optical properties of the composites were evaluated.

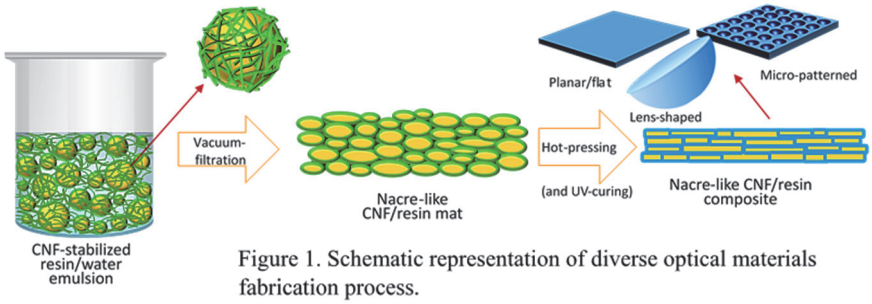

Figure 1. Schematic representation of diverse optical materials fabrication process.

Results and discussion

During emulsion formation, numerous resin droplets of 0.3-10 μm in diameter have been produced. The droplets are covered and stabilized by the suspended CNF-network in the emulsion. Interestingly, after vacuum-filtration a CNF/resin mat with self-assembled 'nacre-like' structure has been obtained (Fig. 1). The nacre-like alternating CNF-resin structure reduces the H-bonding between the CNFs and allows to fabricate a lens-shaped transparent material after hot-pressing (Fig. 2). The fabricated materials uniquely combines high optical transparency (regular transmittance 82% at 600 nm wavelength), high strength and toughness (15 and 24-times than neat acrylic resin, respectively), and a drastically low thermal expansion (1/24th of the neat acrylic resin) at a CNF content of 14-20%.

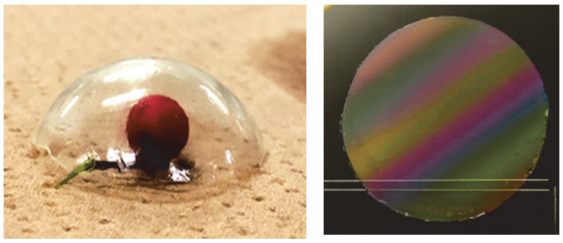

Figure 2. CNF-reinforced lens-like composite (left), and a micro-patterned composite showing beautiful colors (right).

References

[1] Yano, H., Sugiyama, J., Nakagaito, A.N., Nogi, M. et al., *Adv. Mater.*, 17 (2), 153-155, 2005.

ABSTRACTS (MASTER THESIS)

Artificial lignification using wood cell wall models

(Graduate School of Agriculture, Laboratory of Active Bio-based Materials, RISH, Kyoto University)

Tomoaki Natsume

One of factors of making trees enable to support their big body against the gravity is deposition of lignin into gaps of cellulose and hemicellulose in wood cell wall (lignification). This mechanism is thought that wood cell wall forms fiber-reinforced composite structure by lignification. However, this process and mechanical properties changes caused by lignification are still unclear.

In this study, wood cell wall models were prepared using cellulose nanofiber hydrogel. Cellulose nanofiber is the main components of cell walls and plays main structures of them. Cellulose microfibrils were isolated from wood powder (Japanese cypress, 60 mesh) by Wise method and alkaline treatments. Isolated cellulose microfibrils were fibrillated by a grinder to nanofibers. Cellulose nanofiber forms hydrogels by alkaline treatment. In detail, NaOH was dissolved in suspension of cellulose nanofiber and got 8 wt% concentration of NaOH. Next, cellulose nanofiber was treated by centrifugation (11,000 rpm, 30 minutes). The precipitate was neutralized, and got hydrogel of cellulose nanofiber. One of lignin models is DHP (Dehydrogenation Polymer). DHPs made from coniferyl alcohol were used in this study. Coniferyl alcohol, peroxidase, and H2O2 were dissolved in solvent composed ethanol: water=3:1, and cellulose nanofiber hydrogel were immersed into them. After 24 hours, ethanol was vaporized under vacuum pressure. Then DHPs synthesized in hydrogels. Those gels were rinsed by distilled water and repeated DHP synthesis.

Those processes made it possible to reproduce lignification in vitro. Those hydrogels looked like actual wood cell wall in the SEM observation (Fig.1), and compression strength was increased as increasing the time of DHP synthesis. It is thought that gaps of cellulose nanofiber networks are fulfilled by lignin (DHPs) and reinforced. It is also thought that there is some interactions between lignin and cellulose nanofiber because DHPs don't form spherical shapes, and those two components fixed rigidly.

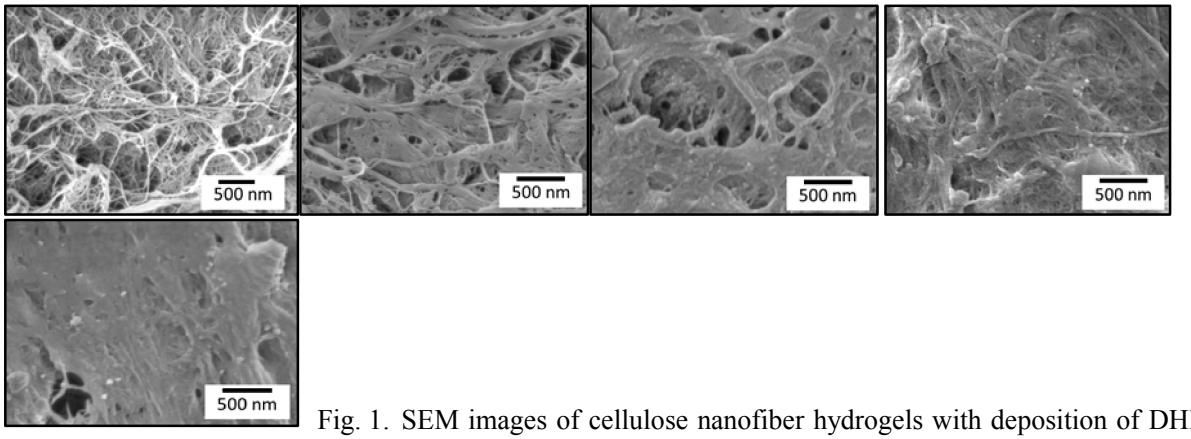

Fig. 1. SEM images of cellulose nanofiber hydrogels with deposition of DHPs (From upper left, the time of DHP synthesis is 0,1,2,3,4)

ABSTRACTS (MASTER THESIS)

The new technical development of wet-spinning with cellulose nanofiber

**(Graduate School of Agriculture,
Laboratory of Active Bio-based Materials, RISH, Kyoto University)**

Momoyo Utsumi, Kentaro Abe, and Hiroyuki Yano

When obtaining a molded product from cellulose, it is necessary to dissolve cellulose once and regenerate it. In that case, special solvents such as carbon disulfide are used, and the crystallinity of cellulose decreases and crystal transformation occurs. However, cellulose, which occupies about 50% of the plant cell wall, originally exists as a crystalline nanofiber having a width of about 3 nm. By using this cellulose nanofiber(CNF), it is considered that a high strength molded body can be produced without dissolving cellulose. Our laboratory already establishes a method for gelling CNF by simple alkaline treatment. Since it can be molded into an arbitrary shape while maintaining the crystal structure of I type, it is not necessary to use special solvents. Therefore, in this research, we aimed to develop new cellulose fiber by spinning CNF under alkaline conditions. On the other hand, it is reported that CNF is uniaxially oriented by utilizing shearing action. [1] As the material with higher degree of orientation is considered to exhibit superior physical properties, the second objective of this research was to arbitrarily set the spinning speed in order to uniaxially orient CNF under alkaline conditions.

Non-cellulose components were removed from Japanese cypress wood meal, and CNF was prepared from the obtained refined pulp using a grinder. CNF was treated with 8% sodium hydroxide aqueous solution and then spun into 2% sulfuric acid using a syringe. At this time, the spinning speed was controlled to 1-100 m / min.

The surface cellulose molecular chain of CNF swelled by alkali treatment, and the cellulose molecular chains entangled with each other by spinning (neutralization step) into the coagulation bath and then a fibrous gel could be obtained. (Figure 1) From the X-ray diffraction results, it was revealed that this spun fiber was a cellulose type I crystal, and succeeded in the production of spun fiber of cellulose I by simple alkali treatment. From the results of the tensile test (Table 1), an increase in elastic modulus and tensile strength was revealed as the spinning speed increased. The X - ray diffraction results revealed that the degree of orientation of CNF increased with increasing spinning speed. Therefore, the orientation of CNF can be controlled by increasing the spinning speed, which contributes to the increase of elastic modulus.

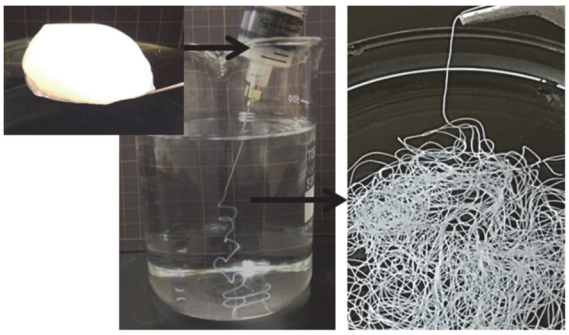

Figure 1. Wet-spinning of CNF

Table 1. Tensile properties of wet spun fibers

Spinning rate (m/min)	Young's modulus (GPa)	Tensile strength (MPa)	Strain at break (%)
1	11.9 ± 2.7	77 ± 6	1.1 ± 0.2
10	12.2 ± 2.8	98 ± 8	2.4 ± 0.7
100	12.7 ± 1.9	112 ± 18	2.8 ± 0.8

Reference

[1] Iwamoto. S, "Structure and mechanical properties of wet-spun fibers made from natural cellulose nanofibers," *Biomacromolecules*, vol. 12, pp. 831-836, 2011.

ABSTRACTS (MASTER THESIS)

Selective acetylation of matrix components in softwood ground pulps

**(Graduate School of Agriculture,
Laboratory of Active Bio-based Materials, RISH, Kyoto University)**

Tomohiro Yagi

The use of lignocellulose biomass remains a challenge in wood chemistry. Wood, the most abundant lignocellulosic resource, has long been used and researched as a raw material. However, wood has certain disadvantages such as dimensional stability, fungal resistance, photostability, and weathering. Chemical modifications can overcome such shortcomings. Specifically, acetylation, the simplest esterification, is an efficient method for improving the properties of wood (i.e., lignocellulose materials). In fact, acetylated wood is now commercialized.

This study prepared matrix-acetylated ground pulp to follow its acetylation process from the initial stage to the final stage of the reaction. Ground pulps, whose component ratio is approximately the same as raw wood, was selected as the sample. Acetylation was chosen as the most typical esterification. In detail, we prepared partially acetylated ground pulps with degree of substitution values of 1.2 (where it was expected that the matrix components were acetylated completely) and elucidated the position that the acetyl groups were introduced under the acetylation of ground pulps. We also investigated the effect of acetylation on thermal stability. Thermal stability is important for the use of lignocellulose materials as filler because plastics are molded from 150 to 300 °C. An increase in thermal stability will make the application to more plastics possible.

The acetylation of ground pulp was followed by heteronuclear single quantum coherence-nuclear magnetic resonance (HSQC-NMR) spectroscopy to investigate the relationship between the degree of acetylation and the introduction positions of acetyl groups during this acetylation. We also examined the effect of acetylation on thermal stability. Seven kinds of acetylated ground pulps with degree of substitution values of 0.19, 0.29, 0.59, 0.74, 1.04, 1.11, and 1.19 were prepared and analyzed using HSQC-NMR spectroscopy. Acetylation was found to occur first on the primary hydroxyl groups of polysaccharides and lignin, followed by the secondary hydroxyl groups of polysaccharides, and finally the hydroxyl groups at the α-position of lignin. The thermal stabilities of the acetylated ground pulps were analyzed using thermogravimetric analysis. The 1% weight loss temperatures of the acetylated ground pulps were higher than that of the ground pulps. The acetylation of the primary hydroxyl groups in polysaccharides and lignin and the hydroxyl groups at the α-position of lignin was more effective in improving thermal stability than that of the secondary hydroxyl groups in polysaccharides.

ABSTRACTS (MASTER THESIS)

Development of inorganic composite wood molding using hydroxyapatite formation reaction

**(Graduate school of Agriculture,
Laboratory of Sustainable Materials, RISH, Kyoto University)**

Zhu Yunqi

Introduction

The depletion of fossil resource and global warming is becoming problems nowadays. Wood as a renewable resource is expected to contribute to restrain those problems. However, the defects of wood such as flammability, easily degradable, poor dimensional stability are problems in the utilization. To resolve these problems, complexation with inorganic compounds has been carried out. However, the complexation has various problems relating to impregnation to wood, chemical safety, and removal of by-products etc. The aim of this research was to develop of wood-inorganic composite molding by using the reaction of hydroxyapatite (HAP) formation. HAP have good biocompatibility and heat-resisting property. In addition, by-products of nitric acid and sodium nitrate generated in the preparation of HAP were tried to use as chemicals for self-bonding of wood.

Method

A HAP aqueous solution was prepared by using calcium nitrate and disodium hydrogenphosphate, and the molar ratio of calcium nitrate and disodium hydrogenphosphate was 5: 3. Wood powder (100 mesh pass) was added to the hydroxyapatite aqueous solution and mixed. The addition ratio of the amount of calcium nitrate and disodium hydrogenphosphate to wood was changed from 0 to 60wt%. After drying the mixture, the mixture powder was poured into a dumbbell-shaped mold for JIS K 7139-1966 A type, and hot-pressed. The obtained molding was stored for a week at 20˚C and RH 60%. As evaluation methods, bending test, boiling test, FT-IR analysis, thermal analysis was performed. The influences of the mixing ratio of the amount of calcium nitrate and disodium hydrogenphosphate to wood, drying condition, hot press condition on the physical and chemical properties of the molding were investigated.

Results and discussion

It was confirmed that wood-inorganic composite molding was obtained by using the reaction of HAP formation. The specific bending properties were improved with increasing the amount of calcium nitrate and disodium hydrogenphosphate up to 20wt%. In boiling test, wood-inorganic composite molding with addition ratio of more than 20wt% had good water resistance. Therefore, it was clarified that by-products brought self-bonding of wood. Figure 1 shows the results of TGA measurement. As the addition ratio of the two compounds to wood increased, the final residual weight increased. This indicated that the content of HAP in the molding increased with increasing the two compounds. The behavior of the molding without adding the two compounds (E 0) had two steps behavior indicating flaming combustion and red hot flame. However, the two steps behavior gradually disappeared as the addition ratio of the two compounds increased. This means that the flame retardancy of the molding was improved by the existence of HAP. As results of IR spectra of the molding after the boiling test, the absorption peaks derived from phosphate ion of HAP were observed.

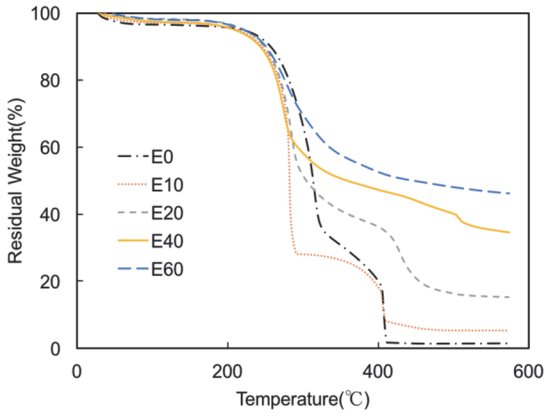

Fig.1. TG of wood-inorganic composite molding. (20℃/min, Air)

ABSTRACTS (MASTER THESIS)

Estimation of in-plane bending strength considering lamination effect

**(Graduate School of Agriculture,
Laboratory of Structural Function, RISH, Kyoto University)**

Tsuyoshi Aoyama

A simulation model based on Monte-Carlo method was developed to estimate in-plane bending strength of cross laminated timber (CLT). The model used mechanical characteristics of lamina obtained from edgewise bending test of them. To consider the effect of gluing each layer, bending test on lamina with cross layer was carried out. Experimental value of in-plane bending strength of CLT and calculated value were compared. The result indicates that cross layer raises the distribution of bending strength and that in-plane bending strength can be estimated by the model.

The model on estimation of in-plane bending strength of CLT

The model assumes that longitudinal layer only can resist against bending moment and that bending strength (MOR)of base material of each lamina is unique in direction of the length of lamina. Knots and finger joints (FJ) are generated as random number according to probability distributions. MOR of each defect is given using regression equations obtained in edgewise bending test of single lamina. The failure of lamina occurs at the moment that the bending stress on the edge of tension side reaches MOR on any point of lamina (base material, knot or FJ) and CLT failed simultaneously with the failure of the first lamina.

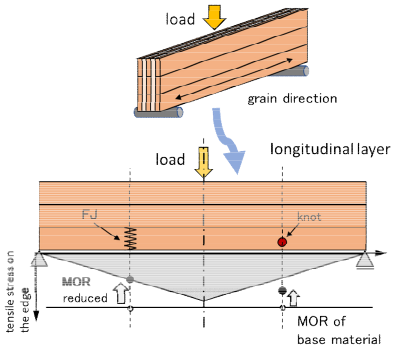

Figure 1. Overview of the model

Bending test of lamina with cross layer

Bending test of lamina with cross layer as shown in Figure 2 was carried out. Specimens were chosen so that they have knot or FJ between the loading points. Table 1 shows comparison in average MOR between specimens with and without cross layers. The result indicates that MOR of specimens with knot was raised by lamination, while in the specimens with FJ the tendency was not found.

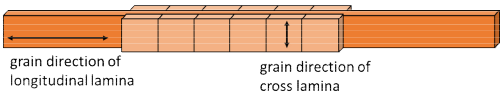

Figure 2. Specimen with cross layer

Table 1. The result of lamina bending test

	MOR without cross layers (MPa)	MOR with cross layers (MPa)
knot	37.5	45.4
FJ	36.6	38.3

Estimation of in-plane bending strength of CLT

Bending strength of seven-layered CLT was compared between experimental value [1] and estimated value obtained from the model described above. Lamination effect was calculated as strength of knots was multiplied by 1.2. The experimental value and cumulative curve of estimated value are shown in Figure 3. It shows that estimated value with lamination effect was larger than the value without the effect, especially in specimens with relatively low strength. In addition, the agreement between experimental and estimated value was better in calculation with lamination effect. In conclusion, in-plane bending strength of CLT can be estimated employing the model and its accuracy would be improved by considering lamination effect.

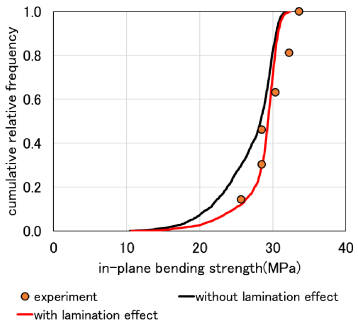

Figure 3. Experimental and estimated value of seven-layered CLT

Reference

[1] Forest products Research Institute, Progress report of promotion of CLT utilization, 2015 (in Japanese)

ABSTRACTS (MASTER THESIS)

Study of Fine Structure of Plasmaspheric Hiss

(Graduate School of Engineering, Laboratory of Computer Simulation for Humanospheric Sciences, RISH, Kyoto University)

Daishi Miyazaki

We analyzed the observation data from the Electric and Magnetic Field Instrument and Integrated Science instrument (EMFISIS) on the Van Allen Probes mission using fast Fourier transform to investigate plasmasheric hiss. Plasmashperic hiss is an electromagnetic whistler mode emission which typically occurs in the frequency range from 100 Hz to several kHz. Recent report says plasmaspheric hiss can generate energetic particles. We examined the fine structure of plasmaspheric hiss which similar to small segments of rising tone and falling tone of chorus subpackets. By analyzing the high resolution data observed mainly in April 2013, we confirmed the characteristics and calculated wave normal angles, degree of polarization, Poynting flux and ellipticity to investigate the plasmaspheric hiss. From these properties, we made a study of generation and propagation of hiss emissions from the equator. We found the propagation often induced convective growth. Plasmaspheric hiss was found even during magnetically quiet periods and intensities during storms or sub storms. We checked if nonlinear wave growth theory of whistler mode chorus emissions can be applied to coherent hiss emissions. We compared the optimum amplitude and threshold amplitude from the nonlinear growth theory and the observational results of plasmaspheric hiss. While some cases show good agreement between the nonlinear theory and observation, we found some cases with discrepancies. We also found cases showing both hiss and chorus emissions as shown in Figure 1. This suggests that physical conditions necessary for hiss emissions may not be much different from those of chorus emissions, and that the nonlinear wave growth model with the threshold and optimum amplitudes for chorus emissions can also be applied to hiss emissions. However, further studies of these emissions along with analyses of energetic electron fluxes providing energy to the waves are needed for identification of necessary conditions for generation of hiss and chorus emissions.

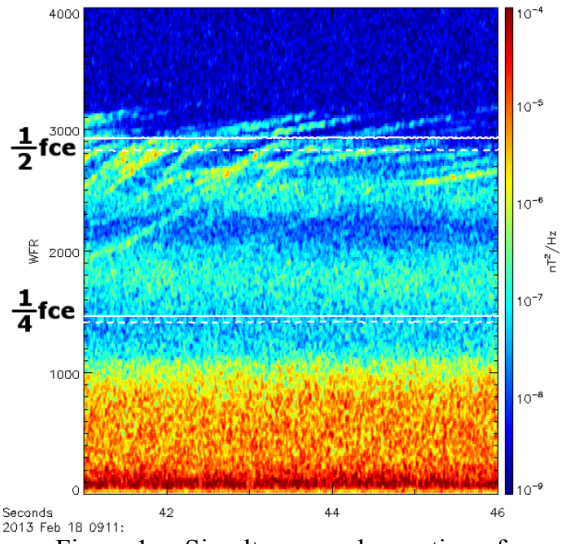

Figure 1. Simultaneous observation of whistler-mode hiss and chorus emissions.

Acknowledgements

The data analysis was performed on the KDK computer system at the Research Institute for Sustainable Humanosphere (RISH), Kyoto University.

References

[1] D. Summers, Y. Omura, S. Nakamura, C. A. Kletzing, Fine structure of plasmaspheric hiss, *J. Geophys. Res., Space Physics*, 119, 9134-9149, 2014.

[2] Y. Omura, S. Nakamura, C. A. Kletzing, D. Summers, and M. Hikishima, Nonlinear wave growth theory of coherent hiss emissions in the plasmasphere, *J. Geophys. Res. Space Physics*, 120, 7642-7657, 2015.

[3] S. Nakamura, Y. Omura, D. Summers, and C. A. Kletzing, Observational evidence of the nonlinear wave growth theory of plasmaspheric hiss, *Geophys. Res. Lett.*, 43, 10,040-10,049, 2016.

ABSTRACTS (MASTER THESIS)

Formation of multiple energy dispersion of H^+, He^+, and O^+ ions in the inner magnetosphere in response to interplanetary shock

(Graduate School of Engineering, Laboratory of Computer Simulation for Humanospheric Sciences, RISH, Kyoto University)

Hiroki Tsuji

The sun sometimes emits a magnetic cloud. There is a shock ahead of the magnetic cloud, called an interplanetary (IP) shock (IP). When the IP shock arrives at Earth's magnetosphere, the particle environment in the magnetosphere is known to be change drastically. Satellite observations have shown that soon after arrival of the IP shock, overall intensity of the ions rapidly increases and multiple energy dispersion appears in an energy-time spectrogram of the ions. In order to understand the response of the magnetospheric ions to IP shock, we have performed test particle simulation under the electric and magnetic fields provided by the global magnetohydrodynamic simulation. On the basis of the Liouville theorem, we reconstructed the differential flux of H^+, He^+, and O^+ ions situated at (7, 0, 0) Re in GSM coordinates by means of the semi-Lagrangian (phase space mapping) method. The H^+, He^+, and O^+ ions are known to be majority of ionic species in the magnetosphere.

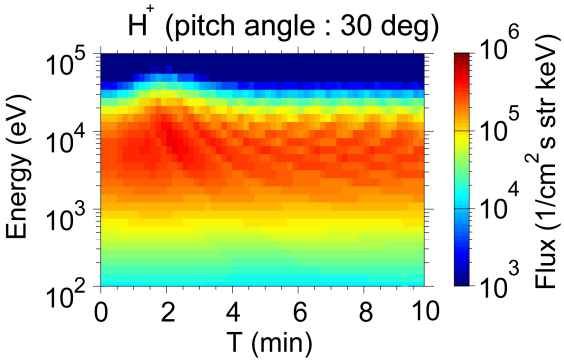

Figure 1. Energy vs. time spectrogram of simulated differential H^+ flux at (7, 0, 0) Re.

Simulation results show that the ions respond to the IP shock in two different ways. First, overall intensity of the flux gradually increases at all pitch angles. As the compressional wave, which is one of the magnetohydrodynamics waves, propagates tailward, the magnetic field increases, which accelerates the ions due to the gyrobetatron. This change is well known. Second, multiple energy-time dispersion appears in the reconstructed spectrograms of the ion flux. The energy-time dispersion is caused by interaction between bouncing ions and compressional wave propagating tailward. When the tailward propagating compressional wave catches up the ion moving toward mirror point at off-equator, the ion gains the kinetic energy efficiently. The ions are primarily accelerated by the drift betatron under the strong electric field looking dawnward. The dispersion is clearly seen in the mirroring ions, but is absent in equatorially mirroring ions. The dispersion appears at higher energy for heavier ions. These features are consistent with the satellite observations. Because the acceleration depends on bounce phase, the bounce-averaged approximation is probably invalid for the ions during the interval of geomagnetic sudden commencement. The result is published in Journal of Geophysical Research Space Physics [1].

Acknowledgements

The computer simulation was performed on the KDK computer system at the Research Institute for Sustainable Humanosphere (RISH), Kyoto University.

References

[1] Tsuji, H., Y. Ebihara, and T. Tanaka (2017), Formation of multiple energy dispersion of H^+, He^+, and O^+ ions in the inner magnetosphere in response to interplanetary shock, J. Geophys. Res. Space Physics, 122, 4387–4397, doi:10.1002/2016JA023704.

ABSTRACTS (MASTER THESIS)

Design of Microwave Sintering Apparatus of Titanium for Industrial Mass Production

**(Graduate School of Engineering,
Laboratory of Applied Radio Engineering for Humanosphere, RISH, Kyoto University)**

Satoshi Arimasa

In modern days, microwave heating is used in a variety of fields, including microwave oven in our daily lives. In 1999, Roy et al. discovered that it can be applicable to sintering various metal alloy powder. Since microwave heating is generally more highly efficient than conventional heating, a number of studies and reports on its application have been conducted in order to employ this technology in the industrial field.

In this paper, we design microwave sintering apparatus of titanium powder for industrial mass production by both electromagnetic simulations and experiments. Electromagnetic simulation needs electromagnetic properties of titanium powder, or its complex permittivity and permeability, which are still unclear for its structural complexity. Therefore before apparatus design, we evaluated its properties by both electromagnetic simulations and experiments. In the evaluation of the permittivity and permeability, the coaxial line method was utilized. In electromagnetic simulations, we simulated two models, single sphere model and unit cells model. By changing a particle radius and an interparticle distance, we obtained a variety of properties of complex permittivity and permeability. In experiments, we measured mixture of titanium powder and quartz powder at various mass fractions and estimated the complex permittivity and permeability of pure titanium powder. Combining the results of both simulations and experiments, we obtained complex permittivity and permeability of titanium powder for the electromagnetic simulations of apparatus design. The apparatus we designed basically consists of a waveguide with apertures and a belt conveyor on which the heated sample is put. Since additional apertures may let microwave energy leak through them, the energy leakage from the apertures as well as absorption energy of titanium powder were investigated. First the apparatus without apertures was investigated, and we can successfully irradiate microwave to titanium powder sample. However in an apparatus with apertures, it is found that the apertures make efficient microwave heating of titanium powder quite difficult.

ABSTRACTS (MASTER THESIS)

Study for Improvement of Oscillation Efficiency and Noise of 2.45 GHz Magnetron

(Graduate School of Engineering, Laboratory of Applied Radio Engineering for Humanosphere, RISH, Kyoto University)

Keita Hirayama

Magnetron has high oscillation efficiency and large noise. In the previous studies, researches on them aren't sufficient. In this thesis, we analyzed the details of them using 3D particle-in-cell (PIC), 3D electromagnetic, and eigenvalue simulations. Here, we used QV, J, and U models as 1kW magnetrons and a HI model as a 6kW magnetron. The QV model is a high oscillation efficiency model. The J model is a low noise model. The U model is an intermediate model between the QV and J models. The HI model is similar to the shape of the QV model which has different size.

First, we utilized the simple model and actual model as the filament of the QV and J models and estimated the oscillation efficiency of them. The results showed that the oscillation efficiency was decreased by the particles accelerated in electric field generated between the cavity resonators. Also, the oscillation efficiency didn't depend on electron efficiency loss which was 1% or less, due to the axial direction component of the particle velocity. Then, we estimated the oscillation efficiency of the QV, J, and HI models by changing the amount of emitted particles. As a result, there was a tendency that oscillation efficiency showed a local maximum value with respect to the anode current in any models, because there was the influence of the RF electric field between the interaction space side and the cavity resonator.

Further, we compared the results of eigenvalues and 3D PIC simulations. As a result, we identified the noise source and also mentioned noise improvement methods. Using this result, we proposed a reduction method of 3 GHz noise source in the HI model. As a result, it was possible to construct an HI1 model, which was improvement of the HI model, with the frequency difference between the oscillation frequency and the spectra of 3 GHz bands increased by 52 MHz. Finally, we conducted experiments. The tendency of the oscillation efficiency with respect to the anode current was consistent with the simulation. The HI1 model could also reduce 3 GHz noise and it proves that the present noise reduction method is effective.

Acknowledgements

This research is collaborative research with Panasonic Appliance Co.

ABSTRACTS (MASTER THESIS)

Study on Wireless Power Transfer between Array Antennas in the Radiative Near Field towards Higher Efficiency

(Graduate School of Engineering, Laboratory of Applied Radio Engineering for Humanosphere, RISH, Kyoto University)

Seishiro Kojima

In this paper, we analyzed the wireless power transfer between array antennas in the radiative near field. We can calculate the power transmission efficiency between array antennas by regarding array them as aperture antennas. However, it is re-ported that there is a considerable gap between theoretical efficiency and measured one in the previous study. As the reason, the theoretical calculation doesn't consider losses which occurs in the transmission. In the previous study, losses were estimated but the examination of concrete loss factors is insufficient. In the radiative near field, an incident wave on receiving antenna is a spherical wave and a loss occurs in power combined circuit because the amplitude and phase of spherical electric field are different at each element. We call it synthesis loss and this was not considered in the previous study.

Therefore, we defined 5 losses to clarify the factors of gap between theoretical efficiency and measured one; synthesis loss, antenna loss, refection loss, beam formation loss and receiving efficiency. Then we estimated the effect of them on transmission efficiency in the simulation and calculated the efficiency compensated the effect of them. As the result, we found that the effect of synthesis loss can not be ignored in the radiative near field. Besides, the estimated efficiency was matched the measurement efficiency and it was shown our method of estimating transmission efficiency is useful.

Finally, we tried to enhance the transmission efficiency by designed a receiving antenna with an adjusted phase difference in the circuit. By using this antenna as a receiving antenna, the efficiency was improved by 0.9 point in the simulation. Further, in the simulation, we realized about 2.5 point increase of transmission efficiency by removing the corner elements of an array antenna when the transmission distance is enough small.

Acknowledgements

Part of this research was carried out by use of Microwave Energy Transmission Laboratory (METLAB) as collaborative inter-university research facility.

ABSTRACTS (MASTER THESIS)

Study on Rectifier for a Satellite Internal Wireless Power Transfer System

**(Graduate School of Engineering,
Laboratory of Applied Radio Engineering for Humanosphere, RISH, Kyoto University)**

Ce Wang

In order to achieve space development in future, it is essential to launch observation and scientific satellites. However, because rocket carrying capacity is limited, reducing the weight of an artificial satellite is an important issue. To solve this problem, an internal wireless system (IWS) for a satellite was proposed. If all the wires can be eliminated, its weight will be reduced by 20% to 30%, and the subsystems designs can increase without the limits of wires. During satellite operation, because subsystems is independent, the stability can also be increased. The wires of an artificial satellite can be divided into two types: signal wires and power wires. In a previous study, the signal wires were reduced with wireless communication devices. In this paper, we proposed a complete IWS system using wireless power transfer technology. The IWS we propose is a wireless power supply system that can be compatible with the internal wireless communication system as well. In this paper, we use a 5.8 GHz charge pump rectifier with high conversion efficiency. Moreover, we theoretically compare the conversion efficiency of a charge pump rectifier and a single shunt rectifier, and experimentally verified the results.

We analyzed the cause of loss in a rectifier circuit and the diodes' voltages and currents in a charge pump circuit. The conversion efficiency can be expressed as the difference from 100% efficiency caused by the transmission line loss, element loss and reflection. When the rectifier circuit is in the matching condition, the reflected component is small enough to be considered 0%. The total loss of a rectifier circuit is generated by the electronic elements. By analyzed voltages and currents of the diodes, however there are two diodes in a charge pump circuit, the diodes loss is the same with a single shunt circuit which is in the same conditions.

Using the results of previous, we designed and made the 5.8 GHz charge pump rectifier and measured its performance practically. In the circuit simulation calculations, the conversion efficiency reached about 77% at 1300 Ω optimum load. The experimentally measured efficiency of the circuit is about 71% at optimum load, which is consistent with the simulation results. Because of the limits of the experimental conditions, the design accuracy is 0.1 mm, which is one-tenth of the typical accuracy of high-frequency circuit design. If we can design and produce this circuit under better conditions, the conversion efficiency should reach about 80%. The highest conversion efficiency so far reached about 80% in a single shunt circuit. Therefore, the results of this experiment also prove that a charge pump circuit and single shunt circuit have the same conversion efficiency.

Acknowledgements

Part of this research was carried out by use of Microwave Energy Transmission Laboratory (METLAB) as collaborative inter-university research facility.

ABSTRACTS (MASTER THESIS)

Improvement of Space Debris Shape Estimation Technique Using MU Radar

**(Graduate School of Engineering,
Laboratory of Space Systems and Astronautics, RISH, Kyoto University)**

Taiki Iwahori

Space debris is considered as obstacles for space exploration, and we have to expand and improve observation method for space debris to reduce the risk of its collision with active spacecraft. In previous researches, the Single Range Doppler Interferometry (SRDI) method was proposed and used. This method requires only a fluctuating Doppler spectrogram caused by the spin motion of debris to estimate its shape. A spectrogram is a visual representation of the spectrum of frequencies in signal as they vary with time. In this thesis, we proposed an improved method of shape estimation of space debris with ground-based observatories.

We introduced Smoothed Pseudo Wigner Distribution (SPWD) for the SRDI method to obtain higher resolution of spectrogram. We confirmed the accuracy of SRDI method using numerical simulation and we also adapted the method with actual data of space debris observed by MU radar. FDTD (Finite-Difference Time-Domain) method is used as a numerical simulation method for radar system observation. We could obtain the correct 2D images characterizing the original shape of space debris when we suppose debris as a set of few discrete points by using SRDI shape estimation. The results of the numerical simulation also shows that, to estimate the shape of rigid body, the accuracy of the estimation needs to be improved. It is because spectrogram cannot distinguish spin motion echo from the echo of targets center. SRDI method was also evaluated by adapting actual observation of space debris which is known its shape. Through the analysis of actual data, we discovered that orbit motion spectral occurs in spectrogram and has negative effect for extracting spin motion spectral. To solve this problem, we proposed an analytic formula of orbit motion spectral and developed elimination method of this spectral. By using this improved SRDI method, we could obtain an image which characterize actual space debris.

ABSTRACTS (MASTER THESIS)

Orbit Determination Technique Exploiting MU Radar

**(Graduate School of Engineering,
Laboratory of Space Systems and Astronautics, RISH, Kyoto University)**

Taiga Nishimura

Space debris are objects in the space including spent rockets, broken satellites and paint chips. Since the velocity of the space debris is on the order of several km/s, it can pose danger to operating satellites and to international space station. Therefore, observation and orbit determination of the space debris are very important problems. In previous study, a tool to design the scheme to observe space debris passing over MU radar based on known orbital elements was developed. In addition, observation method of debris using MU radar has been established. Therefore, in this study, the technique to perform the orbit determination of space debris observed by MU radar is developed. We have developed orbit determination technique using Gauss-Newton method by means to decide orbital elements from plural position vectors estimated from the observation. Our technique can apply for any observed results without considering the time for observation and number of detected points. With this method, elements defining the orbital plane can be estimated with its error is smaller than 1 deg. The results show that if the orbital inclination angle is small and the time for re-passing is short, the observation by MU radar provides enough accuracy to perform the second observation. To improve the accuracy of the estimation, we also study the probability to observe a given debris for several times. The estimation error of orbital period is also improved by the second observation. Moreover if the second observation can be conducted, the estimation errors are improved and the number of observation can also be extended.